NASA Contractor Report 177632

NASA-CR-177632
19940019063

Gas-Grain Simulation Experiment Module Conceptual Design and Gas-Grain Simulation Facility Breadboard Development

J. M. Zamel and M. Petach

CONTRACT NAS2-13408
December 1993

National Aeronautics and Space Administration

NASA Contractor Report 177632

Gas-Grain Simulation Experiment Module Conceptual Design and Gas-Grain Simulation Facility Breadboard Development

J. M. Zamel and M. Petach

TRW Space & Electronics Group
Applied Technology Division
Redondo Beach, CA 90278

Prepared for
Ames Research Center
CONTRACT NAS2-13408
December 1993

National Aeronautics and
Space Administration

Ames Research Center
Moffett Field, California 94035-1000

ACKNOWLEDGMENT

This work was performed under contract number NAS2-13408 sponsored by NASA Ames Research Center and conducted under the management of Mark Fonda. Additional guidance by his science and engineering staff is acknowledged. The work reported was conducted by a number of individuals within TRW who made important contributions. These individuals are listed here in alphabetical order. Dr. Nahum Gat, Dr. Jack Kropp, Christina Luong, Michael Petach, Michael Wolff, and James Zamel.

Table of Contents

List of Figures

List of Tables

List of Acronyms

atm - one atmosphere of pressure
C - degrees Celsius
cg - center of gravity
cm - centimeter
CDR - Critical Design Review
DCE - Droplet Combustion Experiment
EMI/EMC - Electromagnetic interference and compatibility
F - degrees Fahrenheit
fps - frames per second
GGSEM - Gas-Grain Simulation Experiment Module
GGSF - Gas-Grain Simulation Facility
GN_2 - gasious nitrogen
ICD - Interface Control Document
ISPR - International Standard Payload Rack
kg - kilogram
KSC - NASA/Kennedy Space Center
kw - kilowatt
kw_{th} - thermal kilowatt
LEO - low earth orbit
LN_2 - liquid nitrogen
LSE - Laboratory Support Equipment
m - meter
mil - thousandth of an inch
mm - millimeter
NASA - National Aeronautics and Space Administration
PDR - Preliminary Design Review
psia - pounds per square inch absolute pressure
psig - pounds per square inch differential pressure
R&T - Research and Technology
RFP - Request For Proposal
S&T - science and technology
SAMS - Space Acceleration Measuring System
SEM - Scanning Electron Microscope
SSF - Space Station Freedom
STP - Standard temperature (25C) and pressure (1 atmosphere)
TBD - To be determined
Vac - voltage, alternating current
Vdc - voltage, direct current
WBS - Work Breakdown Structure

1 INTRODUCTION

This report delineates the Option portion of the Phase A Gas-Grain Simulation Facility study. The conceptual design of the Gas-Grain Simulation Experiment Module (GGSEM) for Space Shuttle Middeck is discussed in sections 2 through 4. A laboratory breadboard was developed during this study to develop a key function for the GGSEM and the GGSF, specifically, a solid particle cloud generating device. The breadboard design and test results are discussed in section 5. Recommendations for further studies are discussed in section 6.

The GGSEM is intended to fly on board a low earth orbit (LEO), manned platform. It will be used to perform a subset of the experiments planned for the GGSF for Space Station Freedom, as it can partially accommodate a number of the science experiments. The outcome of the experiments performed will provide an increased understanding of the operational requirements for the GGSF.

The GGSEM will also act as a platform to accomplish technology development and proof-of-principle experiments for GGSF hardware, and to verify concepts and designs of hardware for GGSF. The GGSEM will allow assembled subsystems to be tested to verify facility level operation. The technology development that can be accommodated by the GGSEM includes:

- GGSF sample generation techniques
- GGSF on-line diagnostics techniques
- sample collection techniques
- performance of various types of sensors for environmental monitoring
- some off-line diagnostics

Several LEO platforms are available for GGSEM applications. Figure 1 shows these options and lists some of the advantages and disadvantages of each. The Space Shuttle Middeck was selected as the optimum experiment configuration, as is it simple to implement experiments in the middeck, the experiments can utilize human interaction, and the opportunities for flight are more abundant than other locations on the Space Shuttle. The middeck offers an inexpensive method to extend ground-based research to micro-gravity.

The progression of ground-based experiments to micro-gravity platforms often involves the use of low-g facilities such as the NASA KC-135 or a zero-g drop tower. Use of these facilities can provide an inexpensive method (though short duration) for verifying GGSF hardware concepts in low gravity.

The GGSEM middeck concept utilizes much of an existing experiment apparatus design. The existing design is the Droplet Combustion Experiment (DCE) with modifications to replace obsolete subsystems and provide the required GGSEM functions. There are many advantages to utilizing the DCE design for the GGSEM application. The DCE preliminary design has been completed and reviewed, including detailed analyses and safety. An engineering model was built and tested, and is

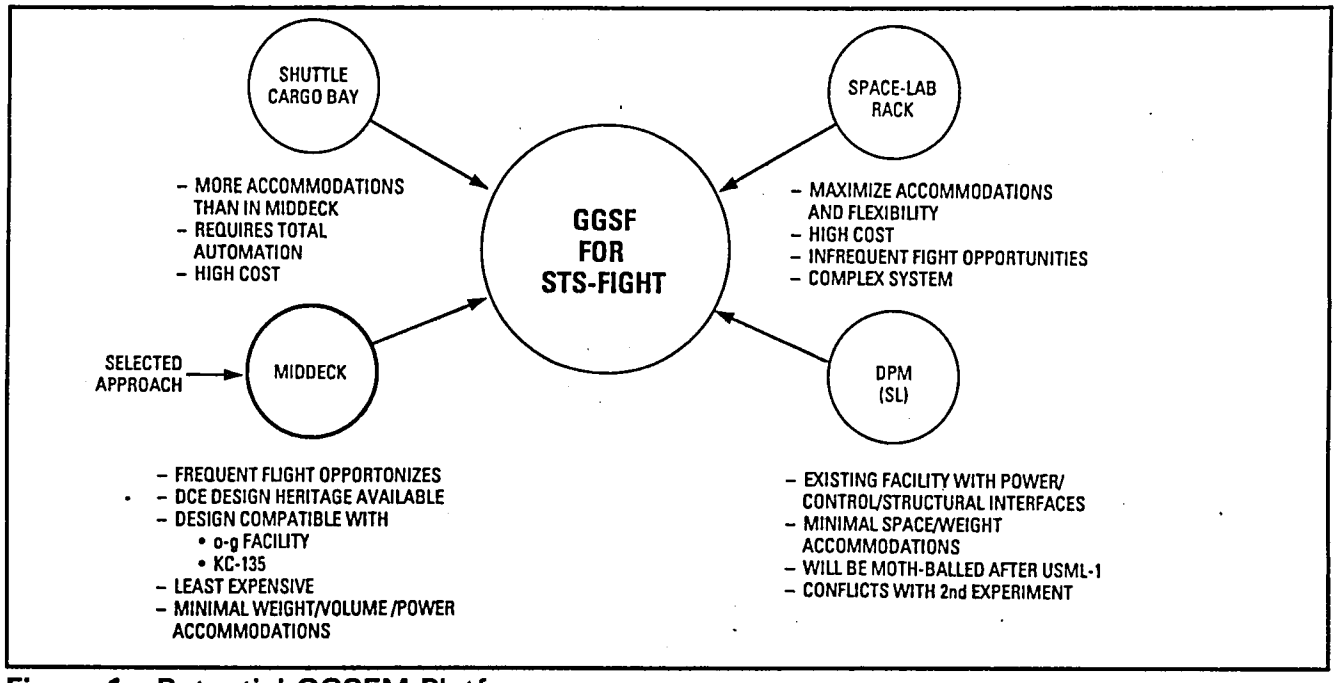

Figure 1 - Potential GGSEM Platforms.

used in the NASA Lewis Research Center 5.5 second zero-g drop tower. The apparatus already has most of the required functions, including a test chamber with ports, middeck interfaces, diagnostics, gas mixture bottles, imaging photography, sample generation, and electrical and electronics for control and data acquisition. These attributes will shorten the GGSEM development schedule, and reduce project risk.

In support of the GGSEM, a breadboard was developed to generate a solid particle cloud sample. This breadboard provides a means of characterizing several major GGSF subsystems, including sample generation, sample collection, sample manipulation, on-line diagnostics, and off-line diagnostics. This device will be used in experiment development, and hardware tests that define hardware performance in meeting science and technical requirements. In addition to being used in a 1-g laboratory, potential low-g platforms for use of the breadboard include zero-g drop towers, low-g aircraft flights (KC-135 or Lear jet), and the Space Shuttle Middeck.

2 GGSEM OBJECTIVES AND REQUIREMENTS

This section defines the GGSEM objectives and requirements for the Space Shuttle Middeck application previously discussed in Section 1. The basic GGSEM objective is to provide a reusable experiment module that:

- meets some of the GGSF S&T requirements and will provide early science return;
- can reduce GGSF hardware risk by allowing early development and testing;
- will provide a platform to accomplish technology development;
- results in a better understanding of the operational requirements for GGSF.

2.1 Science and Technical Requirements

The GGSEM science and technical requirements are a subset of those for the GGSF, which are given in Table 1. The GGSF Phase A Final Report (NASA CR177606) discusses the experiments planned for GGSF in detail, including requirements. Table 2 indicates the applicability of the GGSF experiments to the GGSEM. This assessment is based on the capabilities of the DCE test chamber, which is the bases of the GGSEM design.

Table 1 - GGSF Science and Technology requirements summary as derived in Volume I.

Chamber pressure	From 10^{-10} to 3 bars, with a desire to reach 11 bars
Chamber temperature	From 10 to 1,200 K, with a desire to reach 4 K
Chamber volume	From 1 cm^3 to several hundred liters, various geometries
Particulate matter type	Liquid aerosols, solid-powder dispersions, soot from combustion, high-temperature condensates (nucleation of metal and silicate vapors), low-temperature condensates (ices of water, ammonia, methane, or CO_2), a single liquid droplet, a single or a few particles, *in situ* generated particulate by UV or RF radiation, or by electrical discharge
Particulate size range	From 10 nm to 3 cm
Sample preparation and handling	Sample positioning and levitation
Particulate concentration	A single particle to 10^{10} particles per cm^3
Gases required	Air, N_2, H_2, He, Ar, O_2, Xe, H_2O, CO_2, CO, NH_3, CH_4, and more experiment-specific gases
Diagnostics required	In-line optical systems and off-line sample analyses, including measurements of the grain size distribution, the number density (concentration), optical properties such as index of refraction, emission and absorption spectra, imaging measurement of the grain's strength, mass, density, electrostatic charge, and geometry, collision parameters, including particle kinematic parameters before and after the collision
Experiment duration	From a few seconds, for collision experiments, to weeks, for the biology experiments
Automated facility control and management	Operation of the facility during man-tended phase.

Table 2 - GGSF S&T requirements that fit the GGSEM capabilities.

GGSF Experiment no.	Criteria	Pressure	Temperature	Volume	Appropriate for GGSEM
	GGSEM capability	$0.05 \leq p \leq 1$ atm	cabin (18-27C)	$V \leq 12{,}000$ cc	
1			✓	✓	
2			✓	✓	
3		✓	✓		
4				✓	
5			✓	✓	
6		✓	✓	✓	✓
7		✓	✓	✓	✓
8			✓	✓	
9			✓	✓	
10					
11		✓	✓		
12		✓	✓	✓	✓
13			✓	✓	
14			✓	✓	
15				✓	
16		✓	✓	✓	✓
17			✓	✓	
18		✓	✓	✓	✓
19		✓	✓		
20		✓	✓		
21		✓	✓	✓	✓

2.2 Anticipated Middeck Operations Constraints

Space Shuttle Middeck experiments are constrained to the requirements of NSTS21000-IDD-MDK, which details the interface between the Space Shuttle and the payload. Some of the applicable constraints during operation of the GGSEM on middeck are reproduced in Table 3. Other design constraints are applicable throughout the duration of the Space Shuttle mission, from ground testing at the integration site, to hardware retrieval and packing at the de-integration site. These requirements are given in a variety of documents including:

- NSTS21000-IDD-MDK for loads, environments, interface and installation requirements;
- KHB1700.7 for ground safety during testing, handling, and integration;
- NSTS1700.7 for flight safety from launch to landing;
- NTST21000-SIP-MDK for plans, schedules, and functional agreements.

Table 3 - Operational Constraints of Middeck Experiments Extracted From NSTS21000-IDD-MDK.

Volume:	Each locker or modular unit is 0.056 m^3 (2 ft^3). More than one adjoining module may be used.
Weight:	60 lbs/single adaptor plate with cg 10 in. from attachment face.
Power:	28 Vdc (to 10 amp) 115 Vac (400 Hz, 3 phase: to 3 amp per phase). Approximately 260 W/bus
Automation:	Experiment functions in semi-automated to automated mode. Limited crew involvement is available.
Heat Dissipation:	Active above 60W.
Data Recording:	Internal to experiment, recovered after landing.
Safety:	In accordance with NSTS1700.7 and KHB1700.7
Venting:	Vacuum available throughout the galley vent line.
Installation:	Payload must be attached by approved adaptor plates, or installed in standard lockers.
Pressure:	Ambient, 9.7 - 14.9 psi
Temperature:	Ambient, 18.3 - 26.7°C

2.3 System & Subsystem Requirements

The GGSEM requirements system level requirements, and methods of meeting those requirements are shown in Table 4. Technical feasibility of several GGSF subsystem functions will be demonstrated in the GGSEM. In addition to conforming to the platform requirements and constraints described in section 2.2, the subsystem requirements listed in Table 5 ensure that the GGSEM will provide a compatible test platform to verify GGSF subsystem operations.

Table 4 - GGSEM System Level Requirements and Methods of Accomplishment.

Requirement	Method of Accomplishment
Generate and deploy particles with zero velocity	Provide test cell subsystem deployment mechanism
"Zero-gravity" condition	Provide structure subsystem for experiment installation and operation in the Space Shuttle Orbiter middeck
Provide varying pressures and atmospheres	Provide gas handling subsystem with pre-determined pressures and gas mixtures
Record events, pressure, and temperature	Provide optical subsystem including camera, lighting, and data recording

Table 5 - GGSEM Middeck Experiment and Laboratory Breadboard Functional Requirements.

Subsystem	Function	Middeck	Breadboard
Chamber	Volume	Cylindrical, ~12,000 cc	Cylinder, volume~6 liters
	Environment	Room temp., ~0.1 to 1.0 bar	STP
	Chamber cleaning & physical access	Removable lid (Not opened on middeck); middeck vent line is used for gross cleanup of chamber; universal chamber mount used to test cleaning devices.	Not a sealed container. Can be manually cleaned.
	Diagnostics, observation ports, and interfaces	One large window in lid for observations, video and transmission measurements; small window ports on opposite end for illumination and transmission measurements; port on side-wall for sample generator mounting; side-wall port for scattering experiment light source; gas fill and vent line; universal (internal) chamber mount for future applications.	Clear acrylic chamber with sample introduction port.
Sample Generation	Generate and introduce sample into chamber	Interchangeable sample generator (only one carried on-board); e.g., solid particle dispenser (designed under the breadboard activity), liquid aerosol generator, single particle device, UV source for photolysis	Solid particle dispersion apparatus
Diagnostics	Light scattering, cloud characterization & optical properties	Extinction measurements; angular, forward, & spectral scattering; filter wheel for wavelength selection of broad-spectrum (white light) source in the Si response range of ~300 to 1,000 nm; and laser source (HeNe or diode).	Forward scattering and extinction, HeNe laser, Si detector
	Imaging	Video with 30 fps frame rate & recorder with white illumination source; Spatial resolution TBD	Video and recorder
	Environment monitor	Temperature and pressure; other devices (e.g. humidity, gas composition) can be installed on gas handling port.	None
	g-level	SAMS may be available	None
Sample collection & storage	Collect samples and store for later off-line analysis	Share universal chamber mounts where filters & probes can be installed; or samples collected on a filter during venting of chamber atmosphere; interchangeable filter is stored for post-flight sample analysis.	Samples collected on a slide during settling of particles
Gas handling	Environment for experiment	Each tank (up to 5) contains one chamber fill to a desired pressure with premixed gas composition	Room air
Waste management	Particle and gas clean up to Space Shuttle requirements	Particles collected on filter. Gas passes through scrubber before entering vent line.	None required
Structure	Integrate subsystems and interface with platform	Structure interfaces with standard middeck double locker	Laboratory tabletop
Power	Condition/distribute power	Power conditioning to operate various instruments	110 Vac
Electronics	Experiment control, data acquisition & storage	PC based single-board micro-computer; A/D, D/A board for data input and control; mass storage medium	P/C based data acquisition system and timing circuit

3 KEY SCIENCE AND ENGINEERING TRADES IN MODIFICATION OF DCE

The application of the design from the DCE will result in significant cost and schedule savings, and therefore reduce project risk for the GGSEM. The level of the design for the DCE is PDR for flight system design, and fabrication and test for components and subsystems outside of the structure and gas handling subsystems. For conversion to the GGSEM, the following tasks are anticipated:

- Modify design concept to satisfy GGSEM specific experiment requirements;
- Upgrade design to accommodate new NHB1700.7B safety requirements document (only minor, if any, modifications are required here);
- Modify controller to reflect current technology;
- Resubmit Phase 0 and Phase I Hazards Analyses with updates to reflect modified design, updated electronics, and other changes to meet the requirements of NHB1700.7B (DCE was designed to revision A);
- Complete system design to CDR level;
- Perform phase II and III safety reviews;
- Complete and obtain approvals for materials usage data lists;
- Prepare interface documentation and training documents in support of the Payload Integration Plan (PIP);
- Fab, test, and build flight hardware and integration model;

4 GGSEM DESIGN CONCEPT

The GGSEM concept utilizes the existing DCE experiment apparatus design to conduct gas-grain experiments. The existing design is modified to replace obsolete subsystems, provide the required GGSEM functions, and remove unnecessary DCE functions. The advantages to this approach are that the DCE is designed through preliminary-design, including detailed analyses and safety reviews, Engineering hardware has been demonstrated, and the apparatus already has most of the required functions, including:

- a chamber with ports;
- Middeck interfaces;
- diagnostics;
- gas mixture bottles;
- imaging/photography;
- sample generation (droplets);
- electrical and electronics.

4.1 Experiment Module Description

The GGSEM concept is shown in Figure 2. This concept shows a structure which fits into a standard middeck double locker. The structure integrates a test chamber, light sources, cameras, and other optical components on an optical bench. The non-optical components are integrated separately from the bench in order to isolate vibration and thermal loads.

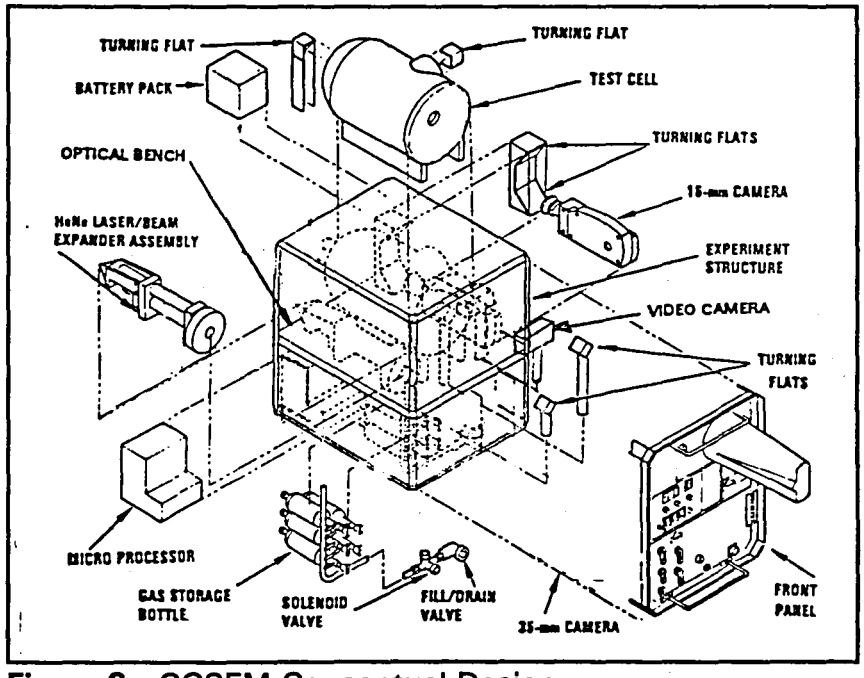

Figure 2 - GGSEM Conceptual Design.

A front panel provides control of the experiment through switches and valves. It also provides the capability of handling push and kick loads while protecting more critical hardware. A viewing port is provided in the front panel, which is aligned to a large port in the test chamber. This allows the operator to monitor and interact with the experiment.

Other features of the front panel include access to storage in the module, fire extinguisher access, handles for installation and removal of the module, and interfaces to the Space Shuttle-provided power and vent lines. Table 6 lists the components, their purposes, and how they are combined into subsystems.

Table 6 - GGSEM Subsystem Components and Functions.

Subsystem	Major Components/subassemblies	Primary Function
Test Cell Subsystem	•Test chamber	containment of samples in controlled environment
	•Sample generation	produce samples to be tested
	•Pressure transducer	monitor chamber pressure
	•Temperature transducer	monitor chamber environment temperature
Gas Handling Subsystem	•Supply bottles	store gases for chamber environment, one chamber fill per bottle
	•Manual fill valves and solenoid valve	transfer stored gas into test chamber, and prevent over-pressure (solenoid valve closes if pressure transducer measures over-pressure)
	•Solenoid evacuation valve	allow chamber evacuation as required
	•Fill/drain vacuum valve	provide interface to Space Shuttle vacuum line
Optical Subsystem	•16-mm camera	Record high resolution data
	•Video camera	provide lower resolution, but larger quantities of data
	•Collimated light source	provide light for diagnostics to be tested, and for cameras
	•Optical components	transfers optical data around compact experiment volume
Structure Subsystem	•Frame	integrates subsystems and interfaces with Orbiter
	•Optical bench	mounts all optical components

4.2 Design Drivers

The GGSEM utilizes an existing design which is a design driver in that it defines the fixed parameters such as chamber volume, number of gas fill bottles, and space available for storage and experiment-specific hardware.

An additional driver is the use of the Space Shuttle middeck, which constrains power usage, cooling, mass, center-of-gravity, operator availability, and other Space Shuttle resource availability (power, vacuum, etc).

These constraints not only affect the design of the hardware to be tested on the GGSEM, but also limit the science that can be achieved. For example, there are restrictions on:

- extensive continuous power - all middeck experiments must share middeck power resources;
- extended undisturbed (vibration or other acceleration loads) operation - extreme quite requirements are limited due to limitations placed on astronaut motion and attitude thruster operation;
- hard vacuum - limited to vacuum available through the middeck vent line.

4.3 Design Layout

Figure 2 shows a GGSEM concept. Subsystem and component concepts were detailed in the GGSEM Conceptual Design Review at NASA Ames Research Center in April, 1992. These concepts are extracted from the DCE design.

4.4 Development Plan

The GGSEM project is intended to utilize technologies, designs, and supporting paperwork from past projects to the extent possible. This is the most cost effective method of providing this device on the planned schedule of an October, 1995 launch date.

4.4.1 Development Schedule - A summary of the development schedule is given in Figure 3. The schedule for the GGSEM project begins with determining the type of tests to be performed on the Space Shuttle, and breadboarding apparatuses that could be used to perform that test. This task would begin in December of 1992, and run concurrent with the preparation of a Statement of Work for development of the GGSEM hardware. The schedule is intended to start flight hardware development with a contract award in early 1994, and support a launch date of October, 1995. This is an extremely ambitious schedule consistent with the new NASA theme of faster, cheaper, and better. It dictates the extensive use of existing technologies, simple designs, minimal hazards and controls, and highly experienced personnel. The DCE and it's design team supports these requirements. The particle generator is the high risk item in the schedule. The DCE incorporated a liquid droplet generator from which certain technologies may apply.

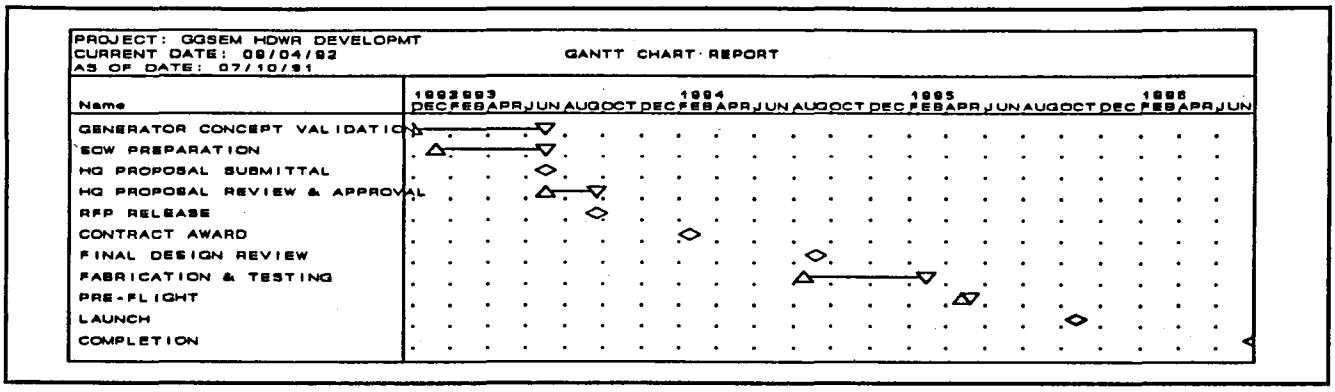

Figure 3. GGSEM development milestones.

4.4.2 Work Breakdown Structure and Task Descriptions - The GGSEM project is divided into three major Work Breakdown Structure (WBS) categories. WBS 1 is for the hardware development such as the design, fabrication, assembly, and test related functions. The second category, WBS 2, is the Space Shuttle Program integration functions required by the Standard Integration Plan for Middeck Experiments (NSTS21000-SIP-MD) such as safety, interface control, crew training, and flight support documentation. WBS 3 are project management tasks which cross the entire project, including the project manager, and the cost and schedule controller. These tasks exchange information required to perform the functions of each.

1 HARDWARE DEVELOPMENT - This WBS category is the hardware development related tasks, starting with a concept, and ending with hardware delivery. The work in this category feeds many of the tasks in the Payload Integration category, and is nurtured from that category as well. The tasks defined here would take place with any hardware development project, whereas the tasks in WBS 2 are specific to the platform for which the hardware is destined.

1A GENERATOR CONCEPT VALIDATION - This task is to develop a concept for a flight device to generate particles. This breadboard generator (excluding its supporting analysis hardware) will be compatible in size and weight with a middeck style experiment to minimize the development and testing required in later phases of the project. The baseline includes a liquid and a solid particle generator.

1A1 PREPARE TEST PLAN - The determination of a particle type to be generated, a viable concept to perform the generation, and the method of verifying and validating the concept is developed during this task.

1A2 DEVELOP BREADBOARDS - The design, review of the design, fabrication, and assembly of the breadboard.

1A3 LAB TEST BREADBOARDS - Perform a variety of performance tests, under varying conditions, modifying applicable parameters, change hardware as required to optimize performance in the lab.

1A4 Micro-G TEST BREADBOARDS - Provide breadboard setup to NASA for micro-g testing in (most likely) the KC-135, or other equivalent platform. The labor involved is support to NASA.

1B RFP PREPARATION - These are NASA tasks to generate the RFP for acquisition of the middeck flight experiment. No payload developer support is expected in these tasks.

1B1 SOW PREPARATION
1B2 HQ PROPOSAL SUBMITTAL
1B3 HQ PROPOSAL REVIEW & APPROVAL
1B4 RFP RELEASE
1B5 PROPOSAL TURNAROUND
1B6 PROPOSAL REVIEW
1B7 CONTRACTING OFFICE REVIEW
1B8 CONTRACT AWARD

1C DESIGN PHASE - This phase of the project includes engineering (design and analysis) tasks such as mechanical, electrical, software, manufacturing, materials and processes, and quality assurance (reliability, configuration management, etc), interface control, design and development models, technical reviews, reports, etc.

1C1 CONCEPT DESIGN - Develop a concept which is based on the Droplet Combustion Experiment and makes the modifications necessary to accommodate the requirements of the GGSEM (for example, add/move ports on the test chamber, add/replace diagnostic devices, etc.).

1C2 CONCEPT REVIEW - Review concept with NASA and support scientists.

1C3 PRELIMINARY DESIGN - Prepare mechanical layouts and electrical diagrams that reflect the concept modifications. These layouts and diagram are detailed enough to support preliminary structural, thermal, reliability, and safety analyses, which are also part of this task. Prepare a preliminary materials list, parts list, and drawing list. Identify any long acquisition time hardware.

1C4 PRELIMINARY DESIGN REVIEW - Review preliminary design with NASA and support scientists. Approve long lead hardware for acquisition.

1C5 FINAL DESIGN - Prepare detailed mechanical and electrical drawings based on the preliminary design. Incorporate review produced changes. Perform structural, thermal, reliability, and safety analyses. Update the materials list, parts list, and drawing list.

1C6 FINAL DESIGN REVIEW - Review final design with NASA and support scientists.

1D FABRICATION & TESTING - This is the fab, assembly, and test of the proto-flight unit, including both the test bed, and the generator modifications from the breadboard phase.

1D1 PURCHASE REQUISITIONS - Preparation of purchase requisitions, approval, competitive bid and vendor selection, and release of purchase orders are included in this task.

1D2 FABRICATION/PROCUREMENT - This is the time and resources required for in-house fabrication and outside procurement (both fabricated and catalog items).

1D3 ASSEMBLY - Assembly of the experiment hardware and software as a unit is performed during this task. Due to the small and integrated nature of this unit, only the particle generator and the electronics are assembled as subsystems, and the experiment is assembled as one system.

1D4 ENGINEERING EVALUATION TESTS - Due to the experimental nature of this unit, engineering evaluation of the experiment following assembly is utilized to fine tune the operation and effectiveness of the unit. Any hardware changes are reflected in the drawings.

1D5 PERFORMANCE VERIFICATION TESTS - These are the formal tests which verify compliance with the Statement of Work, Safety and Reliability requirements, and any additional engineering requirements. These tests include operation, modal testing, vibration and shock tests, minor thermal testing, etc.

1D6 CLEANING - The unit must be particle free to meet the manned module requirements. This task cleans the unit and prepares it for transfer to the off-gassing test facility.

1D7 OFFGASSING TESTING - This is a purchased service (from NASA), and is required for middeck experiments.

1D8 PACKAGE FOR SHIPPING/STORAGE - The experiment is bagged, inserted into a sealed, purged shipping container where it may be stored until use, and shipped to KSC for integration to the orbiter. This is the concluding milestone for hardware development.

1E TRAINING MODEL - A training model is required for training the mission specialists on usage of the experiment. It is representative in size and weight for use in the NASA integration model used during mission planning. The functionality of the training model is very limited, in that only buttons and knobs on the operating panel will be "real".

1E1 TRAINING MODEL DESIGN - This task is the engineering and drafting required to fabricate the training model.

1E2 TRAINING MODEL FABRICATION - In-house and purchased parts and services for fabrication of the model.

1E3 TRAINING MODEL ASSEMBLY & TEST - Assembly of the parts into a model, and verification of the responses to the actions of pushing buttons and turning knobs.

1F QUALITY ASSURANCE - These are tasks which assure the quality of the hardware is consistent with design requirements.

1F1 RELIABILITY PROGRAM - The reliability engineer prepares a reliability plan, performs the appropriate analyses, identifies weaknesses in the design or procedures, and verifies concurrence with the final hardware. This engineer interfaces with other design functions to eliminate low reliability points early in the design phase, and inputs reliability results to the safety engineer (WBS 2D). The reliability requirements are ultimately reflected in the hardware drawings.

1F2 QUALITY ASSURANCE PROGRAM - The quality engineer prepares a quality plan, and verifies compliance with the project requirements. These requirements are specified on drawings and reflect the requirements if reliability, safety, and other design functions.

1F3 CONFIGURATION MANAGEMENT - The configuration manager controls project documentation that affects final hardware configuration, such as plans, procedures and drawings. Hardware is not fabricated without drawings that have been released into configuration management control. This release requires approval signatures from the responsible design engineer, who assures proper review by materials, processes, structural, reliability, and safety engineering functions.

2 PAYLOAD INTEGRATION - This WBS category is tasks specifically associated with the integration of the experiment into the Space Shuttle, and identified as such in the Standard Integration Plan for Middeck-Type Payload (NSTS21000-SIP-MD).

2A SPACE SHUTTLE PROGRAM MILESTONE REVIEWS - These reviews are required for each Space Shuttle mission, and are included here for reference. Some reviews may require support by the payload developer by the Mission Manager, and may be in the form of data input, telecon, or designated representative. Due to the relative simplicity of this experiment, the assumption for this plan is no significant support is required for these reviews.

2A1 Cargo Integration Review (CIR)
2A2 Flight Certification Review (FCR)/Payload Readiness Review (PRR)
2A3 Ground Operations Review (GOR)
2A4 Flight Operations Review (FOR)
2A5 Flight Readiness Review (FRR)
2A6 Payload Management Countdown Review (PMCR)

2B INTERFACE DOCUMENTATION - These tasks prepare, support, and negotiate interface agreements between the payload developer and the Mission Manager, for: mechanical (structural, thermal, fluid), and electrical (power, telemetry, data) interfaces; installation procedures and schedules; operating procedures and schedules; safety, EMI/EMC, and contamination control requirements; and payload removal after flight.

2B1 PAYLOAD INTEGRATION PLAN - This plan is prepared from the Standard PIP for middeck experiments (NSTS21000-SIP-MD) by the Mission Manager with support in the form of input and negotiations from the payload developer.

2B2 PAYLOAD INTERFACE CONTROL DOCUMENT - This task prepares a payload unique ICD by the payload developer, and includes drawings and diagrams for the complete structural and electrical interfaces, describing physical requirements (mounting points, connector types and locations, protruding volumes, weight and center of gravity).

2C PIP ANNEXES - These Annexes are required for standard middeck experiments. They are generally prepared by the Mission Manager with support from the payload developer.

2C1 A-1 PAYLOAD DATA PACKAGE - This annex may be combined with annex 2, but requires the provision of the flight design data to the Mission Manager for review for compliance with mission requirements.

2C2 A-2 FLIGHT PLANNING - The payload developer must prepare, supply, and negotiate the payload crew activities to support this document.

2C3 A-3 FLIGHT OPERATIONS - This document requires a payload operating procedure which is developed and verified by the payload developer.

2C4 A-6 ORBITER CREW COMPARTMENT - This document specifies resources of the crew compartment. The payload developer inputs weight, c.g., configuration drawings, and unique display and control interfaces.

2C5 A-7 CREW TRAINING PLAN - Training requirements will be decided by the Mission Manager based on Annex 2 & 3 input. The plan will require concurrence on tasks and scheduling by the payload developer.

2C6 A-8 LAUNCH SITE SUPPORT PLAN - This plan details the requirements for payload unique support to be provided by the launch site including nominal and contingency requirements for manpower, space, clean-rooms, material handling, etc, for both pre-launch and post landing.

2C7 A-9 PAYLOAD VERIFICATION REQUIREMENTS- This document is prepared by the payload developer in accordance with NSTS 14046. It provides the methods of verifying all payload interfaces, and describes interfaces that cannot be verified.

2D FLIGHT SAFETY - The flight safety is defined by NHB1700.7B, which includes analyses and reviews to verify compliance with the safety requirements. A Safety Engineer is responsible for defining safety requirements specific to this payload, defining verification methods, and verifying the hardware for conformance (inspecting drawings, analysis reports, inspection reports, etc). This engineer interfaces with other engineering functions to help eliminate hazardous conditions beginning in the earliest phases of the project.

2D1 FLIGHT HAZARD ANALYSES - This task is the preparation of the hazard analyses by safety engineers with support from other engineering disciplines.

2D1A PHASE 0 FLIGHT HAZARD ANALYSIS - Conceptual design
2D1B PHASE 1 FLIGHT HAZARD ANALYSIS - Preliminary design
2D1C PHASE 2 FLIGHT HAZARD ANALYSIS - Final design
2D1D PHASE 3 FLIGHT HAZARD ANALYSIS - As built

2D2 FLIGHT SAFETY REVIEWS - These reviews are presentation of the analyses to the NASA Safety Review Board, to obtain design concurrence.

2D2A PHASE 0 FLIGHT SAFETY REVIEW - Conceptual design

2D2B PHASE 1 FLIGHT SAFETY REVIEW - Preliminary design
2D2C PHASE 2 FLIGHT SAFETY REVIEW - Final design
2D2D PHASE 3 FLIGHT SAFETY REVIEW - As built

2E GROUND SAFETY - The analysis for ground safety is based on the requirements of KHB1700.7A. These tasks are to assure safety during ground operations at the integration site. For a middeck payload with few ground and integration operations, or inherent hazards, these series of tasks are minimal.

2E1 GROUND HAZARD ANALYSES - For this experiment, much of the data can be utilized from the flight safety packages, simplifying these efforts.

2E1A PHASE 0 GROUND HAZARD ANALYSIS - Conceptual design
2E1B PHASE 1 GROUND HAZARD ANALYSIS - Preliminary design
2E1C PHASE 2 GROUND HAZARD ANALYSIS - Final design
2E1D PHASE 3 GROUND HAZARD ANALYSIS - As built

2E2 GROUND SAFETY REVIEWS - These reviews are held at the integration facility to review the analyses and designs.

2E2A PHASE 0 GROUND SAFETY REVIEW - Conceptual design
2E2B PHASE 1 GROUND SAFETY REVIEW - Preliminary design
2E2C PHASE 2 GROUND SAFETY REVIEW - Final design
2E2D PHASE 3 GROUND SAFETY REVIEW - As built

2F HARDWARE OPERATIONS - The tasks listed here "pick up" where the WBS 1 left off, i.e. delivery of the finished experiment to the integration facility.

2F1 PRE-FLIGHT

2F1A DELIVERY TO THE PAYLOAD PROCESSING FACILITY - This is the receiving location for payloads that will be integrated to shuttle.

2F1B PAYLOAD INSPECTION - This is the task to verify that the payload has arrived in its proper configuration. This inspection is performed by the payload developer, as well as the facility manager.

2F1C PAYLOAD OPERATION VERIFICATION - The payload developer will perform any testing required to verify proper operation prior to shuttle integration.

2F1D INTEGRATION TO THE ORBITER - This task is solely performed by the integration facility.

2F2 FLIGHT OPERATIONS

2F2A LAUNCH - This task is solely performed by the launch facility.

2F2B ON-BOARD EXPERIMENTS - This task is solely performed by the flight crew.

2F2C GROUND SUPPORT OPERATIONS - If the need for real time interaction with the experimenter (flight crew) is identified, the payload developer and mission scientists will be available to provide required services.

2F2D LANDING - This task is solely performed by the flight crew.

2F3 POST-FLIGHT OPERATIONS

2F3A DATA RETRIEVAL - The removal of data from the orbiter is performed by the de-integration facility, and distribution of the data is per the Annex 8 agreement. Data transmitted to the Payload Operations Control Center (POCC) is available immediately.

2F3B HARDWARE RETRIEVAL - The removal of hardware from the orbiter is performed by the de-integration facility, and distribution of the hardware is per the Annex 8 agreement.

2F3C PACKAGING - Hardware is re-packed into the shipping container.

2F3D SHIP TO STORAGE LOCATION - For storage until next use.

2F3E DATA PROCESSING & ANALYSIS - Distribution, processing, and analysis of data by the science community.

2F3F FINAL REPORT - Preparation of the final report by the science community.

2G CREW TRAINING - This task is performed by the payload developer in accordance with the PIP and Annex 7. The standard requirements for this task include preparation of a training facility, training presentation, and any training aids that are

necessary. This is typically an 8 hour training session for the flight crew and mission planners.

3 PROJECT MANAGEMENT - These tasks report directly to the project manager WBS and span their activities across the project as overseers, to assure the entire project stays within the bounds of requirements, finances, and schedules.

3A PROJECT MANAGER - This is the authority on the project, and includes the manager, assistants as required, and the cost/schedule controller.

3B PROJECT COMPLETION - End of the entire project.

4.4.3 Cost Estimate - The labor estimates for the tasks described in the WBS include all project management, technician and engineering functions (mechanical, electrical, software, safety, reliability, and drafting). The approximate cost of the entire project is estimated at $5.9M including all labor, supervisor and secretarial burdens, purchases, overhead, general and administrative (G&A), and 10% fee.

5 BREADBOARD DEVELOPMENT

A laboratory breadboard was developed to support GGSF experiment and hardware definitions. An examination of the GGSF Science and Technical requirements revealed a need to address dry particle generation techniques. Solid particle dispersion is to operate with a range of five orders of magnitude in size, and eight orders of magnitude in concentration. No commercial device was identified that could fulfill the unique S&T requirements of dispensing the wide variety of materials, sizes, and concentrations of monodispersed particles in a low-gravity environment. Table 7 and Figure 4 summarizes the dry particle S&T requirements that are described in the GGSF Final Report, NASA CR177606.

Table 7 - Dry Powder Properties Extracted From NASA CR177606.

Experiment No.	Materials	Size (μm)	Number Density (No./cc)	Pressure Range (bar)	Temperature Range, (K)
1	Silicate grain	~1	TBD	10^{-3} - 10^{-5}	150 - 500
3*	Salt	0.01 - 1	1 - 10^{4}	0.1 - 1.0	273 - 303
5	Quartz;basalt	0.1 - 1,000	1 - 10^{8}	10^{-4} - 1	221 - 366
8	Carbon	0.1	10^{5}	10^{-4} - 1(10 desired)	233 - 293
13	Olivine;pyroxene	1	10^{5}	0 - 1	77 - 300
15*	Al_2O_3; TiO_2; MgO	0.01 - 0.05	10^{5} - 10^{8}	10^{-6} - 10^{-3}	500 - 1200
17*	Carbon grain (amorphous, hydrated, graphite); silicates	0.05 - 0.1	10^{10}	10^{-10} - 10^{-9}	10 - 300
18	Microspheres (TBD)	0.01 - 20	10 - 10^{5}	1	293 - 373

* Experiments where particles are generated by means other than deagglomeration.

Numerous commercial particle dispensing techniques were investigated to identify those that could dispense a cloud of deagglomerated particles by simple, small, reliable methods, with minimal requirements for carrier fluids that could perturb the experiment. Of these, a blast deagglomerator technique was selected, as it appeared to be the most versatile of the candidates.

To verify the adequacy of the particle generator, a series of performance tests were carried out using representative particle samples of 2.1 and 10.2 μm glass spheres, and 5 to 10 μm Arizona test dust. Limited characterization with these samples was performed as a function of carrier gas pressure and aerodynamic slit width. These tests indicated predictable and repeatable performance of the particle generator concept, though particle concentrations were not high enough to meet the entire range of GGSF S&T requirements.

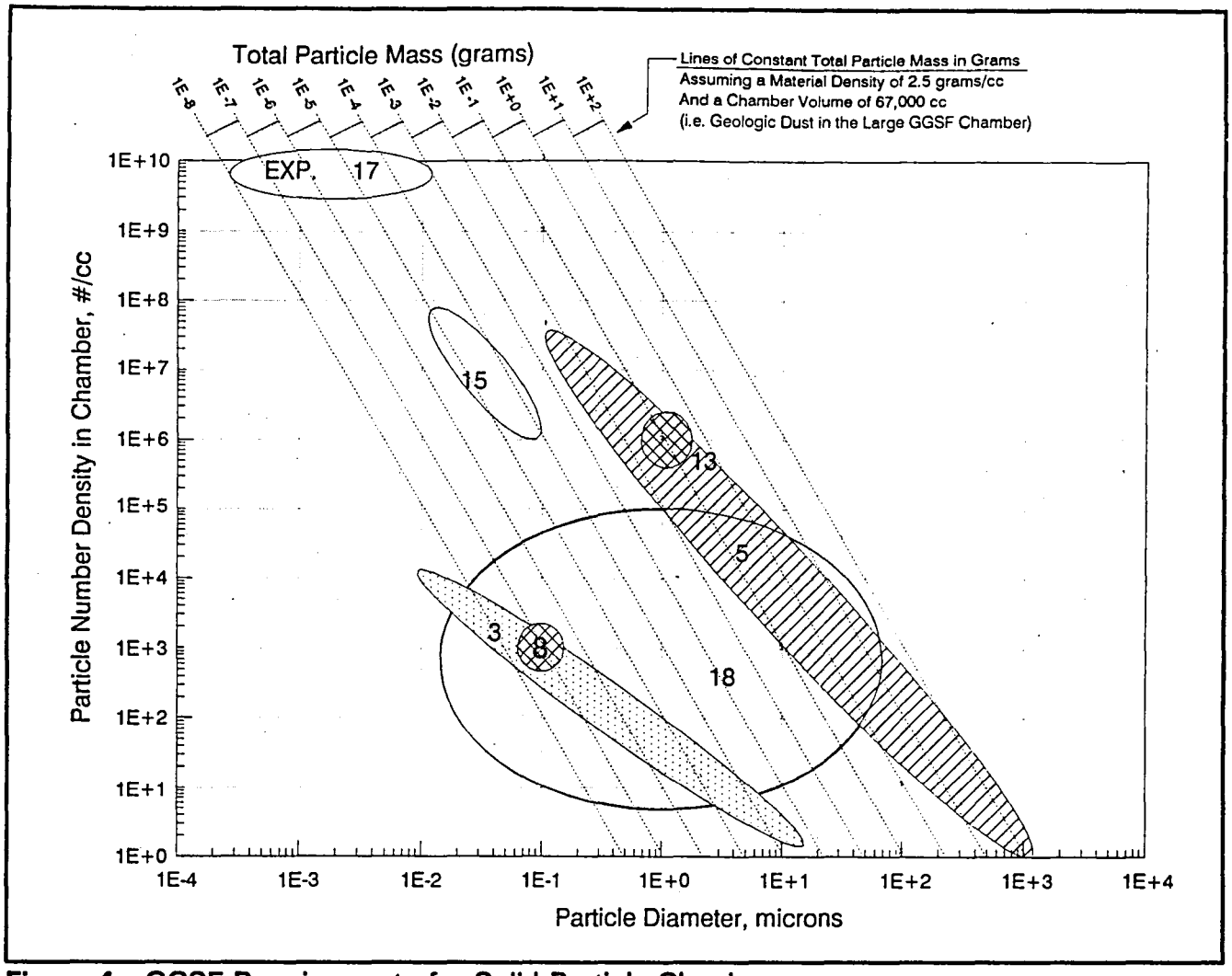

Figure 4 - GGSF Requirements for Solid Particle Clouds.

To determine performance of the particle generator, several diagnostic techniques were utilized. The primary method involved collection of the dispensed particles on a filter, and subsequent microscopic determination of the percentage of mono-particles. A laser beam passing in front of the particle generator output was monitored for extinction as another diagnostic, since dilution of the particles was found to be related to the percentage of mono-particles. A third diagnostic was employed for a limited time in order to qualitatively monitor the cloud motion in the test cell after dispensing. This was a sheet of laser light optically viewed.

The GGSF breadboard can be used to test concepts for sample generation, collection, and manipulation. Cleaning techniques for the chamber windows and walls can also be tested, as the small particles can be sprayed on these surfaces with the deagglomerator. These future studies will help answer science and technology questions and reduce risks associated with the GGSF concepts.

A detailed report on the breadboard development is included in Appendix A. Which details the development requirements, history, hardware, and characterization tests. This section provides an overview of the results of the breadboard development task. The goals and objectives of the breadboard are discussed in section 5.1. The hardware development is discussed in section 5.2, which includes the trades, parameters, and hardware descriptions. Sections 5.3 and 5.4 respectively present the approach to the test plan, and the results of the tests. As the demonstration of the particle generator breadboard was limited during this activity, section 5.5 recommends the further work that would extend our understanding of the breadboard operation and repeatability. To predict the performance of a particle generator with the wide variety of particle types, sizes, and quantities that could be required during the GGSF mission, extensive characterization is required. Section 5.6 discusses how to fully define the performance of this device for the GGSF applications.

5.1 Development Objectives

The goal in developing and building a GGSF laboratory breadboard system was to demonstrate GGSF particle generation techniques and concepts, and perform particle collection and analysis measurements. The primary objectives in developing the GGSF laboratory particle generator breadboard included:

- identification of candidate techniques for storing, deagglomerating, and dispensing dry solid particles that cover a broad range of the GGSF strawman experiment science and technical requirements;
- develop and test laboratory breadboard components that demonstrate the feasibility of the selected particle generation technique to meet a representative subset of the science and technical requirements, including parameters of particle size, type, degree of deagglomeration, total mass, etc.;
- demonstrate the potential for gravity-independent operation of the selected technique;
- qualitatively characterize the flow field (velocity as a function of time in three dimensions) of the dust cloud generated in the test chamber;
- identify configurations and technical issues uncovered during the development and testing of the laboratory breadboard system;
- identify further future development program efforts necessary to fully characterize the selected particle generation device;
- maintain a flexible breadboard configuration allowing for utilization in facilities other than a ground-based laboratory.

5.2 Key Breadboard Trades, Parameters, and Hardware Configurations

The breadboard was designed to fulfill the objectives by allocating requirements to the three subsystems. A particle generator subsystem provides the sample to be generated. The chamber subsystem provides a pseudo-quiescent volume for the sample to be contained within and measurements to be taken. The breadboard was limited to room temperature and pressure, and no attempt was made to control either pressure or temperature during this study although as Table 7 indicates, the experiment requirements span broad ranges of pressure and temperature. The diagnostics subsystem provides the ability to quantify the particle properties.

The laboratory breadboard subsystems and requirements are described in Table 8. The breadboard is flexible in design and application, allowing for the design of many types of experiments, and utilization in facilities other than the ground-based laboratory.

Table 8 - Summary of Breadboard Subsystems.

Subsystem	Breadboard Requirements	Breadboard Description
Particle Generator	• Dispense dry spherical particles, and dust particles, in the 1-10 μm size range, as a cloud of single particles • Provide adequate containment of particles prior to dispensing • Minimize carrier gas for operation • Adaptable to space-based operation (size, weight, robustness, gravity-independent)	• Conical aerodynamic blast-deagglomerator for separating and dispersing particles in a cloud • Cartridge-like storage with pre-mixing gas jets
Chamber	• Approximate volume of GGSF test chamber • Allow visual access for monitoring particle action • Provide ports for particle introduction & collection	Plexiglass cylinder - 60 x 60 cm
Diagnostics	• Monitor particle density at nozzle • Collect particles and perform microscopic analysis of deagglomeration effectiveness • Photograph particles through microscope for qualitative data verification • Obtain representative SEM photos of data • Record operations for performance analysis	• Video (RS-170)* • Laser light sheet illumination* • Angular scattering of laser light* • Extinction • Silicon photodiode • Off-line* - Polaroid Camera - microscope - SEM

* not included in delivered breadboard hardware

The breadboard is schematically represented in Figure 5. A photograph of the laboratory breadboard with the particle generator, test chamber, laser and detector diagnostics, and valve controller is shown in Figure 6. A complete parts list can be found in section 7 of Appendix A.

5.2.1 Particle Generator - The majority of the breadboard effort was devoted to development and characterization of the particle generator. A representative particle generation

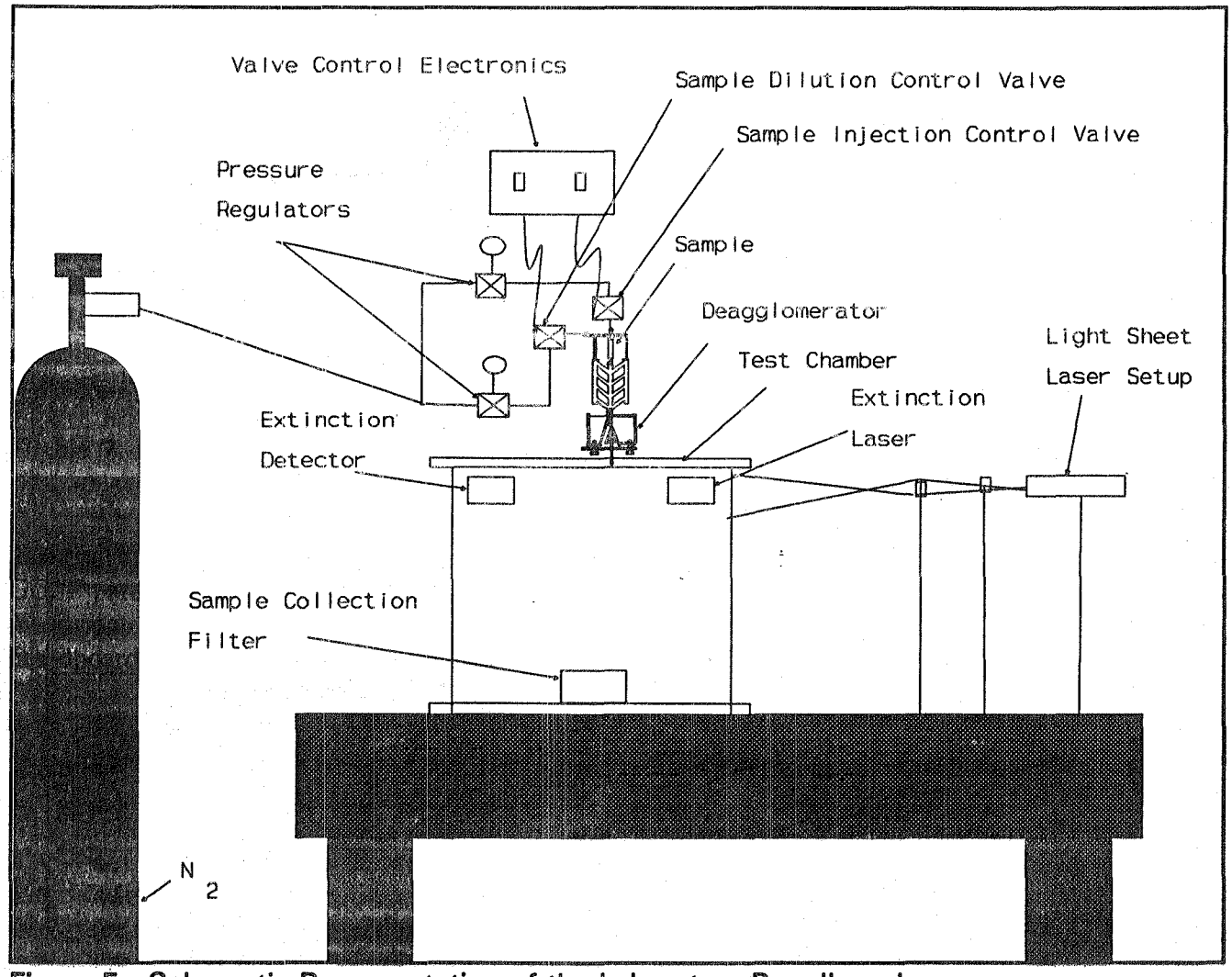

Figure 5 - Schematic Representation of the Laboratory Breadboard.

technique was selected and developed to address several GGSF science requirements. This generator delivers solid particles into the test chamber as a cloud of singlets. Its operation must be for a low-gravity environment, but it must also work in a one-g laboratory. A review of the commercial and laboratory systems revealed that most methods rely on gravity, do not assure complete agglomeration, or use extensive amounts of carrier gas. Some methods only work for large particles (e.g., millimeter size).

Section 4.2 of NASA CR177606, the GGSF Final Report, discussed some of the techniques, which include fluidized bed, aspiration feeder, and auger feeder methods. The selected technology was an aerodynamic deagglomerator, like that used in a micromerograph (described in section 1.7 of Appendix A). This method appeared to have the highest potential for meeting GGSF requirements for a broad range of sizes and quantities, as well as adaptability to low-gravity operation. This deagglomerator functions by shearing particles apart in a gas stream that passes through an

expanding passage. Several modifications were made to the technology to:

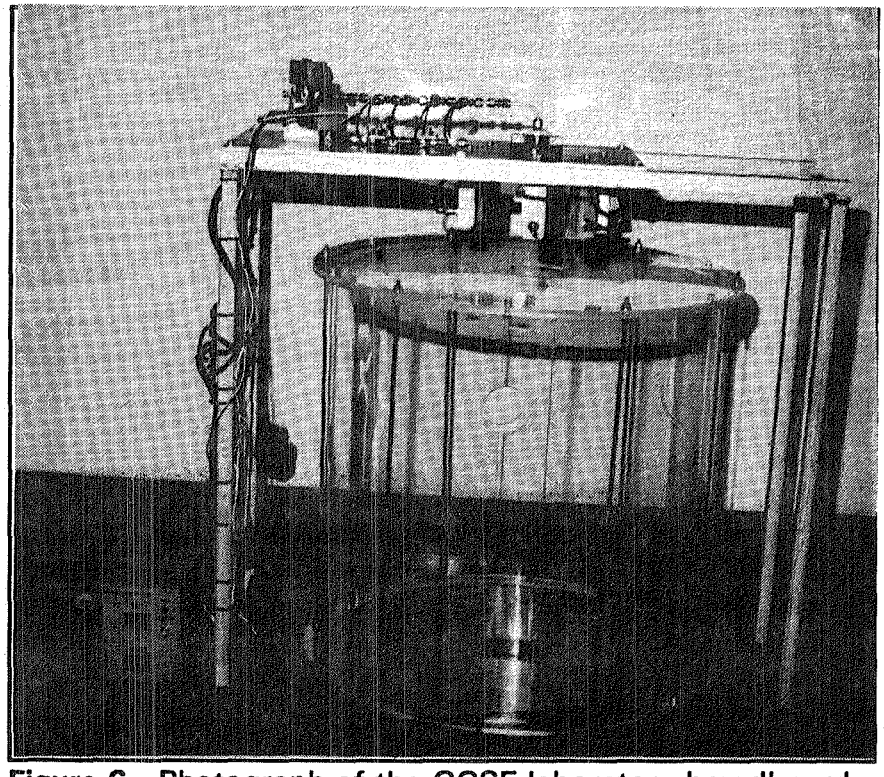

Figure 6 - Photograph of the GGSF laboratory breadboard.

- improve the deagglomeration performance - though no information could be found that quantified performance of the micromerograph deagglomerator, our initial tests indicated that performance was limited to about 65% deagglomeration. The modifications allowed flexibility to vary the parameters that affect the deagglomeration performance, including sample feed rate, sample dilution in the carrier gas, and carrier gas pressure.

- improve sample storage - increasing the quantity of sample material that can be dispersed is required to meet the GGSF science and technical requirements. The micromerograph dispenses approximately 0.05 cm^3, which was increase to .20 cm^3 in the GGSF breadboard. Additionally, decoupling of the storage technique from gravity was required.

- minimize the carrier gas consumption - the GGSF chamber environment is controlled, and introduction of carrier gas must be minimized to avoid contamination of the environment.

The characteristics of the particle generator are described in Table 9. A graphical representation of the particle generator is shown in Figure 7, and a photograph of it is shown in Figure 8.

The blast deagglomerator performance is affected by three distinct, but not independent, operational parameters: storage of particles prior to dispensing, dilution of particles with carrier gas prior to introduction into the deagglomerator, and deagglomeration, or separating of particles into singlets.

5.2.1.1 Sample Storage: Storage of the sample in the particle generator prior to dispersion is an issue. The selected method must:

- be adaptable to the range of particle quantities and sizes required;

Table 9 - Particle Generator Characteristics.

Criteria	Characteristic
Type of particles dispensed	Designed for dry solids, 1-100 μm diameter, may work for broader range of particle sizes Tested using: • Glass micro-spheres, 10.2 μm diameter • Glass micro-spheres, 2.1 μm diameter • Arizona test dust, graded, 5-10 μm diameter
Volume of stored particles	0.08 cc tested with complete success; up to 6.4 cc tested with promising results after more development.
Method of particle ejection	Stored particles pushed out with gas stream, diluted with more gas, and passed through aerodynamic deagglomerator into test chamber. Gas requirement is dependent on percent of deagglomeration and particle type, as indicated in Appendix A.

- keep samples dry and isolated;
- predictably contain and release samples in a low-gravity environment.

The sample storage of the standard deagglomerator is for small quantities of material, on the order of 0.05 cm^3, and depends on gravity to keep the sample in a position for delivery to the deagglomerator. The particles are entrained in a gas flowing over a bed of particles, which also serves as the dilution method.

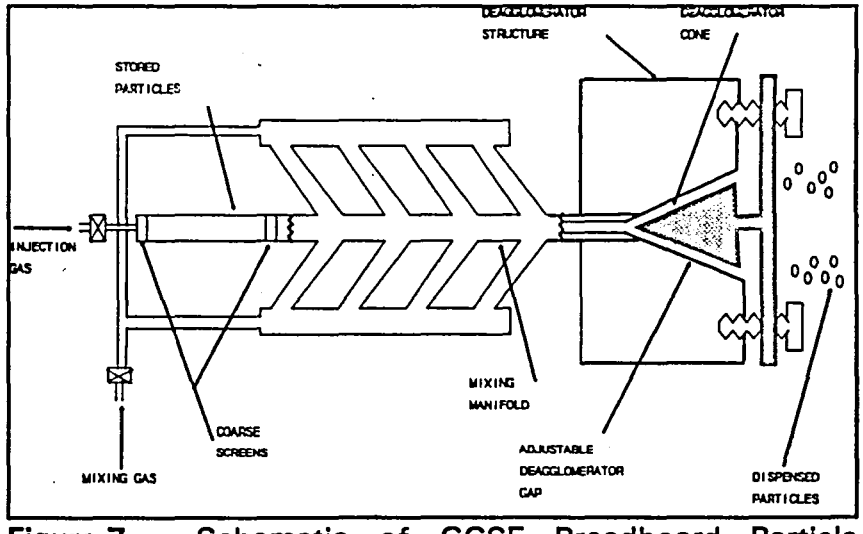

Figure 7 - Schematic of GGSF Breadboard Particle Generator.

For the GGSF breadboard, the sample holder was redesigned to a cartridge type of approach that holds approximately 0.20 cm^3, and can be expanded in size or quantity in order to adjust particle concentration in the test chamber. This method also contains the particles in a known configuration independent of gravity, and can be sealed up to isolate the samples. Appendix A provides more detail on the sample storage.

5.2.1.2 Sample Dilution: In the deagglomerator design, the dilution of particles in carrier gas, and the degree of deagglomeration are intimately coupled. The ability of the blast deagglomerator to deagglomerate aggregates is a function of the number density of aggregates

entering the annulus, which is determined by the dilution of the powder in the carrier gas. The dilution, in turn, is determined by the flow rate of particles out of the sample holder, and the amount of carrier gas introduced into the particle stream.

The redesigned sample holder delivers a cartridge shaped sample charge which is then diluted in a section of tube with several carrier gas feeds along the length. The feed rate of gas into this section can be adjusted to accommodate for particle quantity, size, or adhesion. A more detailed description is presented in Appendix A.

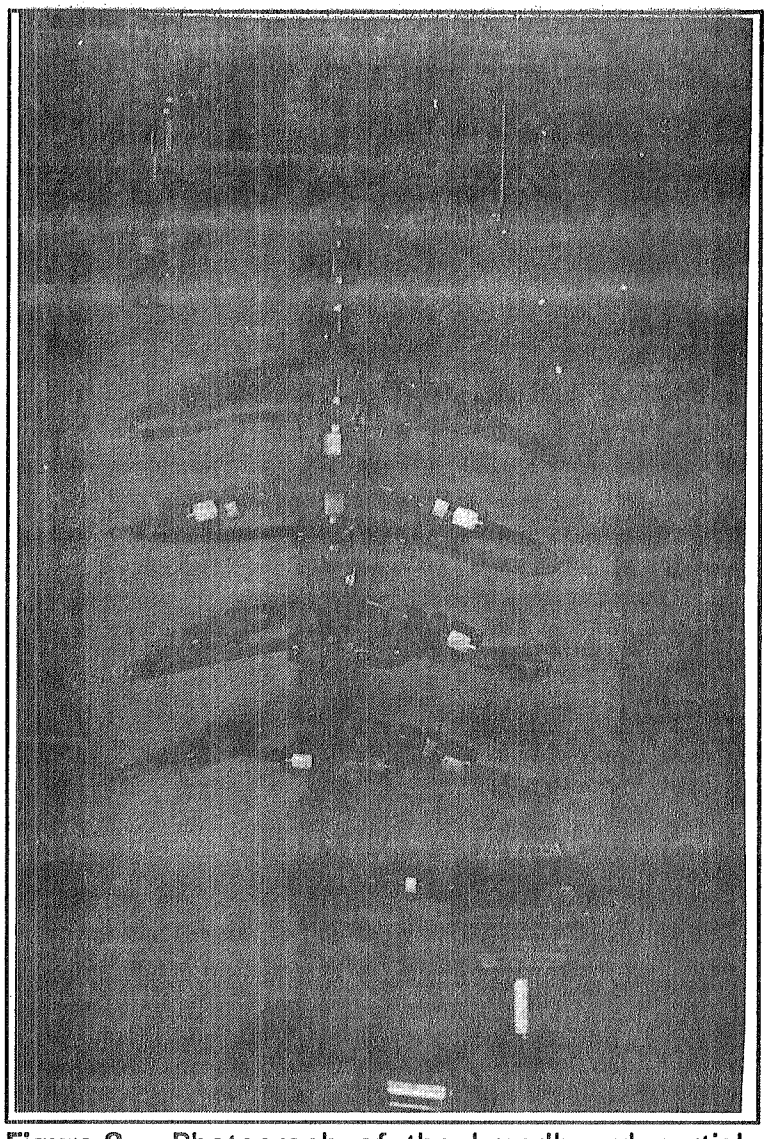

Figure 8 - Photograph of the breadboard particle generator.

5.2.1.3 Deagglomerator: The deagglomerator separates aggregates into single particles. The deagglomerator uses aerodynamic forces generated by passing the carrier gas with entrained particles, through a small slit formed between a male and female cone. The slit width is on the order of several times the particle diameter. The efficiency of the deagglomerator depends, to a certain extent, on the dilution of the delivered aggregates in the carrier gas. The breadboard deagglomerator has an adjustable slit width, as this is the means to modify its performance. This will also allow for use with a large range of particle sizes in one device. Details on the deagglomerator are given in Appendix A, sections 1.10 and 2.1.

5.2.2 Chamber - The breadboard test chamber is intended to contain the particles in an undisturbed gas volume. It allows for 360 degree viewing of the sample inside, and has a volume that approximates the largest GGSF test chamber concept, described in NASA CR177606 (Volume I of the GGSF Final Report) and CR177613 (Volume II of the GGSF Final Report).

The breadboard chamber is a simple plexiglass cylinder with flat end plates, and penetrations for sample introduction, collection, and monitoring diagnostics. The dimensions are approximately 65

cm diameter by 65 cm long. There was no attempt to seal the chamber from the outside environment, or to provide pressure or temperature control. A more detailed description can be found in Appendix A, section 2.2.

5.2.3 Diagnostics - Both in-line and off-line diagnostics are used in the breadboard to characterize the particle samples. Techniques for performing particle characterization are discussed in NASA CR177606, sections 4.3.4 through 4.3.6. A detailed discussion of the breadboard diagnostics is presented in Appendix A, sections 2.3 and 3.1. Some in-line techniques include measurements of light extinction, angular and spectral scattering, and diffraction. The GGSF breadboard is equipped with lasers to provide monochromatic, collimated light, and detectors that can monitor the extinction of the light as the particles pass through the beam.

In addition, imaging was performed to observe the action of the particle cloud. A re-configuration of the breadboard lasers allow passing the beams through optics that formed a light sheet for qualitative flowfield observation.

The off-line diagnostics used included photographic microscopy and scanning electron microscopy. Deagglomerated particles in the quiescent volume of the test chamber were allowed to settle on filters, which were then removed for analysis.

5.3 Test Plan Approach

To demonstrate the feasibility of the particle generation breadboard components to meet a representative subset of the technical requirements, several approaches were undertaken using standard laboratory particle analysis and collection techniques. Deagglomerator performance was addressed by utilizing, and optical microscopy and scanning electron microscopy (SEM) to measure the percent deagglomeration in the chamber's quiescent environment. Additional discussion at the task level can be found in Section 5.3.1, 5.4.1 and in Appendix A. Typical parameter values to be varied are illustrated in the deagglomeration performance validation test flow chart in Figure 9.

The approach used to demonstrate the potential of gravity-independent operation of the particle generation sample holder concept involved the use of high speed cinephotography to view the dilution process at several sample holder orientations. Additional details on the individual tasks and test parameters measured are discussed in Section 5.3.3, 5.4.3 and in Appendix A.

To validate the dispersion flow from the particle generator, a camcorder in conjunction with white light sheet illumination was used to obtain qualitative flow visualization data. Additional detailed information on the individual tasks and test parameters measured are delineated in Section 5.3.2, 5.4.2 and in Appendix A.

The test plan approaches and tasks summarized in Section 5.3 were not geared towards fully characterizing the particle generation device, but instead answered the focused development objectives outlined earlier. Section 5.6 discusses future particle generation characterization needs.

5.3.1 Deagglomeration Performance Validation - Several tasks concerned solely with the dry powder generator's ability to completely deagglomerate powder samples are identified below. The dry powder generator design is functionally similar to the micromerograph deagglomerator and the operating ranges and procedures given in the micromerograph manual were used as guidelines for these tasks.

The resources to test a full matrix of test parameters were not available during this stage of the GGSF program. The result of this test plan is a matrix of test conditions for each powder, as shown in Table 10. The actual values of the operating parameters were generated as the testing progressed (see Appendix A, Table 4). Parameters which were varied include powder type (where size distribution is also considered an attribute of powder type, e.g. 10 micron glass microspheres are considered as a different powder type than 1 μm glass microspheres), powder mass, blast pressure and slit width. Within the scope of this work, potentially important parameters which were not varied or investigated included moisture content of the powder, relative humidity of the carrier gas, agglomeration history of the powder, triboelectric charge buildup in the deagglomerator.

Table 10 - Sample Test Matrix Generated By Test Plan.

Powder Type:	Amount of Powder:		
Degree of Deagglomeration	Pressure #1	Pressure #2	Pressure #3
Slit Width #1			
Slit Width #2			
Powder Type:	Amount of Powder:		
Degree of Deagglomeration	Pressure #1	Pressure #2	Pressure #3
Slit Width #1			
Slit Width #2			
Continue testing until all powders and powder amounts are tested.			

Choose a candidate powder - The powders were chosen from available powders based on size distribution, agglomeration characteristics and powder material. The powder has a size distribution

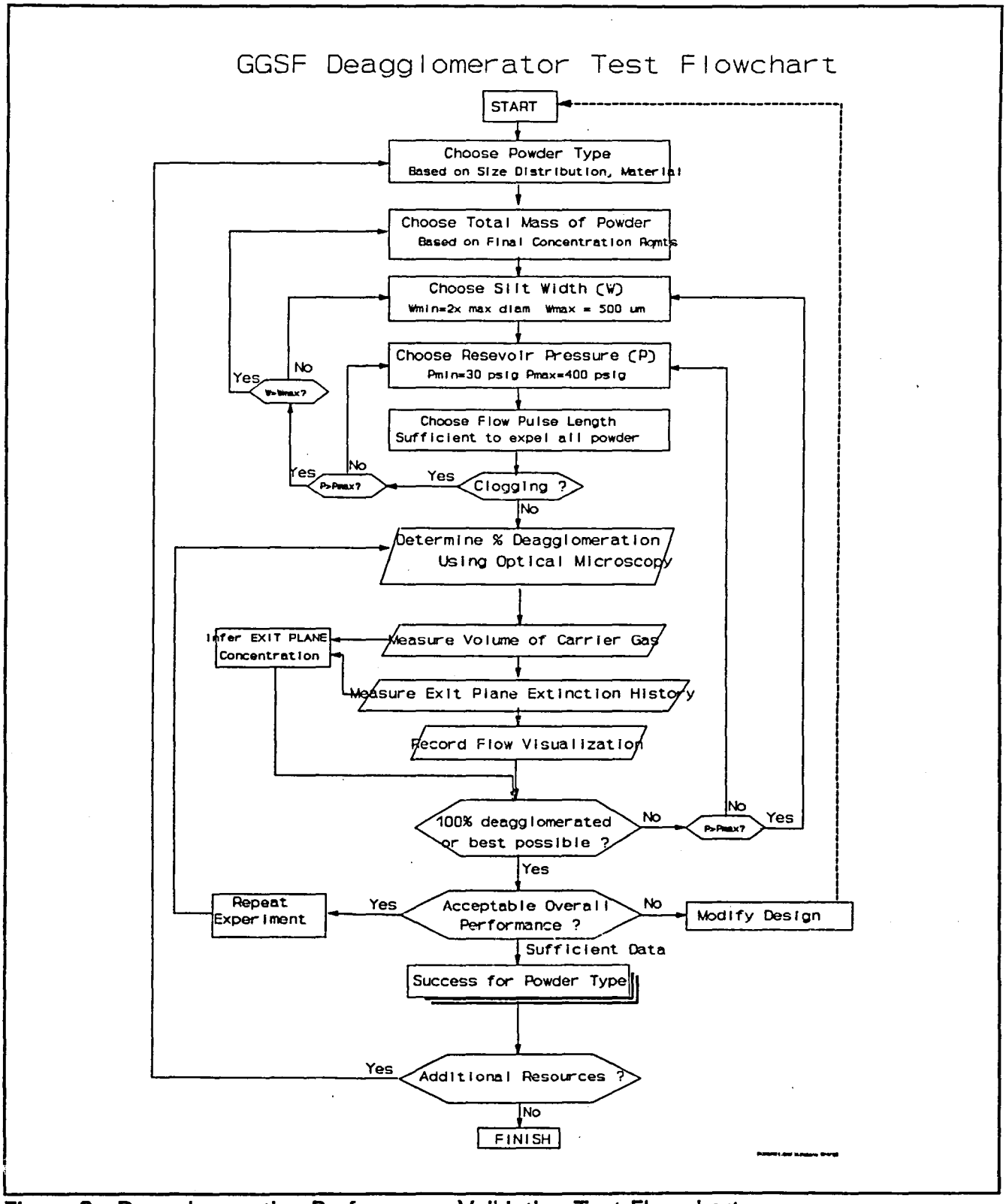

Figure 9 - Deagglomeration Performance Validation Test Flowchart.

that lies within the parameter space of many of the GGSF experiments, is agglomerated in its natural state, and is representative of some of the experiments. Mono-sized particles were used for ease of data reduction. Particles were larger than 1 μm so that optical microscopy could be used and because this is in the operating range specified for the micromerograph. The powders used were Duke Scientific glass microspheres (mono-disperse; $D_{v\,(50)}$=10.2μm and 2.1μm) and Arizona Road Dust with a mean size of 5-10 μm. Some candidates for testing are shown in Table 11.

Table 11 - Some Optional Test Powders.

Powder	Description	Diameter (μm)*		
		$Dv_{(10\%)}$	$Dv_{(50\%)}$	$Dv_{(90\%)}$
Talc	Talcum Powder	tbd	10	tbd
Spheriglass	Glass Microspheres	3	13	22
Spheriglass	Glass Microspheres	13	32	61
Spheriglass	Glass Microspheres	30	64	103
Spheriglass	Glass Microspheres	85	108	153
Duke 364B	Glass Microspheres	6	10	14
AC FINE	Dust	approx 1	approx 40	approx 80

* Particle diameter determined by cumulative volume fraction.

Find the size distribution of the chosen powder when it is fully deagglomerated - The particle size distribution can come from manufacturers data or independent tests. This knowledge is necessary in order to determine the amount of powder needed, and in case pre- and post-deagglomeration comparisons are required.

Calculate total mass of powder needed - This is the mass needed to obtain a distribution of particles throughout the entire chamber volume, of the particle concentration in the range requested by the bulk of the experimenters for the chosen powder's size.

Experimentally determine the optimum deagglomerator slit width and pressure settings - This entails finding the minimum carrier gas pressure, the maximum slit width, and the minimum gas pulse duration necessary to achieve optimum deagglomeration, with minimum amount of carrier gas and without clogging for the chosen powder type and powder amount. The guidelines provided in the micromerograph manual were used to determine the initial choice of operating conditions. The anticipated initial settings were as follows; set the slit width to 4 times the maximum particle

diameter, set the pressure to 30 psig and set the pulse duration for minimum required to clear the powder holder. The pressure was increased and the slit width varied in the test matrix.

Determine the Degree of Deagglomeration Achieved - Nuclepore filters with open face sampling of the quiescent environment powder cloud were used to collect the samples. The Nuclepore filters were manually examined under an optical microscope and a scanning electron microscope. The degree of deagglomeration is based on the number of particles in contact out of the total number. This manual technique is easiest for mono-sized particles, and will get progressively more difficult as the powders become more poly-dispersed.

It was anticipated that the percent deagglomeration would increase as the deagglomerator operating parameters were optimized. If the deagglomeration performance were unacceptable, there would be the need to estimate whether significant reagglomeration were occurring during the time during which the dilution naturally occurs. If it appeared that excessive reagglomeration was probable, the percent deagglomeration achieved at the exit plane would need be to characterized by a laser diffraction instrument or a sophisticated sampling probe that would have to be developed.

Infer the exit plane number concentration - From the mass of powder, the powder size distribution, the volume of carrier gas, and exit plane laser extinction history, an exit plane particle number concentration as a function of particle size distribution is determined.

Infer a fully diluted, final number concentration - From the mass of powder, the powder size distribution, and the chamber volume, infer a fully diluted particle number concentration. Determine if this in an acceptable concentration region of the requested experimental space.

Proceed to test the next powder type - If the new powder is qualitatively similar to a powder previously tested then knowledge obtained from those previous tests are used as guidelines for selecting the initial operating parameter values.

5.3.2 Dispersion Flow Performance Validation - Ideally, the deagglomerator will disperse particles with just enough momentum that they would stop near the center of the chamber, and with just enough turbulence that the cloud would quickly and uniformly diffuse throughout the chamber. This task addresses the characterization of the cloud motion achieved by the candidate dry powder generator.

A camcorder, in conjunction with both floodlighting and light sheet illumination, was used to determine the hardware requirements for obtaining qualitative and quantitative flow visualization data. The temporal and spatial resolution of a high resolution video camcorder (Hi8 or SVHS-C) is sufficient for the majority of the cloud flow visualization requirements.

Our flow visualization tests indicated that at nominal operating conditions the dust/gas jet impinged on the far wall of the chamber. We were able to "stop" the transient dust/gas jet in the center of the chamber using an opposed transient jet of particle-free gas.

Further investigation should be performed when the final design of the deagglomerator and the operating conditions are optimized for deagglomeration.

5.3.3 Dependance on Gravity - High speed cinephotography was used to provide a qualitative understanding of the dilution process of the new design in a variety of sample holder orientations since we cannot obtain 0-g in our lab. To verify the feasibility of this type of cinephotography, high speed movies of the entrainment of three different powder types at one blast pressure and one orientation were performed prior to the generator design changes.

5.4 Test Results

The goal of the characterization of the particle generator was to measure its effectiveness at deagglomeration of particles, placing the particles in a quiescent environment, and operating independent of gravity. This was accomplished by dispensing sample particles under varying conditions including particle type, carrier gas pressure, and deagglomerator slit width. The specific methods, data, and results are detailed in Appendix A, Section 3. A summary of the results and examples of the data are given here.

5.4.1 Deagglomeration Performance - The deagglomerator was tested with three different sample particles. The test plan was organized to optimize the performance of the deagglomerator, i.e. maximize the percent of deagglomeration. To accomplish this, a matrix of 36 tests was performed, and is shown in Appendix A, Section 3. In this matrix, the percent of deagglomeration varied from 64% to 97%, where this represents the ratio of singlet particles to all particles (singlets plus aggregates).

Most of the tests were performed with about 85 mg of sample particles, which represents a concentration of 10^3 particles per cm^3 of 10 μm particles. The parameters that were varied are:

- sample expulsion (or push) pressure - This is the pressure that pushes the sample out of the sample holder and into the dilution section of the particle generator. A high pressure would cause the sample to enter, and proceed through, the dilution section and deagglomerator at a higher rate. The pressure was set at 30, 60, and 120 psi for each of the other variables. The pressure pulse lasts up to 1 second. In general, each variation in slit width had a corresponding optimum pressure setting, often at 60 psi.

- dilution pressure - This is the pressure that feeds the dilution section of the particle generator, determines the amount of carrier gas that mixes with the particles. This is controlled by a combination of the regulator setting feeding this section, and the pressure drop in a tube that has restrictors inserted. The three restrictors used were a 0.15 mm insert, a 0.30 mm insert, and a 0.46 mm insert. The dilution was quantified by measuring the extinction of a laser beam passing through the output plane of the deagglomerator nozzle.

An increase in pressure, and therefore carrier gas, produces increases in deagglomeration percentage.

- deagglomerator slit width - Three slit widths were used, specifically 39 μm, 79 μm, and 118 μm. For the samples tested, 79 μm was generally the best setting.

The majority of tests were performed using 5 to 10 μm Arizona dust particles, selected as a good representative of some GGSF science requirements. Using this sample material, the highest performance achieved, 97% deagglomeration, was the case of a 120 psig push pressure, a 0.30 mm insert and 200 psig regulator setting (extinction for this is about Ln(I/Io)=.25), and a slit width of 79 μm. Several settings provided deagglomeration percentages of better than 90% of mono-dispersed particles. These can be found in the matrix in section 3.2 of Appendix A. Some plots of the results of the test matrix are shown in Figure 10.

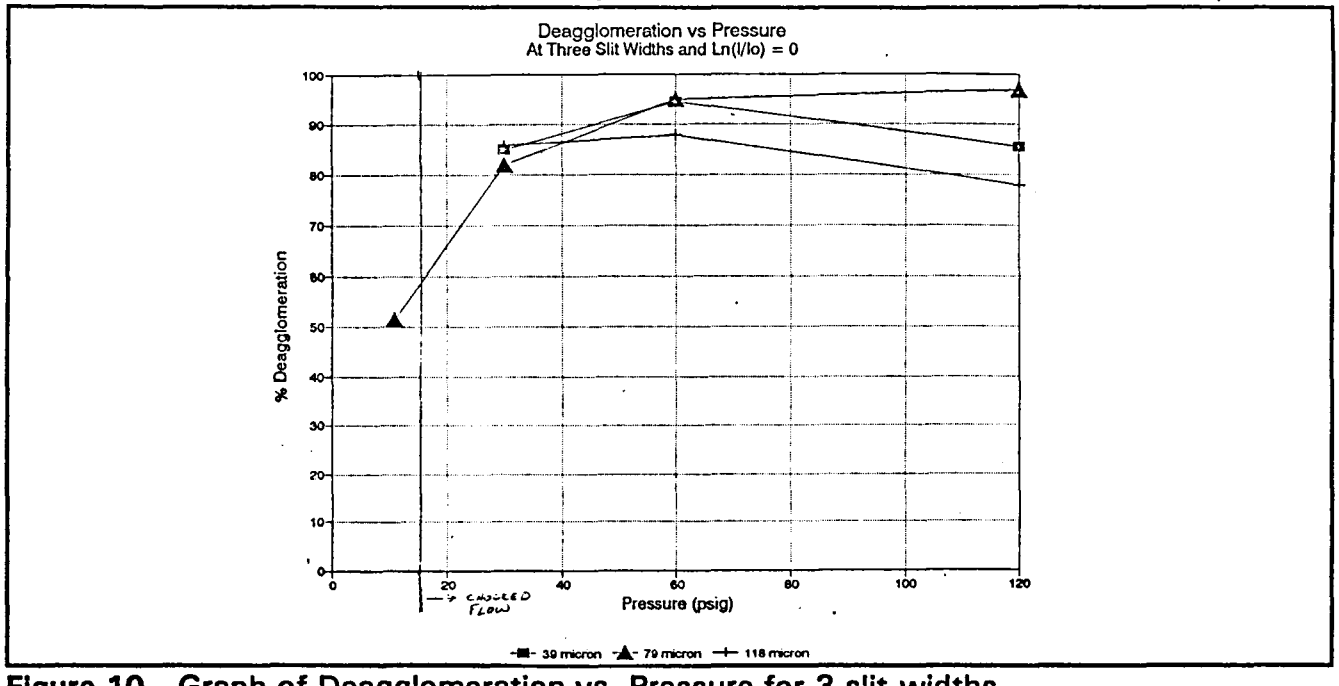

Figure 10 - Graph of Deagglomeration vs. Pressure for 3 slit widths.

A repeat of a few sample test points using the 10 μm glass spheres indicated good correlation with the data acquired using the Arizona dust. Tests performed using 2 μm glass spheres at several test points indicated a reduction of deagglomeration percentage to 86-91%, however, no attempt was made to optimize particle generator settings for this sample material due to the limited resources available.

The degree of deagglomeration was measured by microscopic inspection of particles that settle onto fine filters placed in the quiescent environment of the test chamber. Examples of selected Scanning

Electron Microscope photographs are shown in Figure 11 and Figure 12. More photographs can be found in sections 3.3 through 3.5 of Appendix A.

5.4.2 Dispersion Flow Performance - The dispersion flow was evaluated qualitatively by observing the cloud of dispersed sample in the test chamber by shining a sheet of light through the cloud. It was observed that the particle cloud impacted the test chamber wall opposite the particle generator quite rapidly (on the order of a few seconds or less). This is an undesirable interaction, as particles may be deposited on the wall. Some further investigation showed that a jet of gas, equal in momentum and opposite in direction, may alleviate this rapid interaction, while enhancing the mixing of the cloud in the chamber. More details of this testing can be found in Appendix A, but only a limited amount of data has been collected to date.

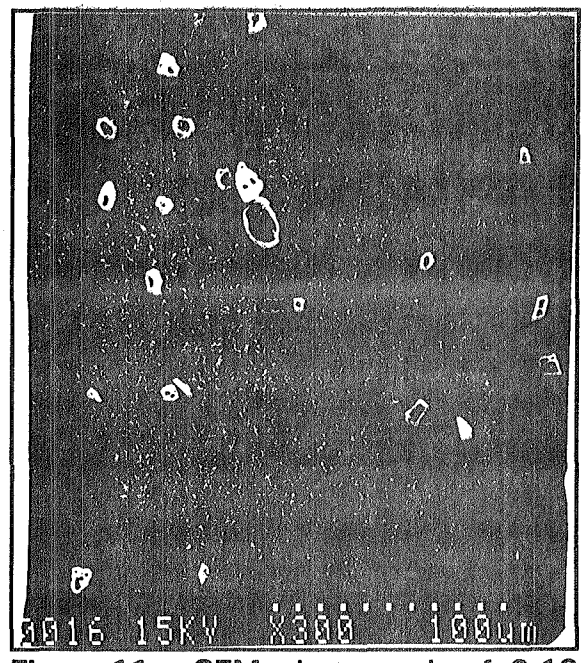

Figure 11 - SEM photograph of 6-10 µm Arizona Test Dust.

5.4.3 Dependance on Gravity - The sample holder that was designed for the breadboard was based on the need to operate independently of gravity. Several qualitative tests were performed to verify this capability. Due to the cartridge type design, the first verification of gravity independence was to operate the sample holder in a horizontal position, and determine if all the sample is expelled during operation. Unexpelled sample would indicate a potential problem. Sample holders of various diameters were tested for this phenomena, from 0.50 inch to 0.05 inch diameter. Above .125 inch diameter, particles were being left in the sample holder; therefore the .125 inch, or 3 mm id tube was used.

The tests were continued at a vertical orientation and the results indicate that the sample holder design is adequate for low gravity operations.

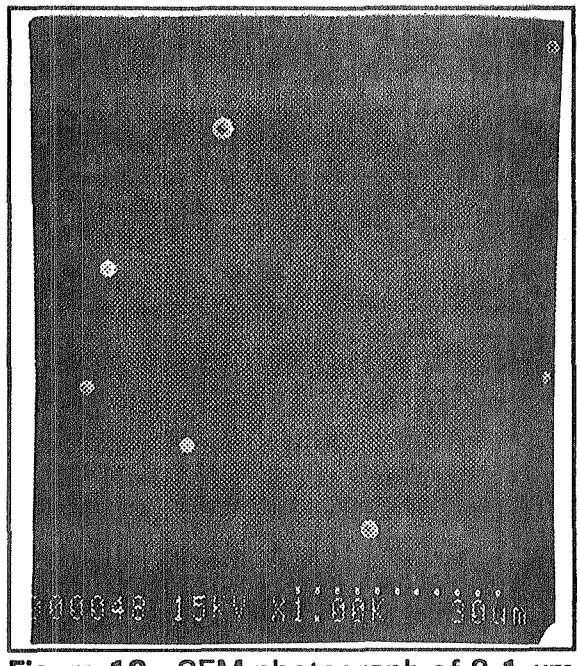
Figure 12 - SEM photograph of 2.1 µm glass spheres.

5.5 Future Recommended Demonstration Tests of the Existing Breadboard

A carefully focused but limited set of data was obtained during this effort. A more complete data set should be obtained to better quantify the performance of the blast deagglomerator under the operating conditions required for the GGSF S&T requirements. These data should be acquired on the breadboard device so deficiencies can be identified prior to the flight hardware design, and flexibility in the science requirements, if any, can be accommodated.

- The mass of particles during this test series was limited to 85 mg. The sample holder can contain up to 200 mg. The test matrix should be expanded to increase the sample quantities as well as other sample material types.

- The accomplished test matrix focused on 10 μm particles, with limited data and no optimization for 2 μm particles, and no data for smaller than 2 μm or larger than 10 μm particles. The breadboard particle generator should be tested with other particle sizes to verify the ability to optimize for, and deagglomerate various particle sizes outside of 10 μm.

- The deagglomeration percentage is very dependent on the dilution of the particles in the carrier gas. The carrier gas can affect the chamber environment detrimentally for some GGSF experiments. A thorough characterization matrix will result in a gas requirement vs. deagglomeration percentage that can be used to better define the GGSF experiments or changes to science requirements that can allow this type of particle generator to be used.

More discussion of this subject is found in Section 5.3 of Appendix A.

5.6 Future Particle Generation Characterization Needs

5.6.1 Design Improvements - Upon completion of the current study, the laboratory version of the deagglomerator still needs additional development. The first and most critical area for further development would be modifications that may be required to increase the quantity of sample that can be dispensed. If additional developments are implemented, some or all of the deagglomeration performance validation tests enumerated need to be repeated. The potential development tasks that can be anticipated at this time are discussed in the subsections that follow.

Another area of possible additional development would be modifications that reduce the weight of the deagglomerator, and automate the adjustment of the operating parameters. These types of modifications would only be reasonable once the operational design has been finalized.

There are several potential modifications which could improve the deagglomeration performance. The majority of these consist of adding an additional deagglomerating section to the system. For example, the addition of an impaction plate is easy to implement. Other potential techniques would

modify the inlet conditions of the annular cone. One example would be an accelerating flow section prior to the annulus that would provide axial stretching of the gas powder mixture to effectively meter it over a longer period of time.

TRW has used qualitative flow visualization techniques to determine the extent of the dusty gas jet penetration into the chamber, and the dispersion flow pattern of the dust cloud within the chamber. Preliminary results showed an undesirable amount of jet/wall interaction with the deagglomerator operating under nominal conditions. Some preliminary investigations looked into the feasibility of using an opposed gas jet or a flow deflector to minimize the wall interaction. Other techniques which have not yet been investigated include inducing large scale mixing currents in the chamber prior to dispersing the powder or just after dispersing the powder. The effectiveness of all of these techniques depends on the experimental chamber pressure. The opposed jet of pure gas appears to a viable means of controlling the location of the particle laden gas jet, but further experimentation will be necessary to determine whether it will work for all combinations of chamber pressure and deagglomerator pressure setting. In addition, this technique cannot be used when a vacuum is required.

The GGSF experiments require a wide range of temperatures and pressures outside of the room conditions at which the breadboard is currently operated. Following more testing at room conditions, the breadboard test chamber should be exchanged for a chamber capable of holing a vacuum, and controlling temperature. The temperature range should be a subset of the GGSF requirements.

5.6.2 Theory, Analysis, and Modeling - A significant effort is required to properly identify the relevant parameter interactions of the particle generator operation, and to develop a model. Appendix B provides background information to the task of a comprehensive investigation for the development of an analytical model and theoretical understanding of the performance and operations of the deagglomerator.

To predict the performance of the particle generator involves modeling the deagglomerator and the sample holder. These functions are interdependent and cannot be totally separated. The performance also depends on various experiment chamber parameters. The discussion in Appendix B is separated into **Powder Sample Lofting, Fluid Mechanics of a Dense Two-Phase Flow, Forces Acting on the Particles,** and **Free Jet Dispersion,** though these topics are not independent.

5.6.3 Proposed Empirical Approach - This section proposes that the performance of the deagglomerator/disperser is characterized only under specific conditions relevant to specific experiments to be performed in the GGSF, as opposed to testing over a broad range of conditions as outlined in the previous sections. This focused approach would produce highly relevant data immediately. Another advantage of this approach is that each experimenter can verify that the deagglomerator does meet the specific experiment requirements, and what conditions are not met.

The disadvantage is that each experiment requires a separate investigation and that a comprehensive understanding is unavailable to be used as a design tool. However, such multiple experimentation

will necessarily lead to the development of a large body of data, and probably to some empirical analyses. Ultimately these contributions will serve as a basis for a comprehensive investigation such as suggested previously.

6 RECOMMENDATIONS FOR FURTHER STUDIES

The success of the GGSF is very dependent on the ability to define meaningful experiments, produce samples that can be used for the experiments, monitoring and measuring those samples during the experiments, and collecting the samples for further investigation. Difficulties can arise from using equipment and processes for these experiments that have not been specifically designed and tested for operation in low-gravity, and with little intervention by personnel.

This breadboard offers the opportunity to clarify experiment requirements by developing and testing hardware concepts that can meet the requirements. The breadboard should be used to:

- further define experiment requirements for particles and data acquisition;
- develop particle generators for the different parameters of particles;
- determine data acquisition methods that adequately monitor particle interactions;
- test concepts for autonomous or remote cleaning of the chamber surfaces;
- convert into a low-gravity lab that can be used for the same purposes and additionally provide early return of GGSF science.

Section 5 of Appendix A offers a more detailed discussion of these recommendations.

7 REFERENCES

1. GGSF Phase A Study Final Report, Volume I - Facility Definition Studies, NASA CR177606

2. GGSF Phase A Study Final Report, Volume II - Conceptual Design Definition, NASA CR177613

APPENDIX A: Breadboard Development Report

GAS-GRAIN SIMULATION EXPERIMENT MODULE

BREADBOARD DEVELOPMENT REPORT

April 1993

Prepared under Contract NAS2-13408

for

NASA/Ames Research Center

Moffett Field, CA 94035

By

Michael Petach

TRW Inc.
Space & Electronics Group
Applied Technology Division
Redondo Beach, CA 90278

A2

Table of Contents

List of Figures

List of Tables

1 BREADBOARD DEVELOPMENT

Several of the anticipated GGSF experiments require the deagglomeration and dispensing* of dry solid particles into an experiment chamber. The GGSF Phase A study[1] reviewed various techniques and devices available for the solid particle aerosol generator. As a result of this review, solid particle deagglomeration and dispensing were identified as key undeveloped technologies in the GGSF design. The present work was undertaken to develop these technologies. This report describes the breadboard, and the characterization that was involved in this phase of the GGSEM.

This task developed a laboratory breadboard version of a solid particle generation system, and provided preliminary characterization of the system's performance. The breadboard hardware emulates the functions of the GGSF solid particle cloud generator in a ground laboratory environment, but with some modifications, can be used on other platforms.

The GGSEM Breadboard was developed to support GGSF concept verifications. This system can be used to test concepts for sample generation, collection, and manipulation. Cleaning techniques can also be tested. These studies will help answer questions and reduce the risks associated with the GGSF hardware development.

The subsystems of the breadboard are described in Table 1. These subsystems are flexible in design and application, allowing for the design of many types of experiments, and utilization in facilities other than the laboratory such as drop towers and aircraft.

Table 1 - Summary of Breadboard Subsystems.

Subsystem	Description
Particle Generator	Dry powder dispenser
Chamber	Plexiglass cylinder - 60 x 60 cm
Diagnostics	• Deagglomeration Gas Pressure • Dilution Gas Pressure • Laser Attenuation
Additional Diagnostics Used During Characterization But Not Part of Deliverable Hardware	• Steady State Flowmeters • Optical Microscope • SEM • Video Camera • Light Sheet Illumination • High Speed Motion Picture • Electronic Balance

1.1 Development Objectives for Solid Particle Generator

The goal in developing and building a GGSF laboratory breadboard system was to

*In this report, the term "dispensing" means the act of distributing the powder uniformly throughout the gas medium, while the terms "deagglomeration" and "dispersion" refer to the act of breaking up aggregates. This distinction is important since the term dispersion is somewhat ambiguous and is sometimes used in the literature as being synonymous with deagglomeration. In addition, the term "powder" will be used interchangeably with "dry, solid particles" for the sake of brevity.

demonstrate GGSF particle generation techniques and concepts, and perform particle collection and analysis measurements. The primary objectives in developing the GGSF laboratory particle generator breadboard included:

- identification of candidate techniques for storing, deagglomerating, and dispensing dry solid particles that cover a broad range of the GGSF strawman experiment science and technical requirements;
- develop and test laboratory breadboard components that demonstrate the feasibility of the selected particle generation technique to meet a representative subset of the science and technical requirements, including parameters of particle size, type, degree of deagglomeration, total mass, etc.;
- demonstrate the potential for gravity-independent operation of the selected technique;
- qualitatively characterize the flow field (velocity as a function of time in three dimensions) of the dust cloud generated in the test chamber;
- identify configurations and technical issues uncovered during the development and testing of the laboratory breadboard system;
- identify further future development program efforts necessary to fully characterize the selected particle generation device;
- maintain a flexible breadboard configuration allowing for utilization in facilities other than a ground-based laboratory.

1.2 Design Criteria for the Solid-Particle Generation Breadboard Hardware

The breadboard hardware design criteria are extracted from the science requirements identified in the GGSF Phase A Final Report[2], and the constraints of the GGSEM, GGSF, KC-135, 1-g labs, and other potential platforms. A summary of the science requirements for experiments that require solid particle clouds is given in Table 2.

1.2.1 Particle Properties - The types of particles, particle diameters, and total mass of particles that must be dispensed can be estimated from the science requirements as interpreted in the GGSF Phase A Final Report[3], and from the dimensions of the proposed GGSF/GGSEM chamber. The range of particle sizes and particle number concentrations requested for solid-particle experiments are shown in Figure 1. Lines showing the total mass of particles required for a given number concentration and particle diameter (assuming a material density of 2.5 grams/cc and a chamber volume of 67 Liters) have been included to illustrate the range of particle masses that must be stored for the different experiments. There is a very wide dynamic range in particle size (6 orders of magnitude), number concentration (10 orders of magnitude), and total particle mass (10

Table 2 - Dry Powder Properties Extracted From NASA CR177606.

Experiment No.	Materials	Size (μm)	Number Density (No./cc)	Pressure Range (bar)	Temperature Range, (K)
1	Silicate grain	~1	TBD	10^{-3} - 10^{-5}	150 - 500
3*	Salt	0.01 - 1	1 - 10^{4}	0.1 - 1.0	273 - 303
5	Quartz;basalt	0.1 - 1,000	1 - 10^{6}	10^{-4} - 1	221 - 366
8	Carbon	0.1	10^{5}	10^{-4} - 1(10 desired)	233 - 293
13	Olivine;pyroxene	1	10^{5}	0 - 1	77 - 300
15*	Al_2O_3; TiO_2; MgO	0.01 - 0.05	10^{5} - 10^{8}	10^{-6} - 10^{-5}	500 - 1200
17*	Carbon grain (amorphous, hydrated, graphite); silicates	0.05 - 0.1	10^{10}	10^{-10} - 10^{-9}	10 - 300
18	Microspheres (TBD)	0.01 - 20	10 - 10^{5}	1	293 - 373

* Experiments where particles are generated by means other than deagglomeration.

orders of magnitude) required, and it is not at all obvious that any single device can cover all these ranges. Part of the development effort, therefore, was concerned with prioritizing the range of particle size, particle type, total mass stored, and number concentration to be covered by the breadboard hardware.

1.2.2 Carrier gas amount and type - The gas pressure requirements for the various experiments, shown in Table 2, which coupled with the chamber volume determines the amount of carrier gas that the breadboard device can utilize without exceeding the required pressure. No carrier-gas based device can be used for the experiments require hard vacuum, and thus cover the entire range of experiment chamber pressures requested. Therefore, part of the development effort was concerned with prioritizing the range of chamber pressures that was deemed acceptable for the breadboard device to produce. Some of the experiments specifically call out the gaseous constituents of the chamber atmosphere. Any carrier gas introduced into the chamber must be compatible with these requirements.

1.2.3 Degree and repeatability of deagglomeration - The degree of deagglomeration required as an experimental initial condition is not given in the GGSF Phase A final report, so a goal of 100% singlets (100% deagglomeration) was adopted without considering this an absolute criterion. No specification for the repeatability in the degree of deagglomeration achieved, or in the uncertainty in estimating the degree of deagglomeration is given, so these were considered parameters to optimize if possible, and to characterize as part of the validation testing.

1.2.4 Gravity independent operation - None of the breadboard hardware functions (storing, deagglomerating, or dispensing the powder) can depend on the presence of gravity if they are to work in a micro-gravity environment, and be used for characterization or other purposes in 1-g environments. Due to the difficulty of testing concepts that rely on the absence of gravity in a

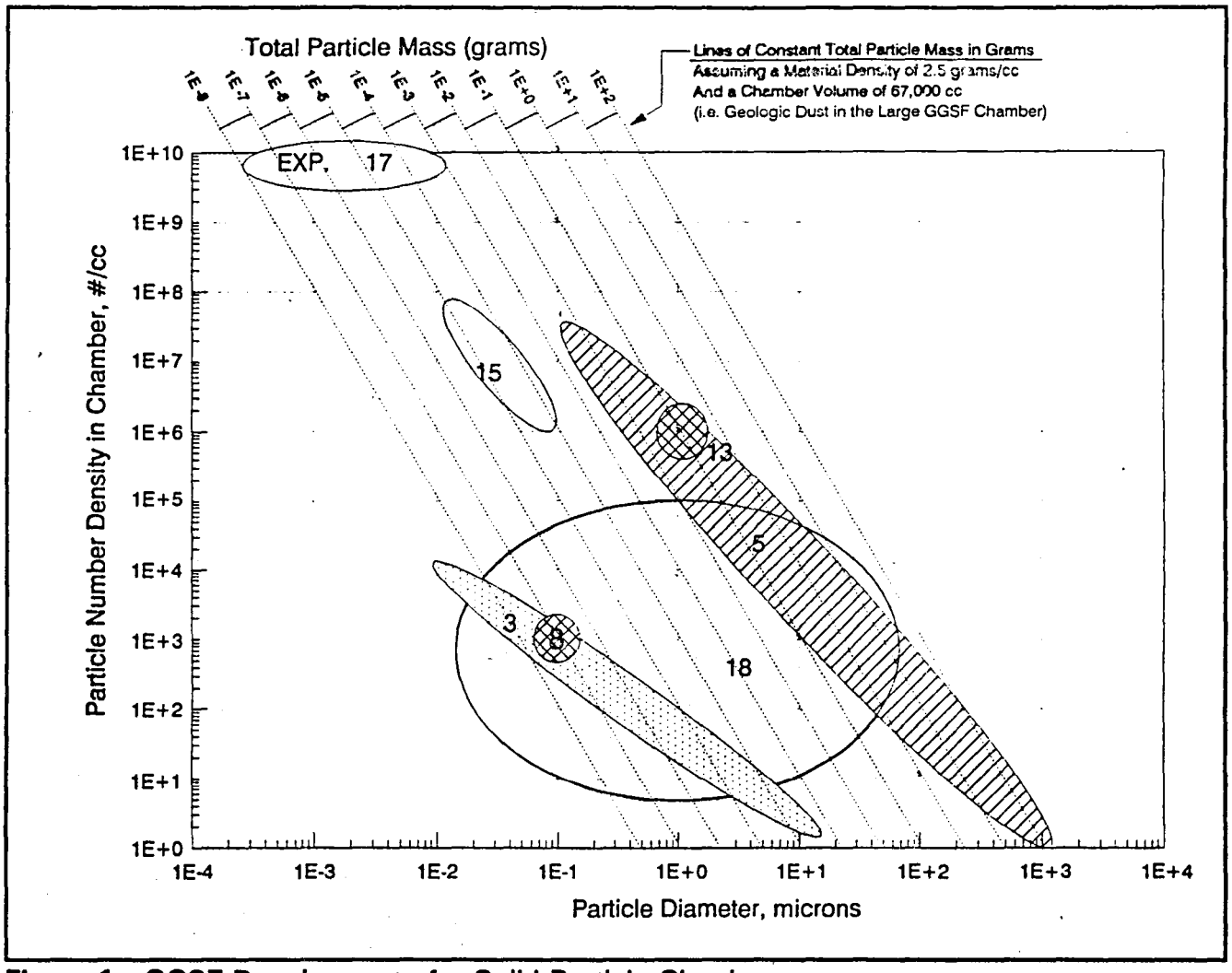

Figure 1 - GGSF Requirements for Solid Particle Clouds.

laboratory situation, a gravity-independent design is desirable.

1.2.5 Logistical considerations; size, weight, and complexity - The particle generator is intended for applications that are size and mass limited. Therefore, the design must be compatible with changes that will bring the size, weight, and mechanical complexity within the these constraints. While all these considerations were used in the design and selection of the breadboard hardware, the weight of the hardware could still be reduced considerably.

1.2.6 Dispensing time - When small particles are dispersed at high number densities, they tend to undergo various processes, such as coagulation, that may alter the nature of the cloud in a relatively short time. The time to dispense the particle cloud into the chamber should be short compared to the time scales over which these processes occur. In addition, the dispensing time should also be short in comparison to the experiment duration. The many orders of magnitude in the ranges of particle size, number density, and experiment duration make it virtually impossible to

define a single design criterion. It is apparent, however, that the dispensing process should take place on the order of seconds as opposed to minutes.

1.3 Review of existing solid-particle aerosol generators

There are several comprehensive reviews of the existing commercial and laboratory solid-particle aerosol generation techniques and devices in the aerosol literature[4, 5, 6, 7] as well as in the NASA CR177606.

There are only a few basic classes of solid-particle aerosol generation techniques to choose from. These can be divided into two main classes; *in-situ* generation of particles, and dispersion of stored particles. *In-situ* generation includes techniques such as exploding wires, arcs, photolysis, and combustion. These techniques typically produce very fine particles in the sub-micron to nanometer size. Techniques based on the dispersion of stored particles can be categorized by the storage medium, which can be solid liquid or gas. Solid binders which sublimate away to release particles have been proposed, but this is an exotic, and as far as we know, untried technique. Storing solid particles in suspension in a liquid is a fairly common technique. The liquid is then nebulized into small droplets containing at most one solid particle, and the liquid is then removed by drying to produce a solid aerosol. The most widely used method for generating solid-particle test aerosols is to store the particles as a dry powder, then pneumatically redisperse the dry powder[8]. The pneumatic redispersion of dry powders can be further categorized according to the methods used for storing, feeding, deagglomerating and dispensing the powder, as well as by particle type, particle size, output concentration, etc.

1.4 Selection of dry dispersion as the candidate technique

All the techniques outlined in the previous section have strengths, weaknesses, and areas where they perform best. There is no single technique that can be expected to cover the entire range of particle types, particle sizes, particle number densities, chamber pressures, chamber gas contents, particle charges, initial particle motions, dispensing times, etc that are required for the GGSF experiments. Therefore, we felt that the technique upon which the breadboard hardware was based should provide the best chance of covering the broadest range of the solid particle cloud experiments.

The selection of a technique based on pneumatic redispersion of a dry powder was based on several factors. First, this technique covers a broad range of the solid particle cloud experiment requirements. The range of particle sizes covered by various dry powder dispensers covers a range from 0.1 micron to greater that 100 microns, with undiluted output concentrations from less than 0.01 g/m^3 to greater than 100 g/m^3, though no one device covers this entire range[9]. Second, this technique works with a wide variety particle type and particle morphologies, unlike the in-situ generation of particles which is limited to a few particle types and cannot generate arbitrary

morphologies. Third, this technique has little chance for contaminating the particle surface, unlike the liquid suspension techniques.[10]

1.5 Literature search and prior work on dry dispersion and aerodynamic deagglomeration

A literature search for work pertaining to experiments, theory and devices utilizing pneumatic dispersion of dry powders yielded a substantial body of work. During the period of performance, these papers were loaned to NASA so that copies could be made for future reference. This literature is referenced throughout the report, but a comprehensive review of it is beyond the scope of this contract.

A few comments summarizing some of the major findings pertaining dry dispersion devices are warranted at this time, though. First, and most important, no fundamental theoretical description of the aerodynamic deagglomeration processes was described or referenced in any of the papers. Several authors describe empirical correlations based on theoretical considerations, but do not develop the theory to a point of comparing their correlations with predictions. Second, no device was described which met all the design criteria for the GGSF/ Option 1 (as discussed in the previous section) breadboard hardware. Third, it became obvious that although there were many design variations, there are certain fundamental functional units that make up every pneumatic dispersion system. These are: a) a dry powder storage device; b) a device or technique for metering the powder into the gas stream at a controlled rate; c) a device for controlling the gas pressure and flow rate; d) a device or technique for preconditioning the powder after it has entered the gas stream but before it has entered the deagglomeration section; e) a deagglomeration section based either on aerodynamic shear or particle impaction. Additional optional components may include; f) a classification section to remove aggregates; g) a dilution section to reduce the number concentration and; h) a charge neutralization section to strip charge built up on the particles during the dispersion process.

Another important point that became evident as a result of the literature search was that the deagglomeration performance of dry dispersion devices depends on the particle number concentration in the device. Interestingly, this phenomenon has been observed in a dry dispersion device based on particle impaction as well as in devices based on aerodynamic shear. A summarized explanation of our understanding of this phenomenon as it applies to shear based devices is included in the next section.

1.6 Dependence of deagglomeration performance on particle number concentration in shear based devices

A heuristic explanation for the dependence of deagglomeration performance on particle number concentration in a shear based device is as follows. The shear in the deagglomerator slit due to the gas velocity gradients is the fundamental mechanism for breaking apart the aggregates. The particle

velocity differences that result from the gas velocity gradients also cause particles to come together, however, resulting in agglomeration. Thus the deagglomeration performance of the device is balance between deagglomeration and re-agglomeration. The deagglomeration term is increased by increasing the shear, which unfortunately also increases the reagglomeration term. A similar situation also exists with the particle residence time in the deagglomerator. The deagglomeration term is increased by increasing the residence time since sufficient time must be allowed for the location and orientation of the aggregates in the shear field to vary over their passage through the slit such that they pass through a maximum. An increase in residence time also allows more time for particles to catch up with one another, though. The only variable which does not increase both terms simultaneously is the particle spacing, i.e., the particle number concentration. The farther apart the particles are initially; the less likely they are to be brought together. Thus, reducing the particle number concentration does nothing to enhance the fundamental ability to deagglomerate particles, but it diminishes the fraction of particles that are reagglomerated.

Iinoya and Masuda[11] showed, experimentally and theoretically, that the deagglomeration performance of a device based on shear is approximately given by the expression,

$$(D_o/Di)^3 = (A/B)\, n_i + e^{(-A0}$$

where D_o = output mass median particle diameter
D_i = fully deagglomerated mass median particle diameter
A = Dispersion (deagglomeration) constant
B = Agglomeration constant
t = mean residence time in the deagglomerator
n_i = initial particle number concentration

which illustrates the points in the discussion above. An interesting point is that when the deagglomeration data is plotted as $(D_o/Di)^3$ vs. n_i the intercept and an estimate of the residence time can be used to determine the deagglomeration constant "A". The slope the shows the relative relationship between deagglomeration and reagglomeration.

1.7 Selection of the Micromerograph as a design starting point

The version of the pneumatic redispersion technique that was selected as a starting point for the breadboard design was chosen based on its ability to handle virtually any powder type, its particle size range, its batch mode operation, and its mechanical simplicity.

The initial design of the TRW breadboard solid particle generator was adapted from a commercial instrument that was developed in the 1950s as part of an instrument for particle size classification.[12,13] This instrument, called a Micromerograph and shown in Figure 2, is composed of a powder storage section, a compressed gas storage section, a deagglomerator section, a sedimentation column, and a microbalance. Figure 3 shows the details of the sample feeder and deagglomerator. TRW acquired a Micromerograph in the late 1970s for use in its pulverized coal combustion

investigations. The Micromerograph was found to be a very reliable instrument and its use led to several important findings.[14]

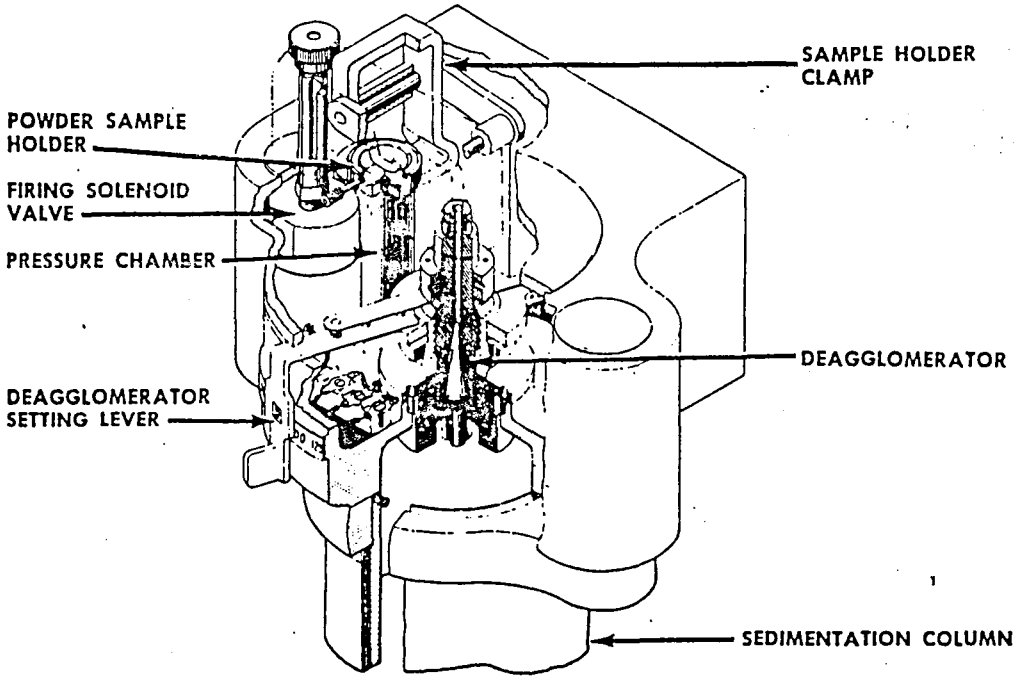

Figure 3 - Micromerograph Sample Feeder and Deagglomerator.

In the Micromerograph, the dry powder sample is stored in a "U" shaped channel at the bottom of curved section of tubing that is connected to small pressure vessel containing compressed gas. A solenoid valve allows the gas to flow over the powder sample, entraining the powder into the gas stream and carrying it to the deagglomeration section.

The deagglomeration section of the Micromerograph consists of a pair of concentric cones forming a very narrow conical annulus through which the dust-laden gas passes. The spacing between cones can be adjusted to vary the annular gap width, and the pressure of the stored gas can be adjusted to vary the flow rate through the conical annulus.

1.8 Literature and prior work pertaining to the Micromerograph

To the best of our knowledge, no quantitative theory of operation of the deagglomerator section of the Micromerograph exists in the literature. A limited qualitative discussion of a possible theory of operation found in one reference[15] suggests that the breakup of agglomerates is related to the shear flow in the boundary layer, but the discussion also indicates that no conclusive evidence exists to support this theory.

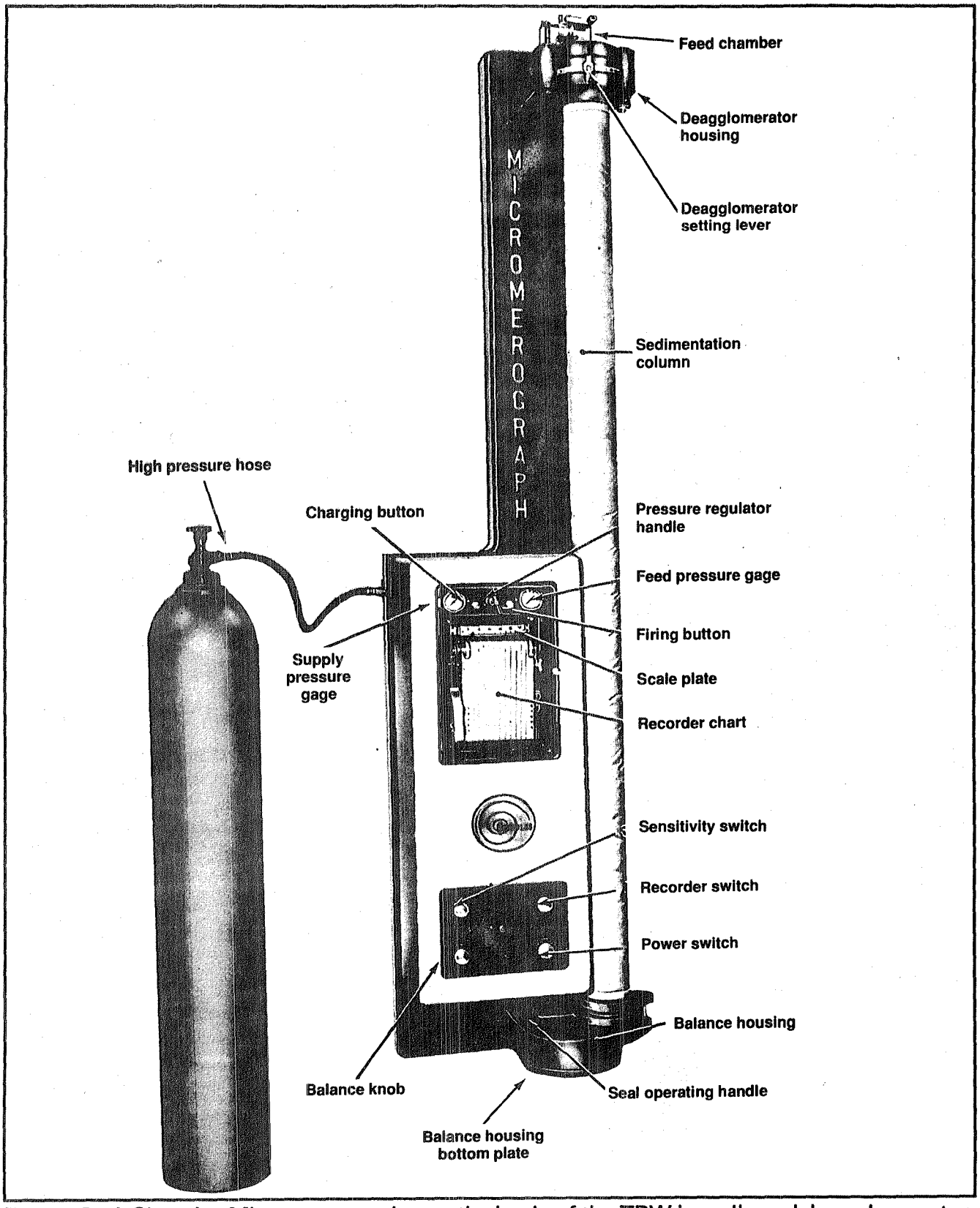

Figure 2 - A Sharples Micromerograph was the basis of the TRW breadboard deagglomerator.

Several papers analyzing the performance of the Micromerograph as a size classification device have been found.[16, 17, 18, 19, 20, 21, 22]
The size classification performance of the Micromerograph has been criticized by several of these investigators based on particle loss to the walls of the sedimentation column, agglomeration during the settling process, and improper accounting for the initial velocity and penetration of the dust cloud. No analysis or measurement of the deagglomeration performance of the Micromerograph deagglomeration section *per se* was found.

A Russian language paper[23] was found which describes experimental deagglomeration results obtained using a modified version of the Micromerograph deagglomeration section, shown in Figure 4. The author was able to obtain 90% deagglomeration (defined as the ratio of the number of single particles to the total number of particles) with 20mg samples of molybdenum, glass and quartz spheres ranging from 1.3 microns to 30 microns in diameter when sufficiently high pressures and narrow slit widths were used. This result was viewed by TRW as a positive indication for the chances of success using this design as a starting point for the breadboard device. In addition, the modifications made in this (Fuchs') version of the deagglomerator were viewed as potentially significant and potentially detrimental to its performance, so we felt that there was the possibility for improved performance. (The author also describes in the same paper a different deagglomeration device which achieved 100% deagglomeration performance, however his later work with it[24] indicates that this performance is achieved at very low undiluted output concentrations, on the order of 1 gram/m^3. In the context of the GGSF/GGSEM mass requirements, this would raise the chamber pressure to unacceptable levels, so this design was not pursued).

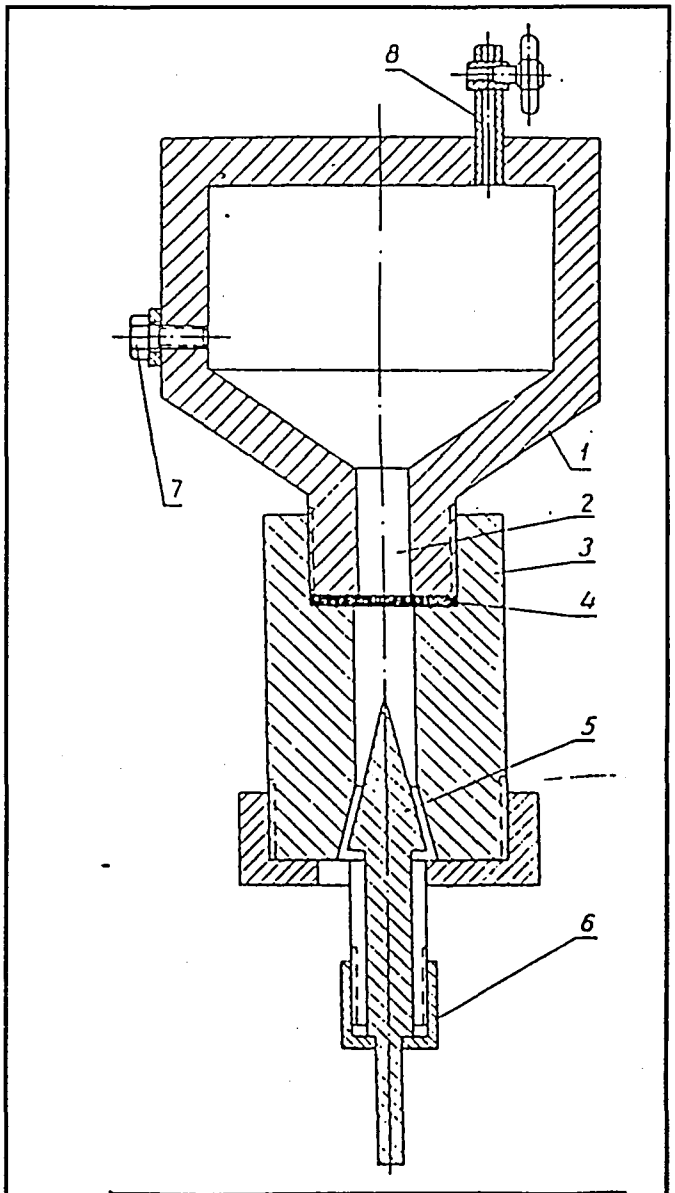

Рис. 1. Пневматическая коробка для распыления порошков:

1—стальная коробка объемом 150 *см*^{3}; *2*—штуцер с внутренним диаметром 9 *мм*; *3*—муфта, навинчивающаяся на штуцер; *4*—мембрана из латуни или целлулоида; *5*—штифт с конической головкой; *6*—гайка, регулирующая ширину зазора между *3* и *5*; *7*—отверстие для засыпания порошка на мембрану; *8*—вентиль, соединяющий коробку с газовым баллоном и с манометром

Figure 4 - Deagglomerator Built and Tested by Fuchs.

1.9 A heuristic explanation for the Micromerograph deagglomerator's conical geometry

The concentric cones geometry of the Micromerograph design forms a converging-diverging nozzle. This fact becomes apparent when the area of the deagglomerator gap is plotted as a function of distance starting in the tube leading to the cones in Figure 5. The area ratio of this nozzle for any reasonably small gap between the cones is such that for pressures above the critical pressure the flow will choke. This was checked experimentally by varying the back-pressure on the Micromerograph while holding the upstream pressure constant and monitoring the gas flowrate. The gas flowrate was observed to remain constant as the back pressure was reduced, indicating choked flow. In the choked condition, the flow will go sonic at the throat and supersonic in the diverging section. This enhances the maximum shear available for deagglomerating particles in two ways. First, the centerline velocity in the gap is higher than it would be if the flow stayed subsonic and decelerated in the converging section. Second the accelerating flow steepens the boundary layer profile. The flow will shock back down to subsonic conditions either at the gap exit or else in the gap, depending on the downstream pressure. It is not known at this time if the shock has any significant effect on the particles.

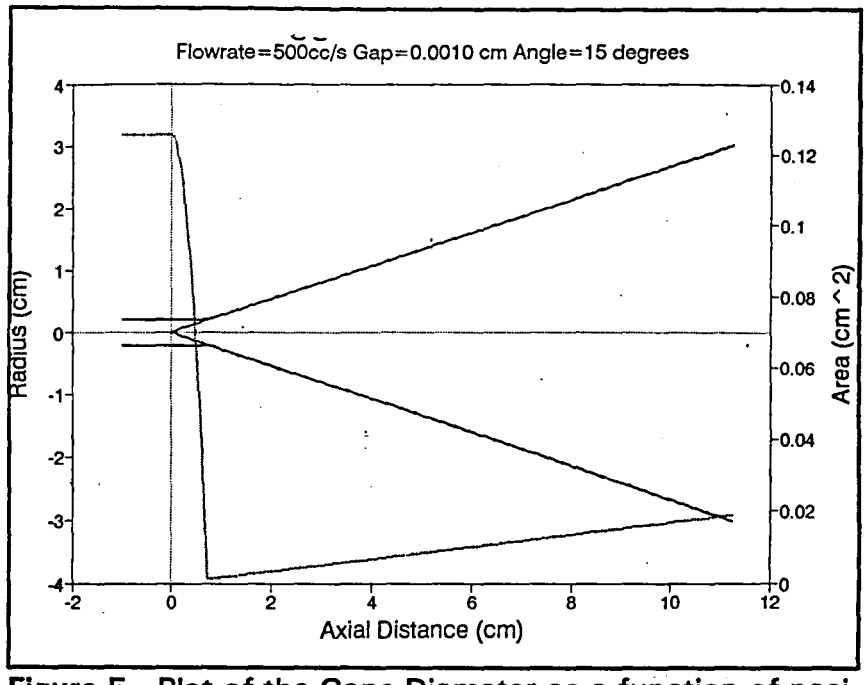

Figure 5 - Plot of the Cone Diameter as a function of position.

Some preliminary estimates of representative flow conditions in the GGSF Micromerograph Deagglomerator were made which support this crude model described above. The powder/nitrogen mixture was assumed to act as a dense gas, and the effects of area change and friction were accounted for. These calculations indicate that the flow is sonic at the minimum area near the start of the conical gap, and the flow accelerates to an average Mach number at the exit of the annular region of Mach 2.5. This result assumes the exit plenum pressure is lower than 200 torr (plenum pressures greater than 200 torr will drive a normal shock into the conical section).

The Reynolds number in the gap is 5000 based on gap thickness, the unit Reynolds number is 5×10^5 cm^{-1}, flow in the gap should be turbulent.

In the present contract no attempt was made to develop a comprehensive theory. The analysis could, however, be used to calculate a first order estimate of the shear layer in the gap region and thus be lead to an evaluation of deagglomeration by shearing forces. The one-dimensional approach could be improved by developing a more realistic model of the N_2/powder two-phase flow in the pre-expansion section and by accounting for gas/solid effects such as reduced sonic velocity, possible suppression of turbulent mixing, and the effect on other thermodynamic properties and flow phenomena.

1.10 Development evolution of breadboard hardware and test plan

The breadboard hardware went through several design and fabrication iterations prior to the final characterization testing phase. During this hardware development stage the test plan, diagnostics and data reduction techniques also evolved. Throughout this process, NASA was kept informed about TRW's reasoning, plans, and actions. Only the points that illustrate the design rational and hardware issues are presented in this section. The evolution is presented along functional/component lines in roughly chronological order in the following sections.

1.10.1 Chamber - The primary purpose of the breadboard chamber is to simulate the larger GGSF chamber for observing the dust penetration flowfield. A transparent Plexiglas cylinder nominally 2 feet in diameter by 2 feet long, with flat Plexiglas ends was initially chosen as the breadboard chamber. The diameter and length simulate the large (67 L) GGSF chamber, but the actual volume of this chamber is substantially larger (approximately 170 liters) because it has squared off ends rather than hemispherical ends. The larger chamber volume and flat ends were not judged to effect the flowfield in the chamber sufficiently to justify the cost associated with using transparent hemispherical ends. Another purpose of the chamber is to provide a clean, quiescent atmosphere from which dispersed particle can be sampled for deagglomeration testing. The final purpose is to contain the dispersed powder so that the lab and the experimenter are not covered with dust. The chamber as originally purchased was found to perform its functions acceptably without significant modification. An additional Plexiglas end piece with a large opening (8" diameter) was made during the deagglomeration testing phase to allow the particle generator to stand off further from the chamber in order to allow access with some of the optical diagnostics.

1.10.2 Diagnostic instrumentation and control circuits - The fundamental functional components of the breadboard diagnostic instrumentation and control circuits remained fairly stable over the course of the development of the breadboard hardware. Minor changes in the actual transducers, the locations of the transducer and the circuits occurred as the development progressed, but these changes do not warrant a chronology. Generic functional descriptions are given in this section simply to provide a backdrop for the development chronology that follows. More detailed descriptions of the instrumentation and control circuits used in the characterization tests and delivered as part of the breadboard hardware are given in the sections describing those tests.

The gas pressures were set using standard laboratory pressure regulators and the pressure settings were determined using standard laboratory test gauges. The pressure history in the deagglomerator

was monitored by a miniature flush-mount strain-gauge type pressure transducer mounted just upstream of the powder sample. Pressure histories were recorded digitally for subsequent plotting and analysis.

Steady-state gas flowrates were determined using laboratory rotameters. No attempts were made to measure time-resolved, transient, two-phase flowrates.

Time resolved number concentration histories were obtained by recording the intensity of a laser beam(s) passing though the dust cloud near the exit plane of the deagglomerator.

1.10.3 Selection of test powder types, sizes and size distributions - Relatively early in the preliminary testing phase it was decided, with NASA/ARC input, that glass micro-spheres and a geologically representative quartz "dust" would be used as test powder materials. Since the literature indicates that deagglomeration becomes a difficult problem with particles smaller than 10 microns, only powders smaller than 10 microns were considered. The literature gives no indication of successful aerodynamic deagglomeration below 0.1 microns, so the present work was limited to powders larger than 0.1 microns. The GGSF/GGSEM science requirements do not indicate the desired particle size distributions, or whether mono-sized particles are desired. It was assumed that narrow size distributions were preferred by the experimenters in order to make data interpretation easier. Powders with narrow size distributions also make the data collection and interpretation in the present validation testing easier, and such powders are potentially easier to deagglomerate than powders with a wide size distribution.

Based on the consideration discussed above and availability, the following powders were selected as test powders:

- Powder Technologies, Inc. 4170H graded Arizona Test Dust, 5-10 μm diameter
- Duke Scientific Corp. 364 Glass Microspheres, 10.2 μm +/- 1.0 μm diameter, 2.3 μm standard deviation
- Duke Scientific Corp, 257 Glass Microspheres, 2.1 μm +/- 0.5 μm diameter, 0.9 μm standard deviation.

Size distribution and chemical composition data for these powders is shown in Figure 6 through Figure 8, and Table 3. SEM photographs showing individual particle morphologies are included as part of the data and results section of this report.

1.10.4 Powder sample conditioning - The preliminary deagglomeration tests of the Micromerograph were done with the PTI dust as it was shipped to us from the vendor; with no special attention to keeping it dry. We noticed, however, that the Duke Scientific Glass Microspheres are packaged in gas-tight jars with desiccant capsule inside, whereas the PTI dust containers had no such provisions. Duke Scientific verbally indicated that quartz powders are hydrophilic and "disperse" best when "bone-dry." This is consistent with experimental results quoted by Fuchs[25] in which it was found that "fluidization deteriorates with the addition of some hundredths of a percent of water to a powder of glass spheres with r=150 μm". We characterized the moisture content of the PTI Powder we had been using by putting an 11.4 gram sample into an

150 F oven and weighing it at intervals until the weight decrease had stabilized. We then removed it from the oven and weighed it at intervals until the weight increase had stabilized to insure that the measured loss in weight was not due to loss of powder due to handling. Just to be on the safe side, we repeated this cycle once again with the same sample. The results indicate that the PTI dust absorbs about 0.3% moisture by weight when stored as it was shipped to us. The PTI dust does appear to flow more uniformly in the jar when it is dried than when it is moist. Based on the comments by Duke Scientific, Fuchs' quotation, and our qualitative observations, we decided to do all official testing with dry powder. This gave us control of a parameter which is very likely to effect the dispersion of the powder.

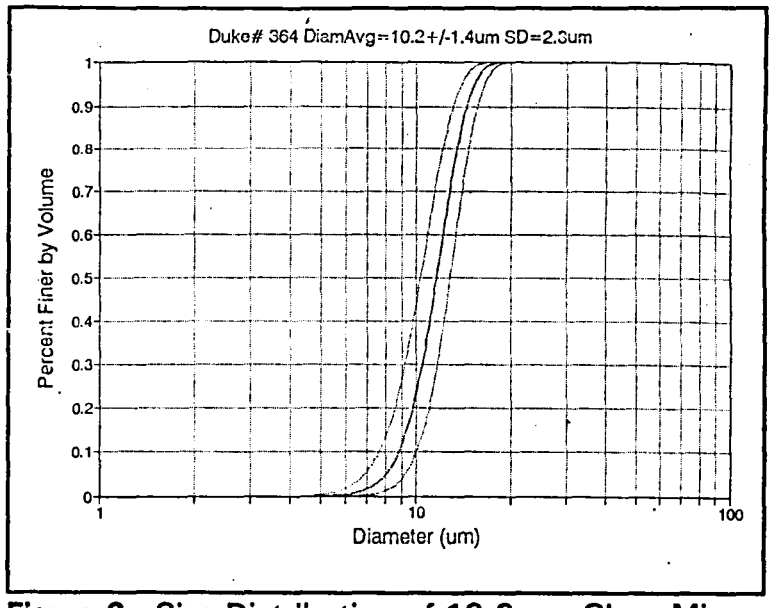

Figure 6 - Size Distribution of 10.2 μm Glass Microspheres.

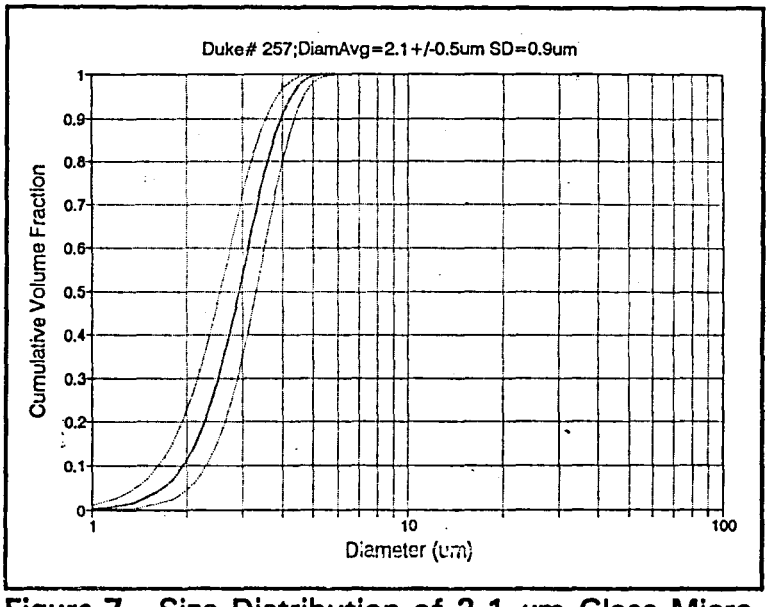

Figure 7 - Size Distribution of 2.1 μm Glass Microspheres.

1.10.5 Flowfield Control - Ideally, the solid particle generator would disperse the particles with just enough momentum that they would stop near the center of the chamber (assuming that there was already gas in the chamber to provide drag to stop them), and with just enough turbulence that the cloud would quickly and uniformly diffuse throughout the chamber.

TRW used a camcorder in conjunction with both flood lighting and light sheet illumination to obtain qualitative flow visualization data of the flowfield produced by both the Micromerograph solid particle generator and the preliminary version of the TRW solid particle generator. These flow visualization tests indicated that at nominal deagglomerator operating conditions and with the chamber at ambient pressure the dusty gas jet impinged on the far wall of the chamber. We were able to "stop" the transient dust/gas jet in the center of the chamber using an opposed transient jet of pure gas produced by a second simulated deagglomerator.

Table 3 -Arizona Test Dust Properties

TYPICAL CHEMICAL ANALYSIS OF PRODUCT LIST PP2G - STANDARDIZED ARIZONA TEST DUST CONTAMINANT COARSE AND FINE GRADES REFERENCE SAE J726 SPECIFICATION			
Chemical	% of Weight	Chemical	% of Weight
SiO_2	65 - 76	MgO	0.5 - 1.5
Al_2O_3	11 - 17	TiO_2	0.5 - 1.0
Fe_2O_3	2.5 - 5.0	V_2O_3	.10
Na_2O	2 - 4	ZrO	.10
CaO	3 - 6	BaO	.10

At NASA's direction, no further work was done concerning the control of the powder penetration and diffusion into the chamber. The opposed jet hardware was not included in the list of deliverable hardware.

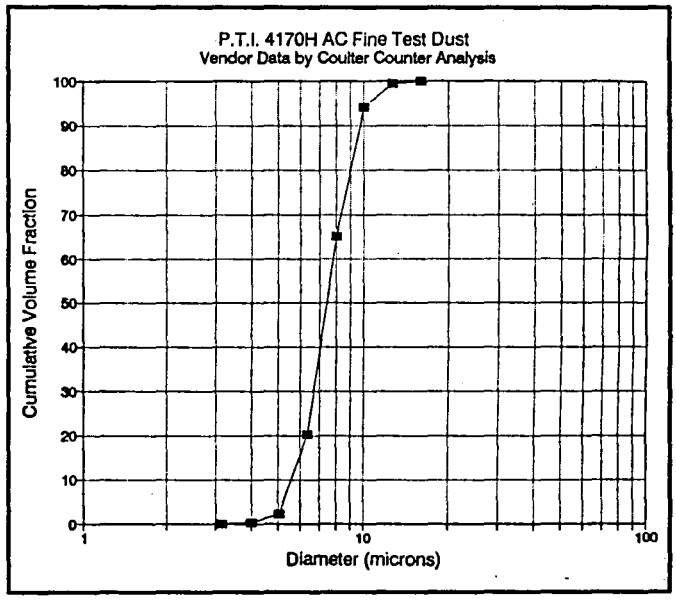

Figure 8 - Size Distribution of 5-10 μm Arizona Test Dust.

1.10.6 Deagglomerator, powder sample holder and concentration control system development chronology and rationale - As the development testing progressed, it became apparent that in Micromerograph design the sample holder subsection and deagglomeration subsection functions are intimately interrelated. The degree of deagglomeration is dependent on the shear in the annular gap, and thus on the gas flowrate. The gas flowrate in turn determines the powder entrainment rate, which in turn determines the particle number concentration presented to the deagglomeration section. The circle is completed by the fact that the deagglomeration efficiency is dependent on the concentration of particles presented to it. Therefore, there was an interrelated, interactive development process for these functional subsections of the hardware. This process resulted in a final design in which the functional subsections are decoupled (or at least much less strongly coupled). The description of the development process that follows cannot be conveniently broken down into functional blocks, however, so the development is described in roughly chronological order.

1.10.7 TRW deagglomeration subsection hardware development - A preliminary version of a deagglomeration section, shown in Figure 9, and powder sample holder, shown in were designed and fabricated based on the fundamental design and dimensions of the Sharples Micromerograph, but which incorporated features making them easier to machine, and more amenable to laboratory use.

Preliminary tests indicated that the male cone (pintle) was not concentric with the female cone of this preliminary version of the TRW deagglomerator, resulting in an asymmetric gap and asymmetric gas/dust flow. Though it is not certain that this necessarily results in degraded deagglomeration performance, the asymmetry makes characterization of the gap setting difficult, and

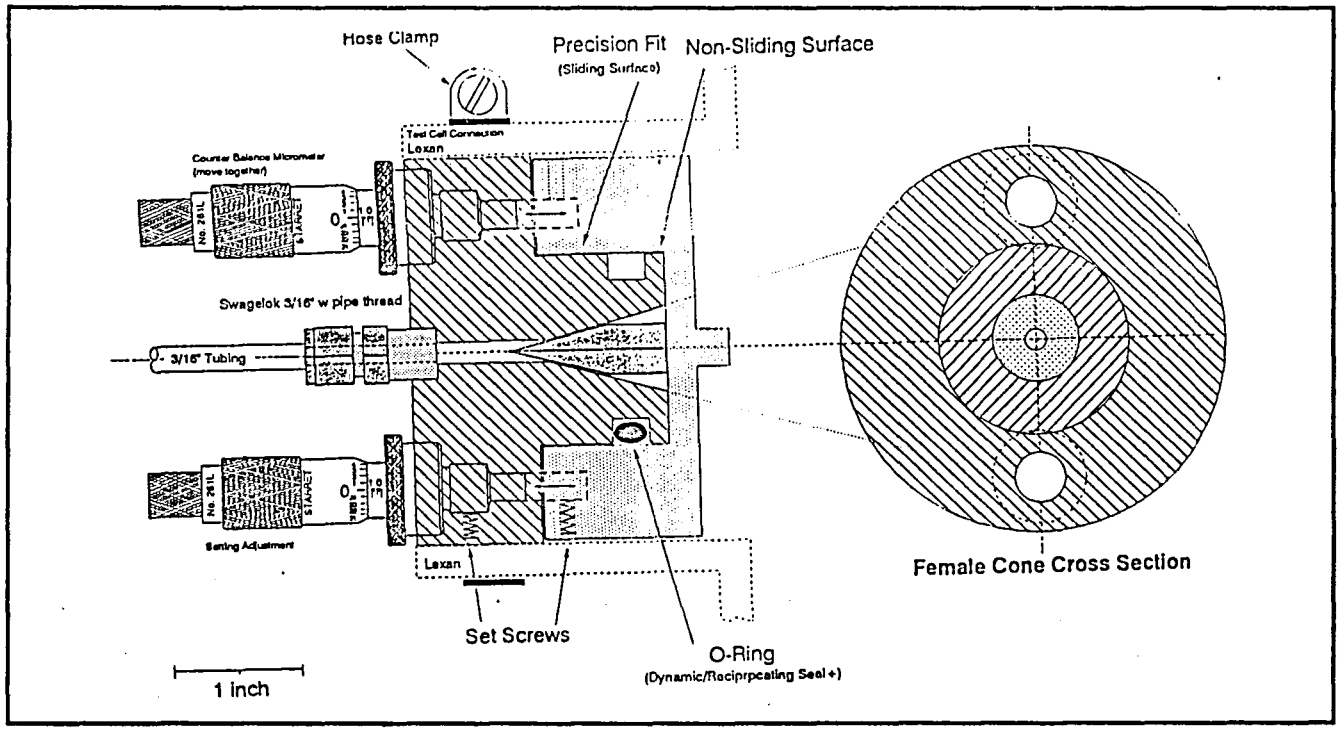

Figure 9 - Section of Aerodynamic Deagglomerator.

the asymmetry was causing dust buildup where the cones touched. The lack of concentricity was found to be due to a combination of factors. First, unequal extension of the two independent micrometers that adjusted the relative positions of the cones would result in the pintle being cocked relative to the female cone. Second, the web holding pintle was not concentric with the female cone. Finally, the male and female cone angle were not well matched. It is not surprising that these issues arose considering tight mechanical tolerances which are required. For example, a 25% eccentricity in a 40 micron gap arises from pintle being just 10 microns (4/10,000ths of an inch) off center. Similarly, a 25% decrease in a 40 micron gap over the 25 mm length of the conical annulus occurs if the pintle is cocked by 0.02 degrees or if the cone angles are different by more than approximately 0.02 degrees.

Several design and fabrication iterations were made using a Plexiglas female cone piece so that the relative positions of the two cones could be visually inspected. Based on this effort, a new design and fabrication procedure evolved which significantly improved the matching of the cone angles, the concentricity of the cones, and the repeatability of the cone positioning.

In the final design machining procedure the male and female cones are turned in a lathe in which the tool post setup is not broken down between operations, so that both cones are machined with the same setting of the tool angle. A spare male pintle was also machined during this process while the tool post was still set up. This procedure results in the accurate matching of the male and female cone angles.

The final design also allows the male cone to "float" in an oversized hole, so that it can be easily aligned in the two translation axes without special tools or jigs. Once aligned, we found that the pintle did not need to be realigned upon disassembly and reassembly. If for some reason it should need realignment, however, or if a new pintle needs to be installed, the realignment process is straightforward. The retaining bolt that holds the pintle into the web is simply loosened allowing the pintle to "float." The gap is the decreased until the male and female cone are in intimate contact (and thus aligned), and the retaining bolt is tightened.

The two adjustable micrometers for setting the slit width were removed. The final design uses insert rings of different thickness to set the slit width. This design minimizes the tendency for the male cone to cock relative to the female cone and allows repeatable repositioning of the cones. This design is not very amenable to automated or remote changes in the gap spacing, however. This issue will need to be addressed this design is to be used in an unmanned space based system.

1.10.7.1 Preliminary deagglomeration tests with the Micromerograph system: While the breadboard deagglomerator design was being finalized, preliminary testing of deagglomeration performance was done using TRW's Micromerograph solid-particle dispersion subsystem. The purpose of this testing was to get a first order indication of the performance potential and to debug the instrumentation and data collection techniques.

The particle dispersion subsystem was removed from the Micromerograph sedimentation column and mounted over the breadboard chamber, facing downward. An open face Nuclepore filter holder (47 mm diameter) was mounted at the bottom of the chamber to sample the fully diluted ("farfield") particle cloud produced by the Micromerograph. Previous flow field visualization had shown that the dust/gas cloud impinges on the far wall of the chamber within approximately 1 second when no opposing jet is used, so there was little chance for reagglomeration to take place. The Nuclepore filters were then be manually examined under an optical microscope to determine the degree of deagglomeration.

In these preliminary experiments with the Micromerograph deagglomerator the deagglomeration performance increased as the total powder sample mass was decreased. Though there was a general trend, the performance did not improve beyond about 65% singlets when the powder mass reduced below 40 mg. Based on high speed movies of the dust entrainment obtained using the TRW preliminary sample holder design, it was hypothesized that this is because the initial flow pulse

impinging at an angle unto the dust bed "plows" up dust which causes an initial spike in the concentration. The initial spike was thought to be only a weak function of the total powder mass in the sample holder.

This hypothesis was tested using a laser transmission diagnostic to obtain time-resolved relative concentration histories at the deagglomerator exit plane and the data are shown in Figure 10. This hypothesis gained support when replotting the data showed that the degree of deagglomeration correlates fairly well with the peak dust mass concentration that occurs during the dust dispersion. This hypothesis gained further support when subsequent tests with a modified sample holder showed that if the peak concentration and the total stored masses are decoupled such that the peak concentration can be varied independently from the total powder mass, the degree of deagglomeration scales with peak concentration and not with total stored mass, as shown in Figure 11.

The fact that the degree of agglomeration achieved in a shear type deagglomerator depends on the dust concentration is documented in the literature[26,27,28] although no general theory is given. Empirical dispersion and agglomeration constants are sometimes given for various types of deagglomerators and operating conditions, but none are available for the Micromerograph.

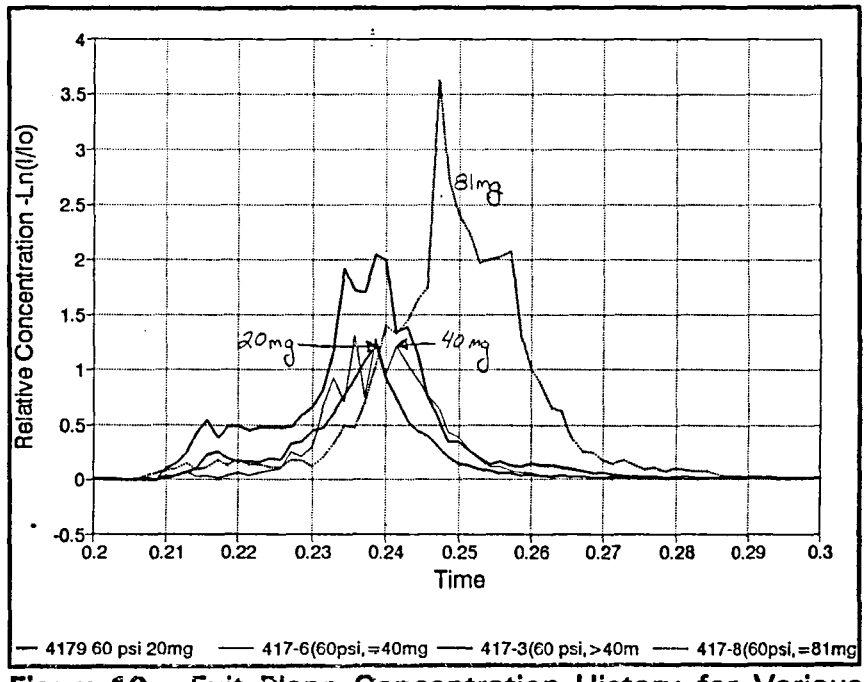

Figure 10 - Exit Plane Concentration History for Various Powder Masses.

Based on preliminary data obtained with the Micromerograph as part of this effort, and experimental results quoted in the literature, TRW and NASA agreed that the test matrix would vary the dust concentration (as indicated by laser transmission data obtained downstream of the deagglomeration section) instead of the total dust mass stored as had originally been proposed.

1.10.7.2 Sample holder redesign: Based on the testing described in the previous section, it was apparent that the sample holder, shown in Figure 12, needed to be redesigned in such a way that the number concentration could be decoupled from the total mass stored so that the deagglomeration efficiency could be improved. In addition, it also became apparent at this time that the sample holder's role in determining the particle concentration was gravity dependent. In the

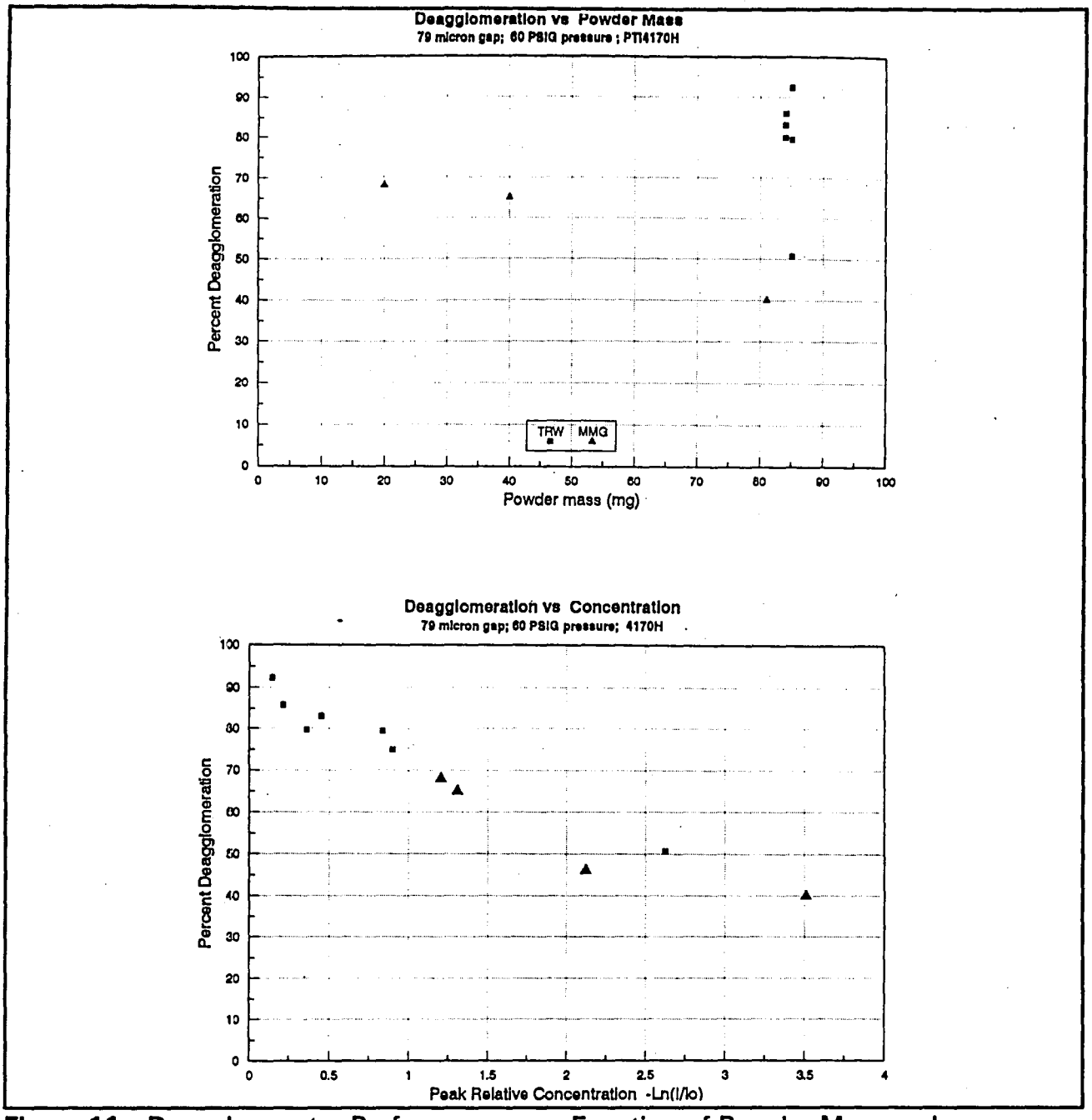

Figure 11 - Deagglomerator Performance as a Function of Powder Mass and Concentration.

Micromerograph (and the original TRW design), the powder sample forms a flat bed at the bottom of a curved channel with an open passageway formed over the dust. The dust metering was initially thought to be done solely by entrainment of the dust by the flow of gas as it flows over the bed of dust. High speed movies, however, indicated that the initial gas flow pulse "plowed" a substantial portion of the dust bed up into the flow, followed by an entrainment type process that removed the

rest of the dust. The time history of the particle concentration presented to the deagglomerator in this design is obviously dependent on the gas flow initially impinging onto the "top" for the powder sample then flowing "over" the powder sample. This is a gravity dependent situation, since in 0-g there is no way to insure that the powder will be at the "bottom" of the sample holder as it is in 1-g. Thus, there were two compelling reasons to redesign the sample holder.

The redesign effort was a two pronged approach which addressed both issues simultaneously by mixing dilution gas with the dusty gas flow downstream of a gravity independent sample holder but prior to the deagglomerator. Several design and fabrication iterations were required to obtain a satisfactory design. The design considerations for the "premixer" dilution scheme and for the gravity independent sample holder are described in the next sections, followed by a section describing the testing.

Dilution gas "premixer" Design Considerations

The fundamental concept is simply to add gas to the dust laden gas stream after it leaves the sample holder and before it reaches the deagglomerator in order to reduce the mass concentration of dust entering the deagglomerator. Conceptually, an arbitrarily reduced particle number concentration can be obtained by adjusting the flowrate of dilution gas relative to the dust-gas flowrate and providing adequate mixing.

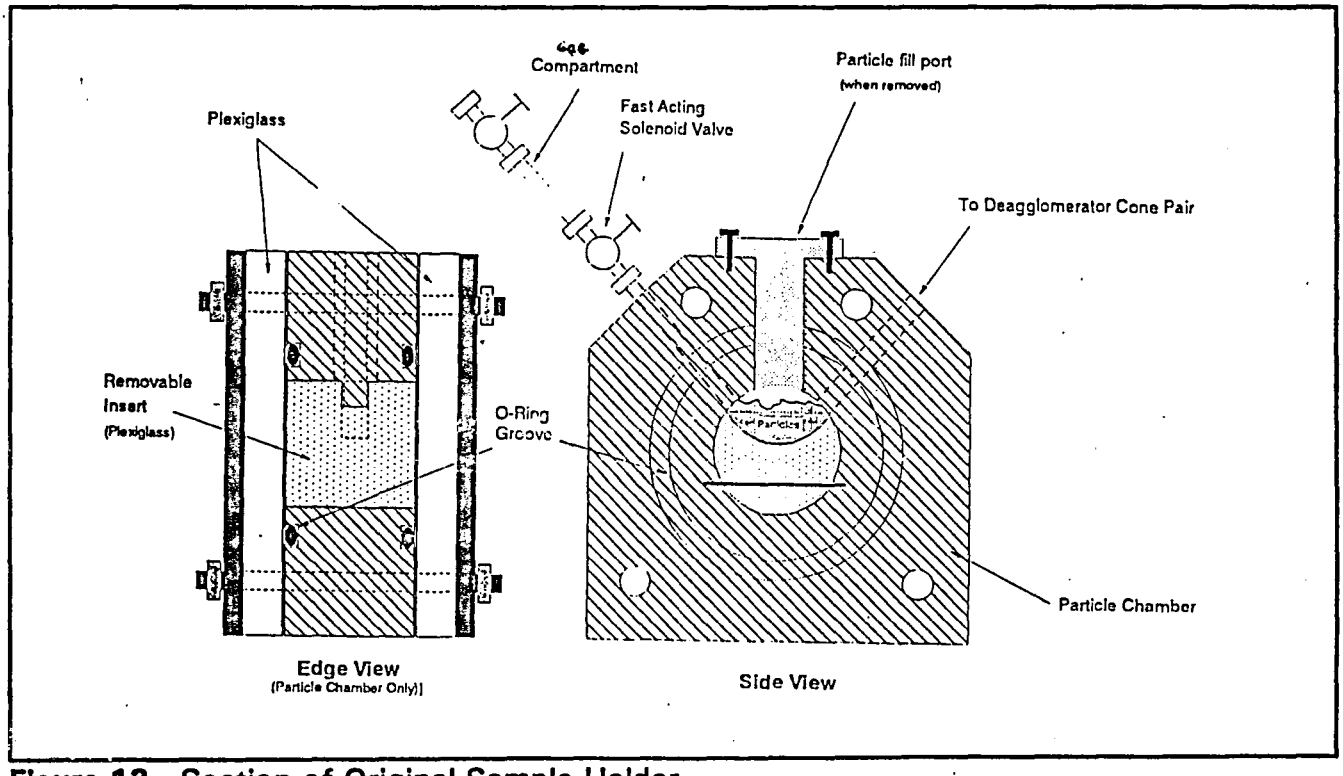

Figure 12 - Section of Original Sample Holder.

The mixing energy can be provided both by the dusty gas flow and by the dilution jets. The velocities in the mixing sections should be kept high enough to prevent particle settling or build up on the wall.

The dilution section must break up the powder into manageable aggregates and mix it with a sufficient (but not excessive) amount of gas prior to reaching the deagglomerator. This process must be repeatable and predictable, of course.

0-g Sample Holder Redesign Considerations

The foremost requirement of the sample holder is that all of its functions be performed completely independent of gravity. The role of gravity in most sample holders is to control the location of the powder within the holder, which allows energy to be concentrated in a particular location. For example, the powder may be held at the "bottom " of a flask with gas flow directed at the "bottom" of the flask with a gas exit at the "top" of the flask. This allows the local energy to exceed the cohesive and/or adhesive binding energy of the powder particles to each other or to the walls.

Gravity independent operation requires that either the functioning of the sample holder be completely independent of the powder's position within the sample holder volume, or else that the powder's position within the sample holder volume be controlled without relying on gravity.

If the sample holder volume is substantially larger than the total volume of powder, the breakup of the powder mass into manageable size aggregates and the subsequent mixing of these aggregates with the carrier gas can all be accomplished within the sample holder volume. However, in this case it is virtually impossible to know *a-priori* where within the sample holder the powder will be located at the start of a test. Therefore, enough energy must be imparted uniformly throughout the entire volume to break up and mix the powder, wherever it may be. If the flow energy is not concentrated, then an excessive amount of gas is required. The only apparent way out of this dilemma would be to put a fan in the sample holder to impart energy to the gas stored in the sample holder without requiring additional gas.

If the sample holder volume is virtually the same as the total stored powder volume, it is obvious that the powder location is very well controlled without relying on gravity. In this case, though, the powder cannot be broken up and mixed within the sample holder volume since the powder already completely fills the sample holder volume. Therefore the powder must be moved from its storage location into a larger volume where it can be broken up and mixed. Thus either a mechanical or aerodynamic metering is required. An additional consideration for this type of design is the form-factor of the sample holder volume, for example whether it is preferable to use a long narrow tube, a spherical volume or a large thin disk. The choice of form factor depends on how the dust is to be moved from its storage location to the mixing location.

The total mass (and therefore total volume) of powder that must be stored and dispensed obviously impacts the design of the sample holder. The mass of powder required is determined by the science requirements for the particle number densities. The volume of powder is found by dividing the required mass by the bulk density of the powder in its "loose-packed" form. Using Experiment no.

5 as a straw-man design goal, the required particle number density for nominally 10 μm diameter particles ranges from $1x10^3$ to $5x10^4$ particles per cc (see Figure 1). For the 67 liter chamber this corresponds to a range from a low of

$$67\ x10^3\ cc\ x\ 1\ x10^3\ particles/cc = 6.7\ x10^7\ particles$$

to a high of

$$67\ x10^3\ cc\ x\ 5\ x10^4\ particles/cc = 3.3\ x10^9\ particles$$

The mass per particle is found from the particle volume times the particle density as

$$4/3\ x\ 3.14\ x\ (5x10^{-4}\ cm)^3\ x\ 2.5\ g/cc = 1.3\ x\ 10^{-9}\ g/particle$$

Thus the range of particle masses required using 10 μm particles for experiment 5 is from

$$6.7\ x10^7\ particles\ x\ 1.3\ x10^{-9}\ g/particle = 8.7\ x10^{-2}\ g$$

to

$$3.3\ x10^9\ particles\ x\ 1.3\ x10^{-9}\ g/particle = 4.3\ g.$$

The bulk density of the PTI powder is about 1 gram/cc, so the sample holder volumes for this type of powder in this particle size must range from 0.087 cc to 4.3 cc.

Sample Holder Redesign Tests

TRW built prototype versions of several sample holder designs based on sample holder volumes significantly larger than the total powder volume, and several versions based on sample holder volumes which equal to the bulk volumes of powder. Several variations on each of these basic designs were attempted. These prototype designs were built from transparent materials so that the powder flow could be seen and videotaped. Designs that showed promise based on visual observation were also characterized using the laser transmission signal at the deagglomerator exit location.

In the initial design, the function of the sample storage and sample dilution are combined in one component. The first series of tests were done with a swirl chamber that had tangential injectors. The second device was a modified DeVilbiss Model 175 Dry Powder Blower. Both these design variations were found to be unacceptable for several reasons. First, the flow energy was not well distributed throughout the chamber volumes, allowing recirculation zones where the particles would collect or "dead" zones where the particles would fall out. Second, particles tended to coat the walls of the chambers, since the shear at the walls was very low. Due to the large surface area of the wall, a significant fraction of the powder was left on the walls. Therefore, the very large sample holder volume designs were not pursued any further.

The first design in which the sample holder dimensions were equal to the bulk powder dimensions was simply a logical extension of the Micromerograph design. In the Micromerograph sample holder the dust sample sits in a flat bed at the bottom of a curved channel with an open passageway formed over the dust. Our thought was that if we were to fill the channel entirely with the dust we would have a gravity independent holder, but with the high dust concentration characteristics of the leading edge of the present Micromerograph. Therefore, if we were to add a subsequent dilution section we could reduce the dust concentration in a controllable manner to an acceptable level. To this end we built a device which hold approximately 80 mg of PTI dust in a 0.10" diameter by 0.50" long cylinder. This cylinder is followed by an 12" long section of 0.125" ID Plexiglas tubing which has three sets of opposed 0.020" diameter jets at approximately 4" spacing. The results obtained with this device were highly encouraging, with the minimum concentration for 72 mg of PTI 417 dust being approximately 70%. The only drawback of this design is the limited amount of dust it holds.

The next design was an attempt to simply increase the volume of dust. In this design we used a cylindrical sample holder 1/2" in diameter by 2" long (6.5 cc max volume). This large diameter cylinder was joined to the 1/8" ID Plexiglas tube by a 7.5 degree half angle cone. This design failed to exhaust all the dust from the cylinder. All the dust that was below the level of the 1/8" tube section remained in place for any reasonable gas flow. Obviously this design had a major flaw in 1-g operation, apparently because the flow rate and/or shear in the large cross section is insufficient to move the dust up the incline from the large diameter section to the smaller diameter section.

The next design variation was to put an Plexiglas insert into the large diameter cylindrical storage section to reduce the diameter to 1/4" (and thus increase the flowrate for a given gas pressure and remove the need to "push" unsuspended dust up the incline). We were able to repeatably exhaust all the dust from this chamber. When we used glass microspheres (Spheriglass #5000 glass beads) we were able to achieve a relatively uniform laser transmission signal throughout the course of the dust dispensing, with the exception of a high concentration pulse at the end. The PTI 4170H graded Arizona test dust did not behave as well, however. With this powder, the concentration history was very sensitive to the "push" flow to dilution flow pressure ratio, and would go from no dispensing at all to dispensing too rapidly with just a 1 or 2 psi change in pressure. It was virtually impossible to get predictable, repeatable results with this dust in this design.

We then decided to try using a plunger to mechanically push the dust plug out of the 1/4" ID Plexiglas insert into the dilution/mixing region. We found several surprising results with this setup. First, the plunger tended to "stick" when the dust plug was under pressure, even though it moved freely with the dust plug at ambient pressure or with no dust at but at full pressure. Second, even when the plunger was pushed at a slow steady rate, the resulting transmission signal was unsteady and had several regions of low transmission. Third, 1" to 2" long sparks were produced which appear to originate at the end of the dust plug ad whose timing seemed to correspond to the high concentration "lumps" in the transmission signal. Our current explanation for these effects is that the dust is packing more densely when the static pressure is raised because the gas does not have time to diffuse throughout the particles and equalize the pressure. The increased packing causes the hard, sharp quartz particles to dig into the softer Plexiglas and lock the dust plug into place. Any

irregularities in the initial packing are magnified when the gas pressure increase causes additional packing. These inhomogeneities cause the plug to break apart irregularly, resulting in the lumpy characteristic of the laser transmission signal. When large lumps of the dust plug break off, a large charge imbalance is created, leading to the sparking which was observed.

In order to alleviate the sticking of the dust plug and the sparking, we fabricated a polished stainless steel insert. This in fact did eliminate the sticking, although not the sparking. In an attempt to reduce the lumpiness of the plug breakup we moved one of the breakup jets to the inner diameter of the insert. We were still not able to eliminate the lumpy breakup, however.

At this time we decided to go back to the first design, with which we had achieved the most repeatable, reliable results.

Based on the decision to use this concept as the basis for our design, we built a metal version of it and did three repeated tests to verify its repeatable consistent response.

Method For Extending the Range of Powder Masses of the Sample Holder

In the final design, the dust sample is contained in a cylindrical volume which is equal to the bulk volume of about 75-100 mg of PTI dust. This amount of dust is just barely sufficient for the lower limit of experiment #5's requirement for 10 μm particles, as interpreted in the Phase A study. In order to dispense the amount of dust required for the upper limit of experiment #5, 50 to 60 such volumes would need to be dispensed. We propose a system that is similar to the revolver in a pistol. A large, thick cylinder would have 40-60 holes drilled in it at equal intervals. These holes would be filled with dust, and stationary plate at the front and back of the cylinder would trap the dust in the holes. The cylinder would sequentially rotate each hole into alignment with the gas source and the dilution/mixing tube. While the hole and the tube are aligned, the dust would be ejected from the hole into the mixing section. The result of this type of mechanism would be a series of "puffs" of dusty gas mixture into the chamber.

In summary, several gravity independent sample holder design concepts were fabricated and tested. Based on these tests, a design concept was chosen which meets all the requirements listed above except the first. The design can be extended to an arbitrarily large total mass of powder, however, by adding a mechanical device (e.g., stepper motor) to sequentially bring powder "cartridges" into position. The deagglomeration performance testing was done with a single powder "cartridge", without building the mechanical loading device in order to be able to meet the test plans within budget.

2 BREADBOARD DESIGN

2.1 Solid Particle Generator

The TRW solid particle generator is comprised of three main functional blocks: the powder sample holder, the dilution control system and the deagglomerator. A schematic representation of the solid particle generator is shown in Figure 13.

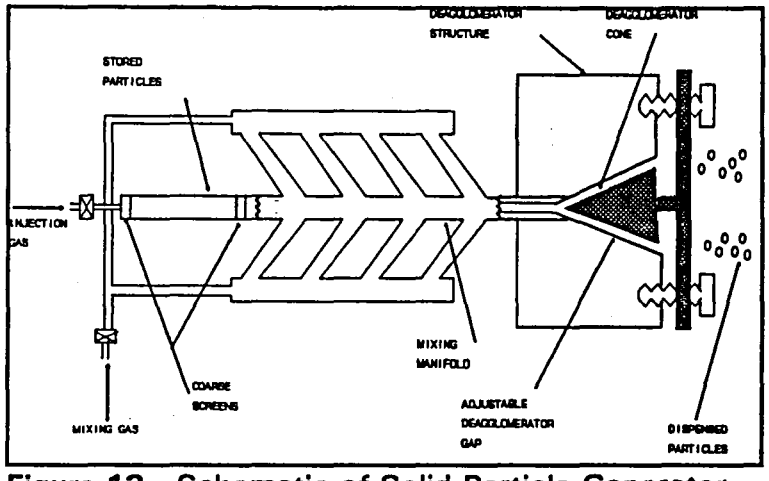

Figure 13 - Schematic of Solid Particle Generator.

2.1.1 Sample Holder - The final breadboard hardware version of the powder sample holder is strictly a laboratory proof-of-principal implementation of the design concept. When reading the hardware description, keep in mind that there are proposed modifications that would allow it to fly on the KC-135, which are in section 9.2 "Design and Engineering Improvements".

The sample holder consists of a 1.40" long section of 3/16" diameter 6061-T6 aluminum tube with an inner diameter of approximately 0.112". This tube is terminated at one end with a Swagelock connection to a 3/16" swagelock tee. There is a 400 mesh stainless steel screen sandwiched between to 80 mesh screens at the junction between the tube and the tee. These screens hold the powder in the tube as the powder in poured into the opposite end of the tube to form a cylindrical plug of loosely packed dust. Although the opening in the 400 mesh screen are larger than the particle diameter, the powder cohesion allows the powder to bridge the openings. The mass of dust determines the height to which the dust plug fills the tube. The length of the powder holder tube can potentially accommodate up to 200 milligrams of PTI dust, though only 85 mg has been tested in it to date. Once loaded into the tube the powder can be lightly packed by dropping a #34 drill blank or the rear of a #34 drill (provided with the hardware) down the open end of the tube onto the dust plug. In this state the powder will remain as a dust plug when the tube is put into a horizontal position. The dust plug will also remain in place if the sample holder is inverted and held with the open end facing down. In the present hardware there is no provision for closing off the open end of the tube to insure that the plug of dust remains in place, so the experimental procedure must not shake or jar the sample holder if it is in a horizontal position prior to firing.

The open end of the sample holder mates to the dilution section via a "swagelock" fitting. Since this connection is made and broken for each test, nylon ferrules were used. The screened-off end of

the sample holder mates with a ASCO model 8262G11 solenoid valve which controls the timing of the gas flow that dispenses the powder.

2.1.2 Concentration Control System - The concentration control system consists of four pairs of opposed jets that inject dilution gas into the main flow. Each pair of opposed jets (Figure 14 and Figure 15) consists of a 3/16" swagelock union with two pieces of 1/16" tubing penetrating the opposite walls at approximately 20 degrees. The 1/16" tubes are silver soldered onto the modified swagelock union.

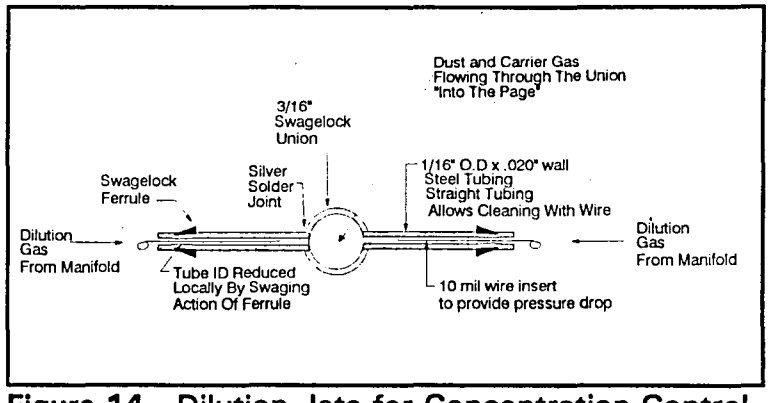

Figure 14 - Dilution Jets for Concentration Control.

Thick wall (.020") 1/16" tubing was used to obtain a high intrinsic pressure drop and to keep the velocity in the tubes high. The swagelock ferrules on the 1/16" tubing were purposely over-tightened to swage down the tube inner diameter locally by a few thousandths of an inch. This local restriction was then able to be further constricted to various degrees by inserting wires of different diameters (included with the breadboard hardware), as discussed in the previous section. The 1/16" tubes were kept straight so that cleaning wire can be inserted in the event of clogging.

The pressure drops obtained with this system using .010 inch diameter wires and the nominally 80 micron slit width are shown in Figure 16. The operating range of the dilution flow can be read from this figure for a given desired deagglomeration pressure. The range of dilution pressure settings that can be used for a 60 psig deagglomeration condition are illustrated in Figure 16 by the arrows. Dilution gas flows are limited on the low end since the dilution flow manifold pressure must be greater than the required deagglomeration pressure. High dilution gas flows are limited by the mixing plenum chamber pressure which must be lower than the deagglomeration pressure.

Obviously, a different set of dilution flow pressure setting ranges will result from the different back pressures produced at different slit widths and with different inserts in the jets. The operating ranges for all the slit width and insert combinations used in the final hardware deagglomeration characterization tests are shown in Figure 16 through Figure 21.

The swagelock union forming each opposed jet pair is followed by a 1.25" long section of 0.125" inner diameter T6061 aluminum tubing to promote mixing. There is an 80 mesh steel screen across the tube at the exit of each swage lock union, again to promote mixing.

The 1/16" dilution jet tubes are fed by a manifold of 1/8" copper tubes carrying dilution gas from the dilution flow solenoid valve (ASCI model 8262G11).

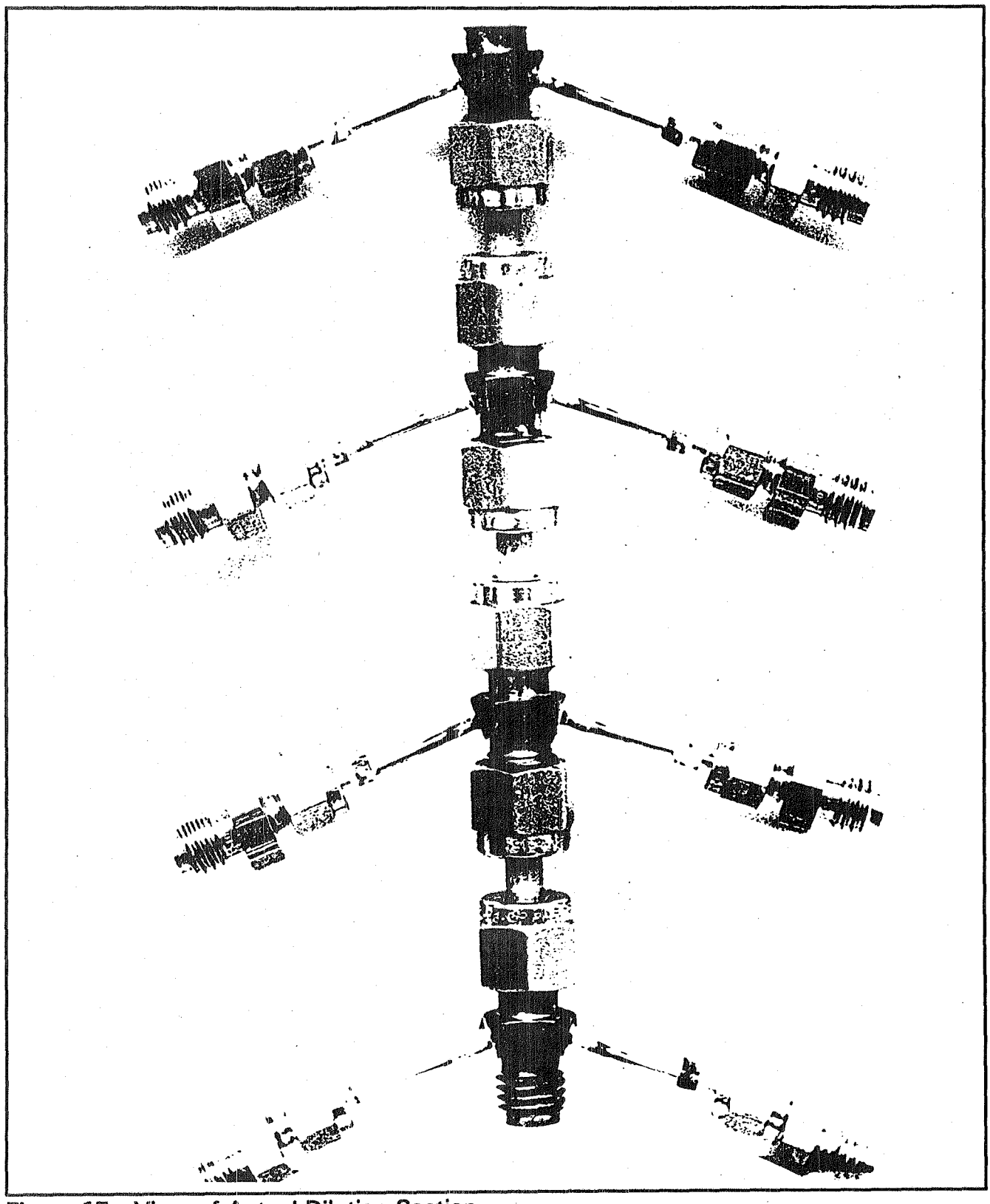

Figure 15 - View of Actual Dilution Section.

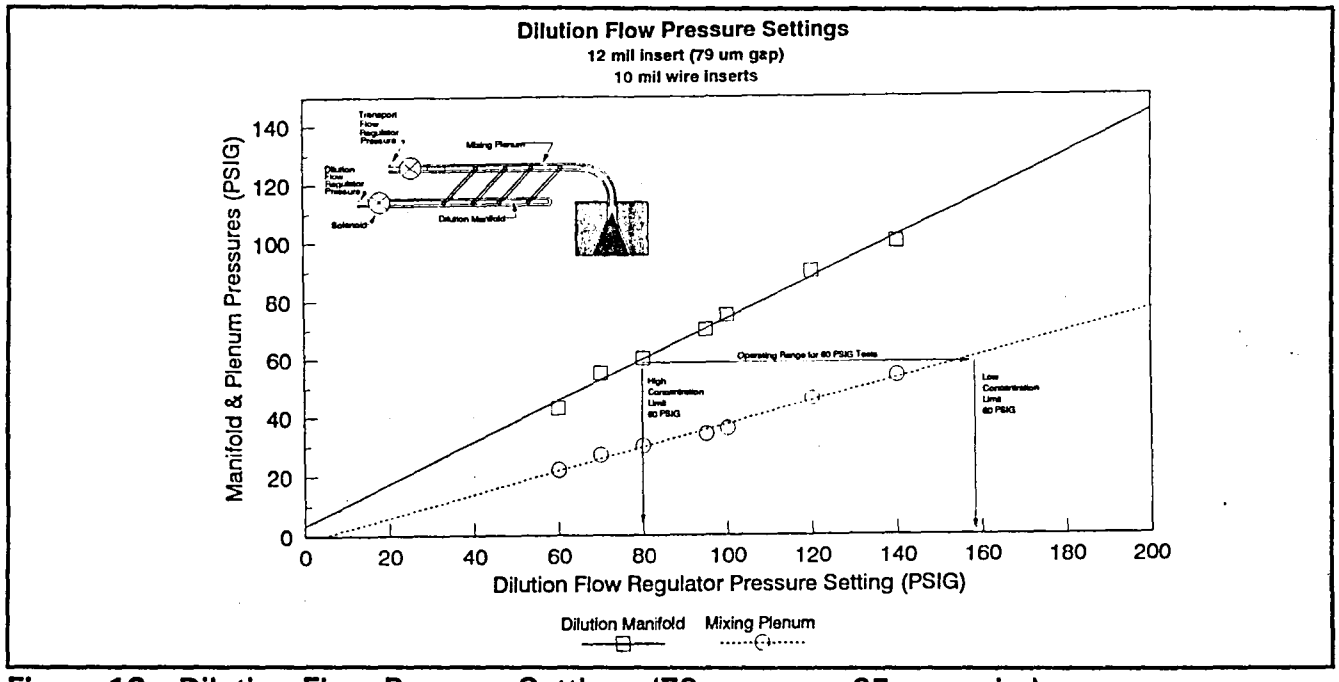

Figure 16 - Dilution Flow Pressure Settings (79 μm gap, .25 mm wire).

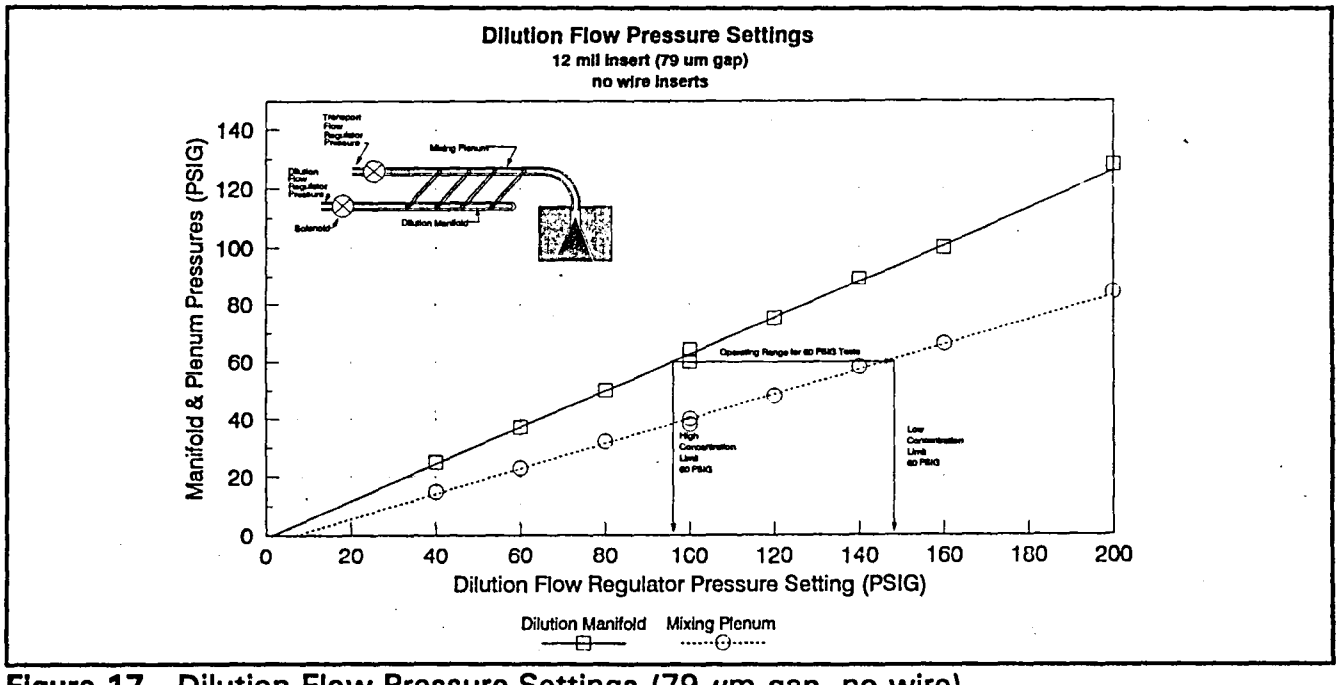

Figure 17 - Dilution Flow Pressure Settings (79 μm gap, no wire).

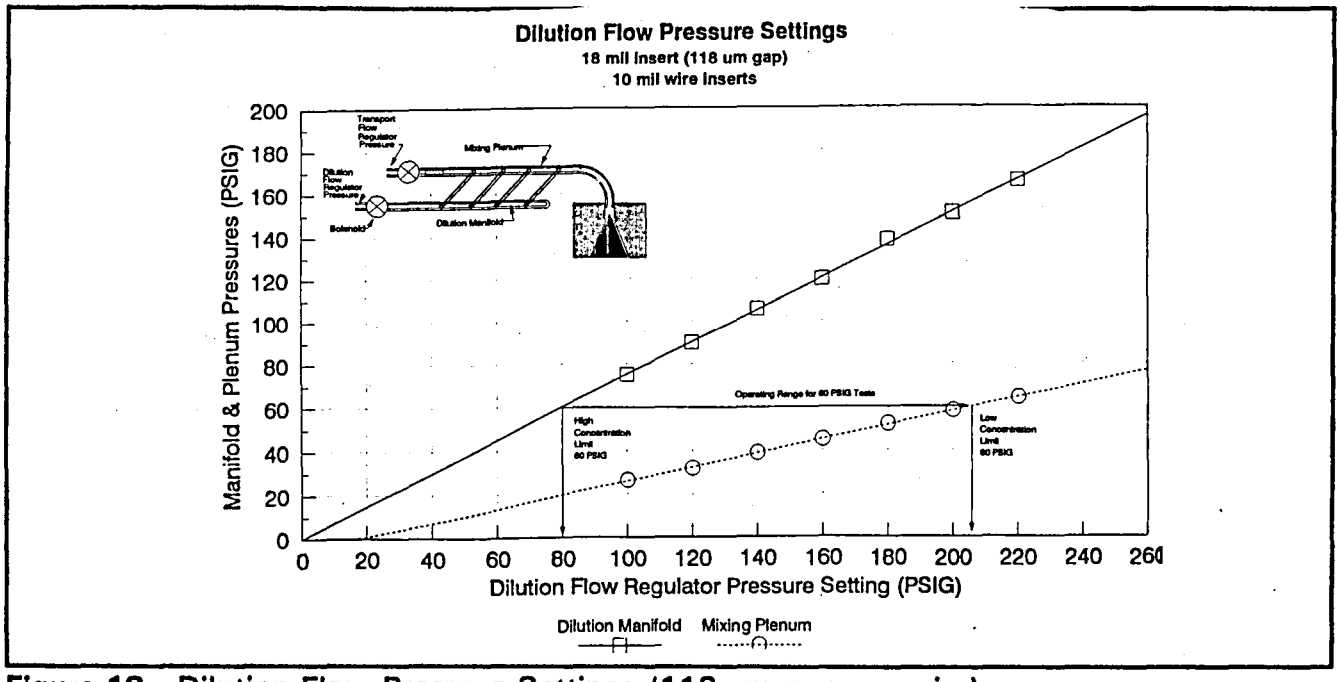

Figure 18 - Dilution Flow Pressure Settings (118 μm gap, no wire).

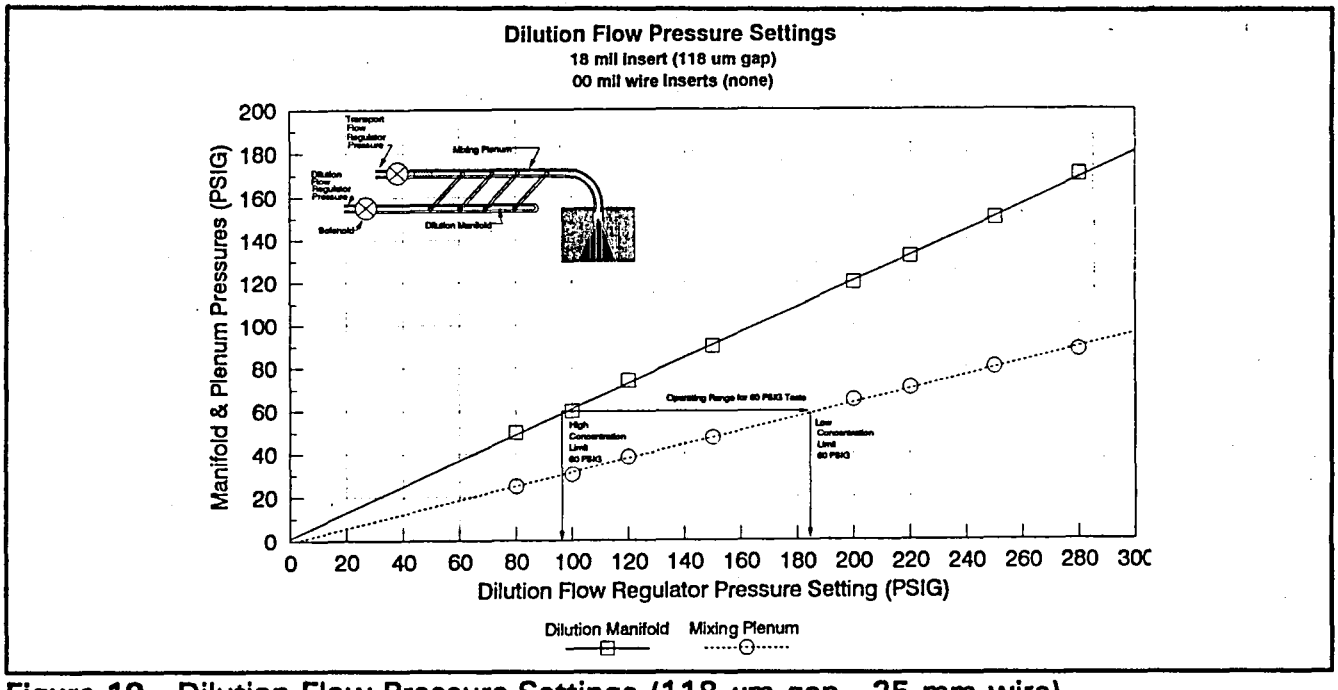

Figure 19 - Dilution Flow Pressure Settings (118 μm gap, .25 mm wire).

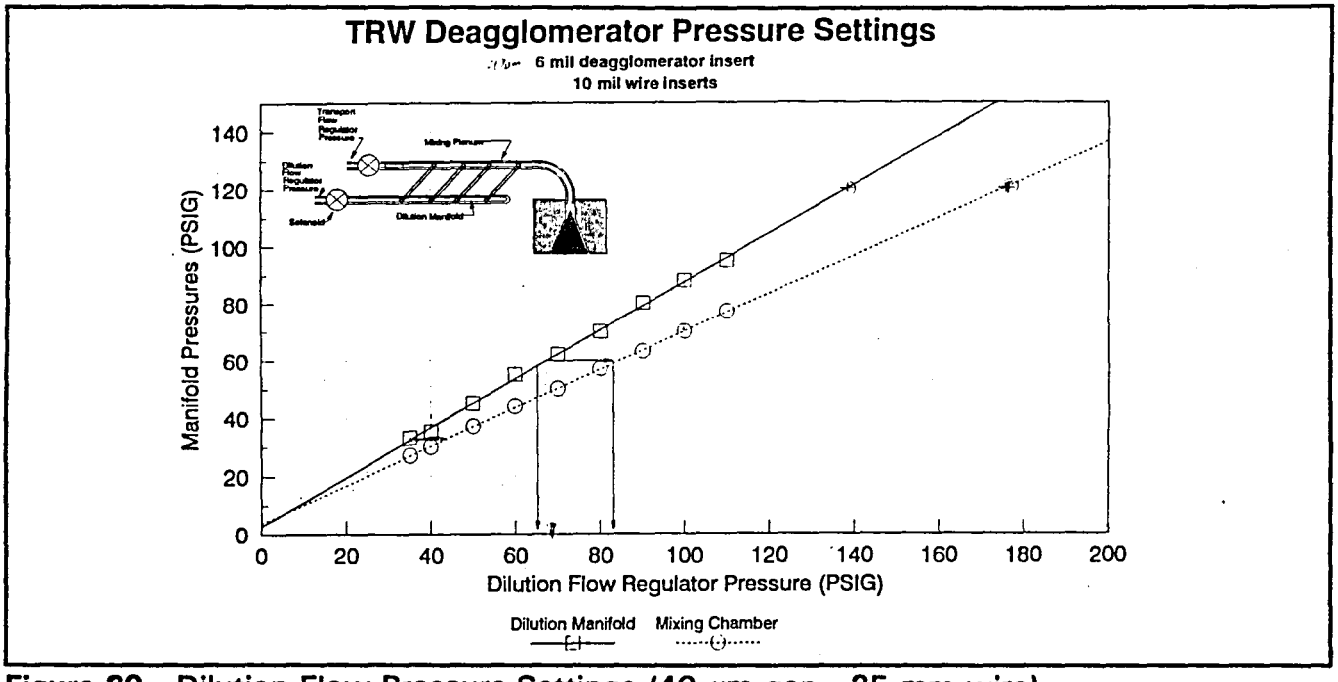

Figure 20 - Dilution Flow Pressure Settings (40 μm gap, .25 mm wire).

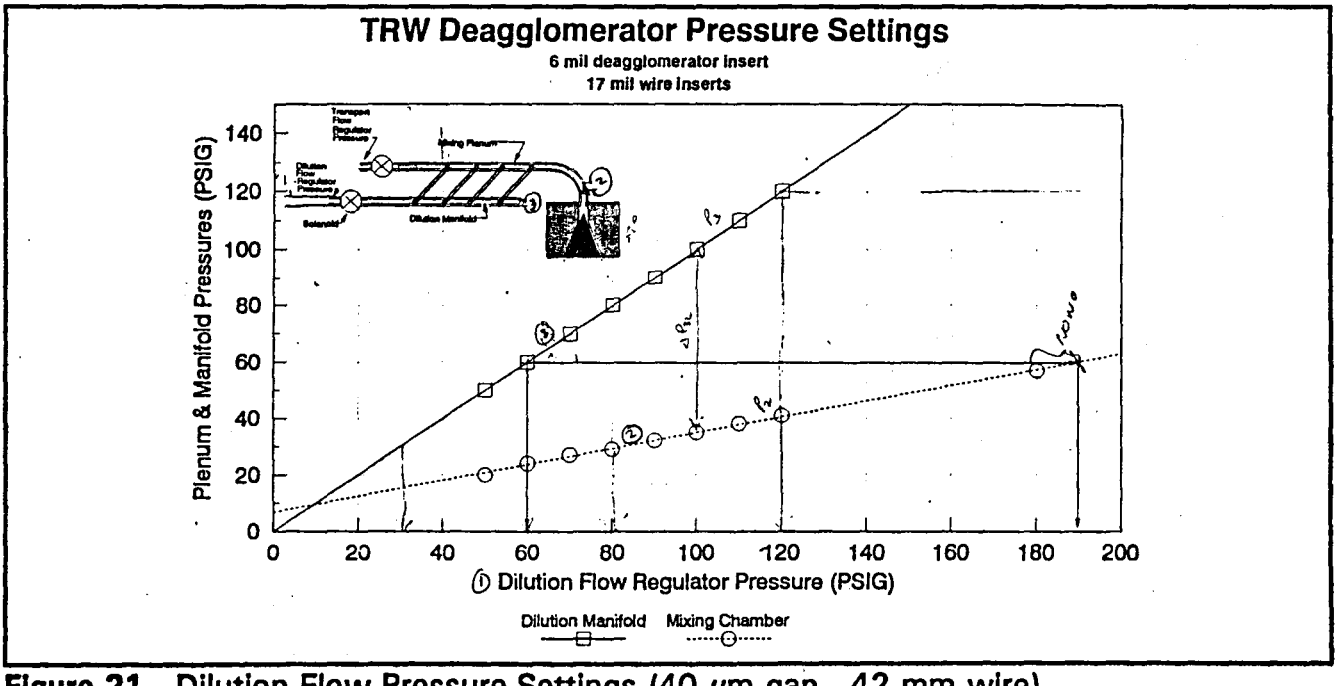

Figure 21 - Dilution Flow Pressure Settings (40 μm gap, .42 mm wire).

2.1.3 Deagglomerator - The deagglomerator section, shown in Figure 22, consists of a pair of concentric cones with an adjustable gap, or slit width, between the cones. The dimensions of the cones and the tubing leading up to the cones are approximately the same as those of the Micromerograph. A spare male cone (pintle) is provided with the breadboard hardware.

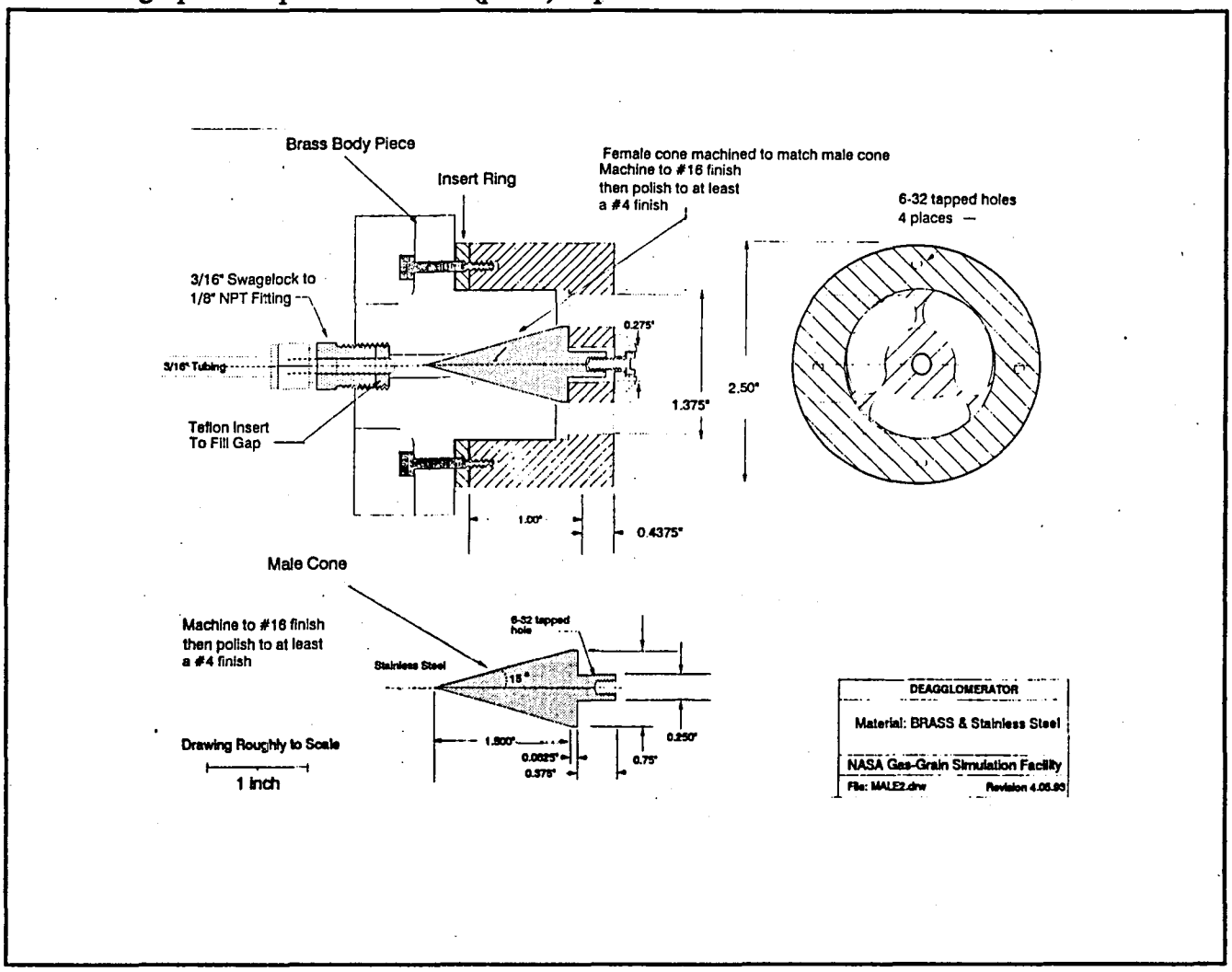

Figure 22 - Final Version of the Deagglomerator.

The breadboard hardware design uses insert rings of different thickness to set the slit width. Four insert rings corresponding to slit widths of 39, 79, 118 and 145 microns are included as part of the breadboard hardware.

The steady-state flowrates of pure GN_2 through the deagglomerator are shown in Figure 23 as a function of upstream pressure for the four gap settings.

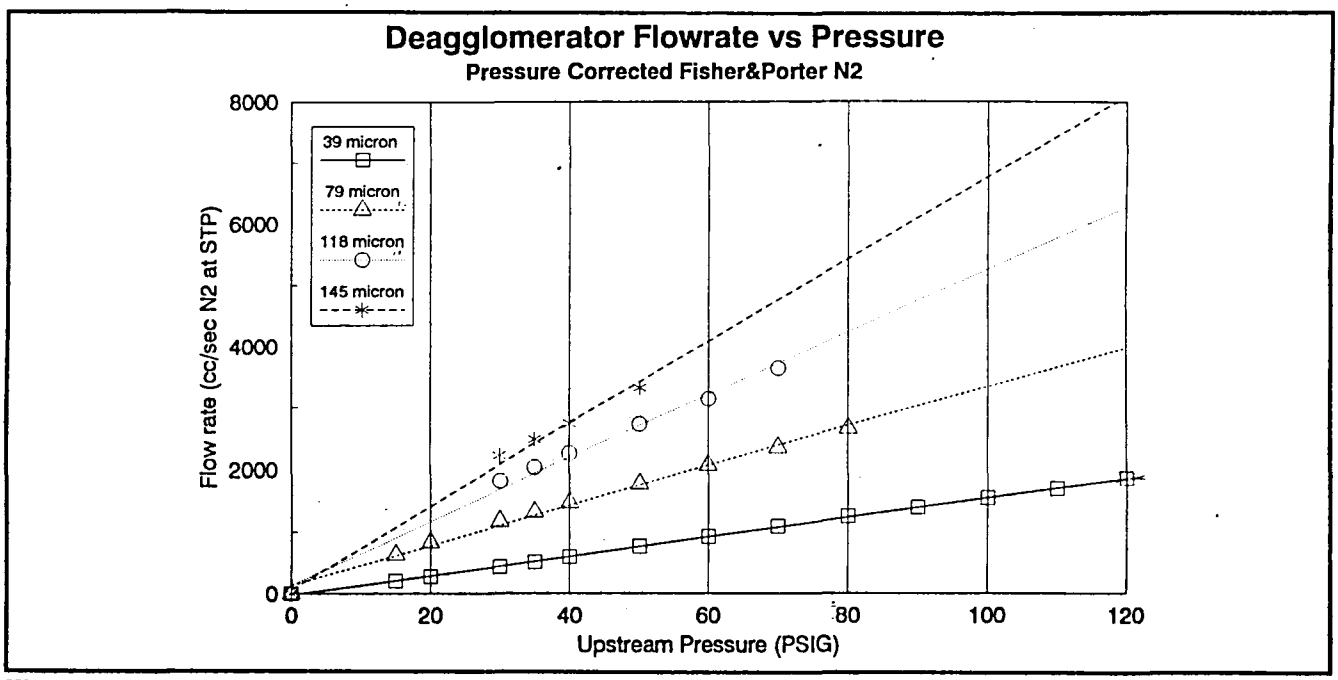

Figure 23 - Deagglomerator Flowrate vs. Pressure at 4 Gap Settings Used.

2.2 Chamber

The breadboard chamber consists of a transparent Plexiglas cylinder nominally 2 feet in diameter by 2 feet long, with flat Plexiglas ends. The diameter and length simulate the large (67 L) GGSF chamber, but the actual volume of this chamber is substantially larger (approximately 170 liters) because it has squared off ends rather than hemispherical ends. The larger chamber volume and flat ends were not judged to effect the flowfield in the chamber sufficiently to justify the cost associated with using transparent hemispherical ends. An additional Plexiglas end piece with a large (8" diameter) opening was made during the deagglomeration testing phase to allow the particle generator to stand off further from the chamber in order to allow access with some of the optical diagnostics without modifying the existing endpiece.

2.3 Instrumentation and control circuits

The control circuit provides the timing for the opening of the two solenoid valves on the solid particle generator, and it provides a signal for timing reference or for triggering a data acquisition system. This circuit drives the solenoids directly via two solid state relays. This timing can be initiated manually using a pushbutton switch on the front panel or by driving a TTL input low using the BNC connection on the front panel. The control circuit has thumbwheel switches on the front panel for individually setting the delay and duration of the opening of each solenoid valve. A schematic of the control circuit is included in the appendix.

The solid particle generator instrumentation consists of two pressure transducers for monitoring the pressures in the deagglomerator and dilution control sections, and three laser/detector pairs for monitoring particle concentration at the exit plane.

The pressure transducers are miniature flush-mount stain gauge type pressure transducers (Entran EPX-10W-250) with sub-millisecond response. The pressure transducers have a range of 0-250 PSIG and provide a signal of approximately 0.5mV per PSIG when excited with 10VDC. The data sheets (including calibration) for these transducers are included in the appendix. The pressure transducers are mounted into the bodies of each solenoid valve on the downstream side of the valve.

The lasers are InGaAlP laser diodes (LaserMax MDL-100-670-3) which provide approximately 3 mW at 670 nm. The lasers are powered by 6VDC supplied by wall-transformer type power supplies (provided as part of the hardware) or they can be powered by batteries (not provided as part of the hardware). The lasers have been mounted in aluminum standoffs that also function as heat sinks, so if the decision is made to move them to other locations they should remain in the aluminum standoffs unless alternate heatsink is provided. The aluminum standoffs are mounted such that the three laser/detector pairs form a plane approximately 75 mm downstream of the deagglomerator exit as indicated in Figure 24. The detectors are large area silicon photodiodes (UDT-PIN-10DP) connected to 1K ohm load resistors which convert the photocurrent into a voltage signal. The photodiode/load resistor combination's linearity has been verified up to an output signal of 250 mV (see Figure 25), and in their present configuration the unattenuated signal is approximately 200 Mv.

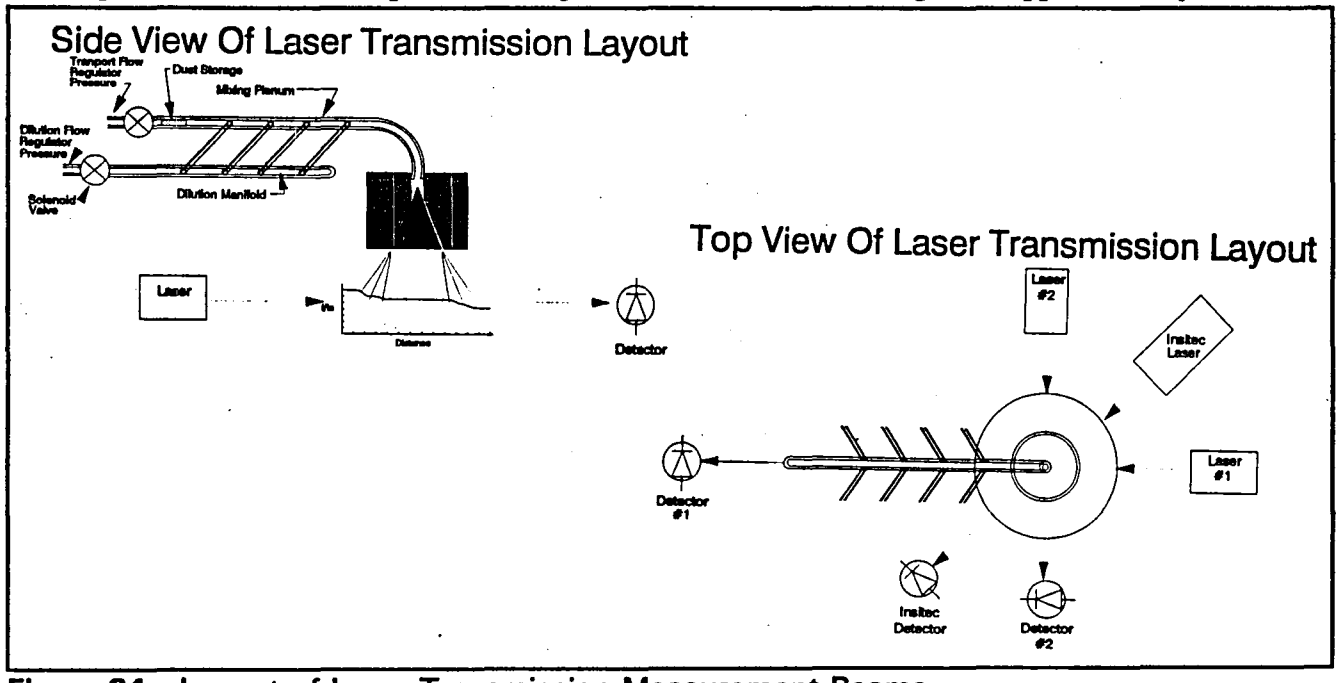

Figure 24 - Layout of Laser Transmission Measurement Beams.

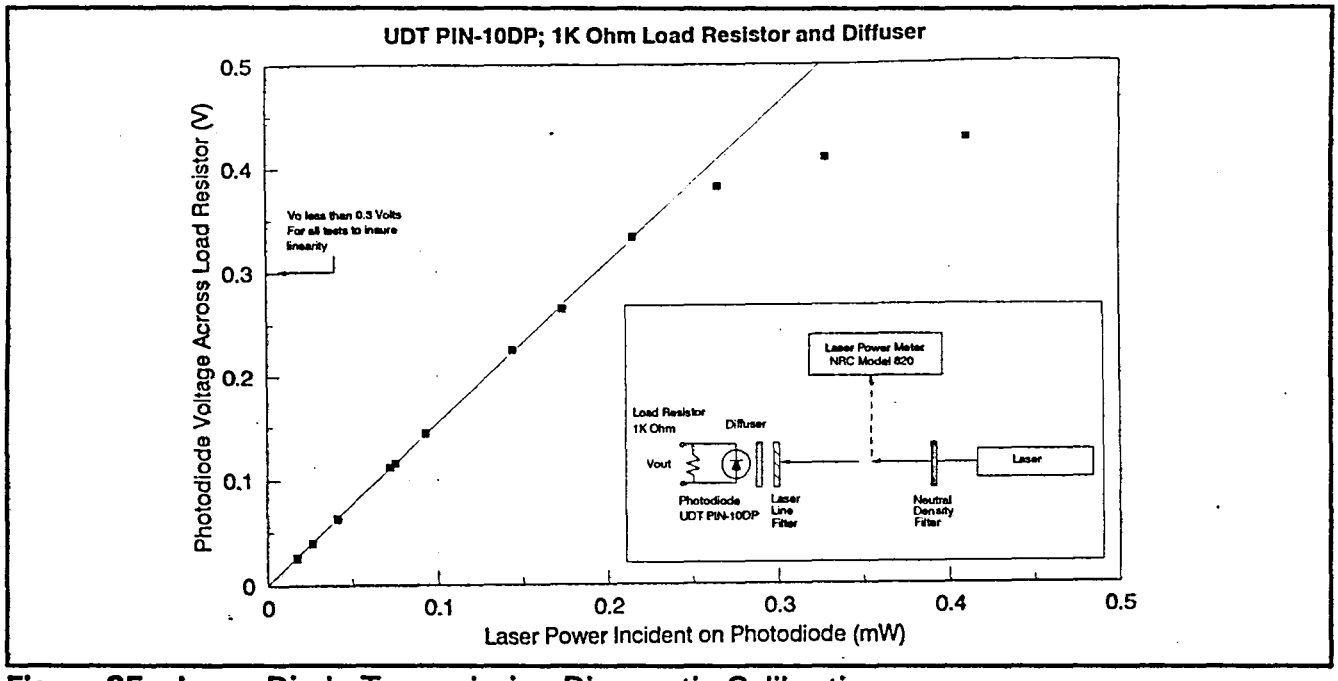

Figure 25 - Laser Diode Transmission Diagnostic Calibration.

2.4 Mounting hardware

The breadboard solid particle generator and laser transmission diagnostics are mounted on an elevated platform which straddles the chamber. The solid particle generator is centered over the top of the chamber pointing at the bottom of the chamber in the same configuration used in the performance testing.

2.5 Flowfield Control

No breadboard hardware was provided to implement the opposed gas jet concept for preventing the dust/gas jet from impinging on the far wall, as directed by NASA/ARC.

3 Deagglomeration Performance Characterization Approach and Results

The deagglomeration performance characterization tests were performed using the approach described below.

3.1 Test plan approach, instrumentation and procedures

The test matrix is the result of repeated discussions between NASA/ARC and TRW. The matrix is an attempt to achieve a balance between the desire to vary a large number and range of parameters so as to provide a complete characterization of the hardware performance, and the limited budget available.

The test matrix calls for measurements of the deagglomeration performance at three slit widths, three gas pressures, and three "exit-plane" particle number concentrations using the 5-10 μm graded Arizona Test Dust (PTI#4170H). TRW was also directed to perform a limited number of tests with the 10 μm and 2 μm glass Microspheres, and opted to do these tests at the "optimum" slit width, pressure and exit plane concentration as determined by the results with the graded Arizona Test Dust.

There are many other parameters which potentially effect the deagglomeration performance of the system but which were not explicitly defined during the discussions that lead to the test matrix. We held all these other parameters constant if possible. A short summary of the most relevant of these follows:

1) The test PTI powder was stored in an oven at 150 F to insure a completely dry state, or at least a uniform moisture content during the course of testing.

2) The gas used was GN2 produced from the boil-off of LN2 and pressurized with the TRW facilities booster pumps. The relative humidity of this gas was not measured but it was assumed to be essentially zero.

3) All tests were done with the deagglomerator exiting into ambient laboratory air, i.e., a chamber pressure of 1 atm. No attempts were made to characterize the variations in barometric pressure, temperature or humidity.

4) No attempts at charge neutralization were made either to the gas entering the system or to the dusty gas exiting the deagglomerator.

5) The deagglomerator materials (brass steel aluminum, etc.) were held constant throughout the testing. No attempts were made to choose materials which minimize triboelectric effect, nor was any attempt made to estimate triboelectric effects.

The physical layout of the solid particle generator, chamber and diagnostics are show in Figure 26. The solid particle generator was mounted above the chamber with the deagglomerator exit pointing downwards at a particle sampling filter located at the center of the bottom of the chamber. Before entering the chamber, the dispersed dust passed through laser beams which were used to determine the exit-plane concentration history.

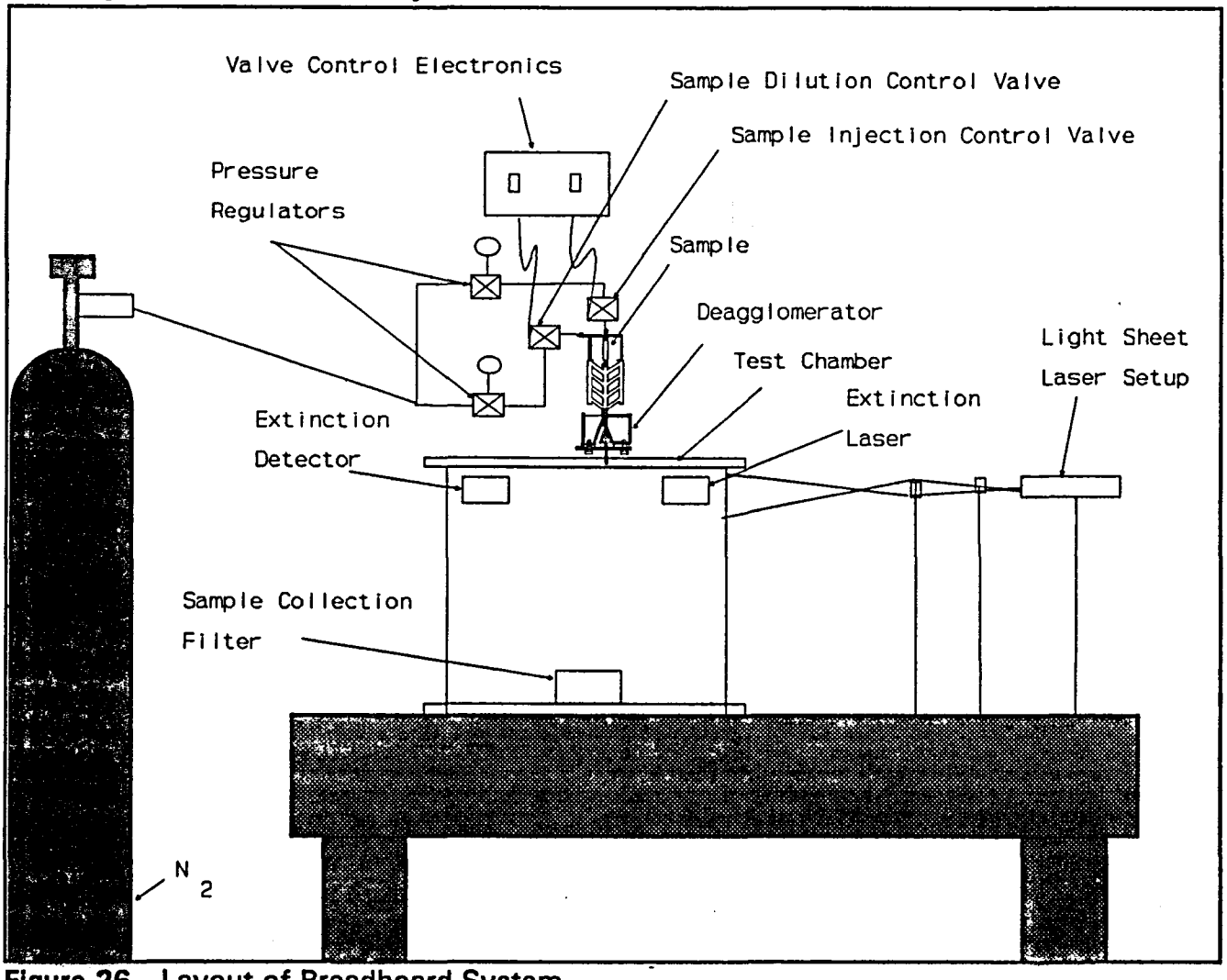

Figure 26 - Layout of Breadboard System.

The steady state clean gas flowrate data for the various deagglomerator slit width settings was obtained using a gas rotameter (Fisher & Porter tube # P-1/2-30-Lb-24/38 with a 6909-A4481-A1 scale calibrated for GN2 at 100 PSIG) and gas pressure test gauge (Matheson Gas 63-5562). The rotameter readings were corrected for the actual pressures according to standard practice.

The pressure history for each test was obtained from a flush-mount stain gauge type pressure transducer (Entran EPX-10W-250) which was mounted in the body of the "transport flow" solenoid body just upstream of the powder sample holder. The pressure transducer excitation was supplied

by a laboratory power supply, and the differential amplification required for the stain-gauge bridge was accomplished using an EGG Model 113 Preamplifier. The pressure data was recorded on a computer based data acquisition system for subsequent display and analysis. This single transducer allowed both the dilution flow pressures and the deagglomeration pressure condition to be recorded for each test.

The timing of the gas flows was controlled by a pair of laboratory pulse generators triggering solid state relays that energized the two solid particle generator solenoid valves (the final breadboard hardware version of this timing circuit was not completed till near the end of the testing and was not used during the actual testing, although its timing performance was verified separately later). The flow to the dilution manifold was initiated first to allow the manifold to come up to full pressure. Approximately 100-200 ms later the transport flow solenoid valve was opened. Both valves were left open for approximately 1 second. The transport flow solenoid was shut off first, followed by the dilution jet flow. This order was chosen so than there was no chance of driving dust into the dilution flow manifold. A typical pressure trace is shown in Figure 27, along with the resulting laser transmission trace. The total gas flow duration was purposely set to be far longer than was required to dispense the dust. In the present set of deagglomeration tests there is no concern about the amount of gas injected into the chamber. There was no a-priori knowledge of the time it would take to dispense the powder at a given setting, so the gas flow durations were made long compared to the expected dispensing times. In the flight operation of the hardware the gas flow duration would be shortened, of course.

The powder mass loaded into the sample holder was measured using a Sartorius model A200S Electronic Analytic Balance with a resolution of 0.1 milligram. The empty sample holder was tared then filled with dust until the desired dust weight was obtained. The sample holder was filled using a modified laboratory spatula to "pour" the powder into the sample holder tube as it was held in a vertical position. Several spatulas worth of powder were required to achieve the nominally 85 milligrams powder mass used for the tests. Between each spatula worth of powder the sample holder was tapped lightly to insure that the powder settled fully and formed a plug that completely filled the sample holder tube cross-section. After the desired weight of powder had been loaded, the sample holder was held in a vertical position and a #31 drill blank was inserted into the top of the sample holder tube and allowed to fall onto the powder to further insure that the powder was all in a plug form.

Some post-test weights of the sample holder were obtained and compared to the pre-test empty sample holder weight to determine the mass of dust remaining in the sample holder, but this was discontinued when no significant masses were measured (less than 1% of the initial stored powder mass). This finding does not preclude powder deposition losses in other portions of the solid particle generator, however. This possibility was explored using the laser transmission diagnostics, as described near the end of this section.

The peak exit plane concentration was inferred from the laser transmission signals measured 75 mm downstream of the deagglomerator slit exit. Three laser beams formed a plane perpendicular to the flow exiting the deagglomerator, one beam along the axis of the flow from the sample holder to the deagglomerator, one beam perpendicular to this axis, and a third beam at 45

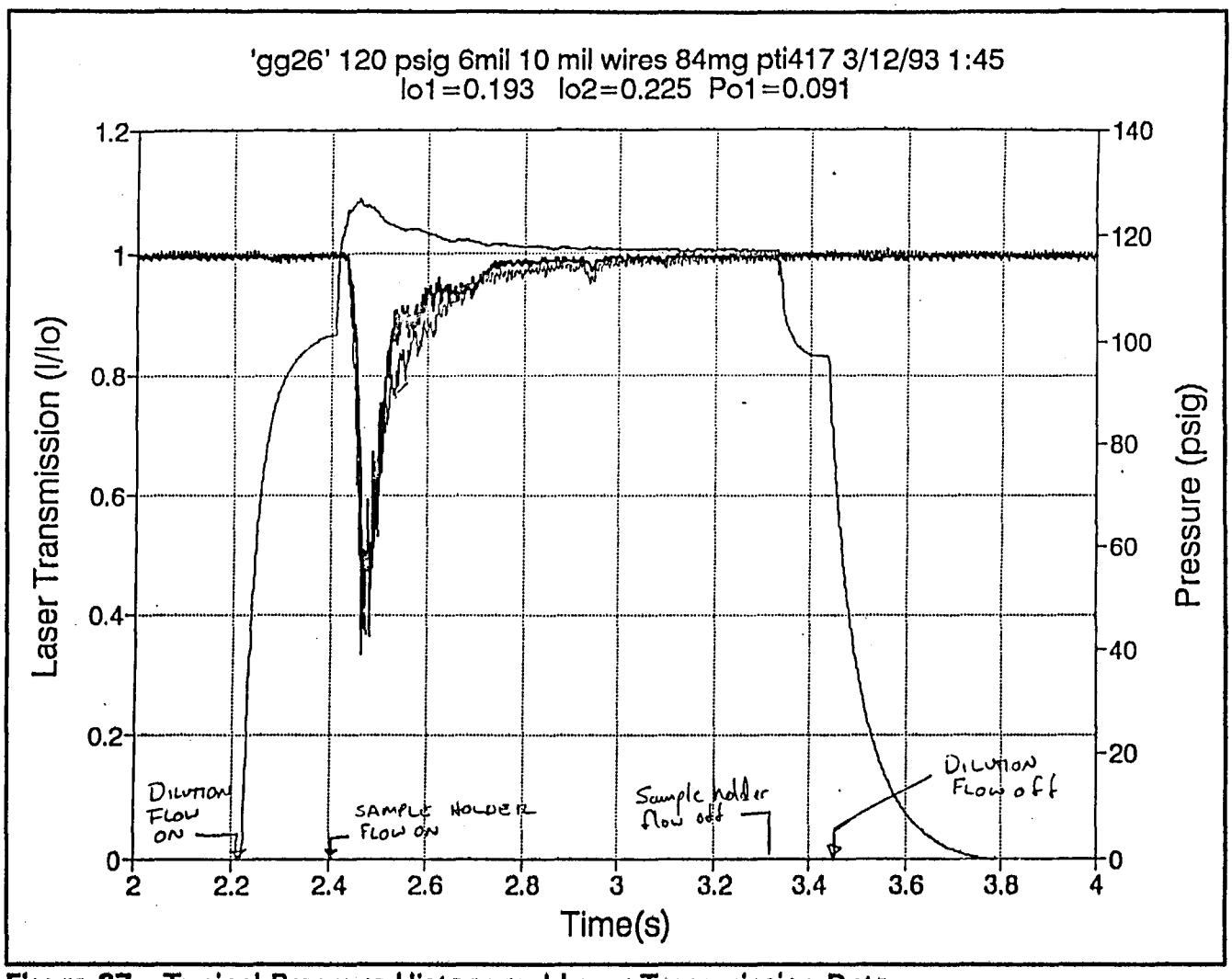

Figure 27 - Typical Pressure History and Laser Transmission Data.

degrees to the other two. The multiple beams allowed the uniformity of the dust concentration around the annulus to be estimated and so that an average spatial concentration could be determined. One of the laser detector pairs was part of a commercial particle sizing instrument. The other two laser detector pairs consisted of low power (~1 Mw) laboratory laser and a UDT PIN-10DP silicon photodiode terminated with a 1K Ohm load resistor. This load resistor value provides a conveniently large voltage of approximately 200-300 Mv at I_o while maintaining excellent linearity.

In the ideal case, the dust concentration could be found directly from the laser transmission signal using Beer's Law in the form:

$$C_m = -2\rho D_{32}/3Q_e L \ln\left(\frac{I}{I_0}\right)$$

where

C_m = mass concentration (gram/cm^3)
ρ = particle density (gram/cm^3)
D_{32} = Sauter (or Surface Weighted) Mean Diameter (cm)
L = Optical Path Length (cm)
Q_e = Extinction efficiency (=2 for this diameter and wavelength)
I/I_o = Transmission (%)

since all the terms in the grouped term (2 p D_{32}/3 Q_e L) on the right hand side of the equation would be known. In the present case, though, all the terms can be estimated accurately except the path length. The laser beams cross an annular jet in which the concentration is probably not nearly uniform along the beam path, so it is not clear what equivalent path length to use (or how to integrate along the beam path).

An order of magnitude estimate for the path length can be obtained by assuming that the dust uniformly fills in the cone defined by the extension of the 15 degree half-angle deagglomerator pintle out from end of the pintle (where the diameter is approximately 2 cm) to the laser beam location (75 mm beyond the end of the pintle), where the diameter is approximately 5 cm. In that case, assuming fully deagglomerated PTI dust, the following values

ρ = 2.5 (gram/cm^3)
D_{32}= 7x10^{-4} (cm)
L = 5 (cm)
Q_e =(2 for these diameters and wavelength)

yield a conversion equation of

$$C_m=(1.2\times10^{-4})\ \ln\left(\frac{I}{I_0}\right) \quad (g/cm^3)$$

A potentially more accurate estimate was obtained by integrating the laser transmission signals in the form -ln (I/I_o) over the duration of the flow (Figure 28). Using an analogy in which the dust/gas mixture is treated as a very-dense pseudo-gas, a mass balance shows that the total mass passing a point is obtained by integrating the product of the pseudo-gas "density" and volumetric flowrate over time. The pseudo-gas volumetric flowrate can be assumed to be equal to the clean gas volumetric flowrate and constant over the test duration. The pseudo-gas "density" due to the dust is given by

$$-K \ln (I/I_o)$$

as shown above. Since the lasers only respond to the dust phase of this pseudo-gas, the coefficient K can be obtained by equating the integration equal to the total dust mass stored and ignoring the density of the gas. This procedure was carried out for a variety of test conditions, yielding values of K from 7.4 x 10^{-4} to 3.6x 10^{-4} with an average value of 5.0 x 10^{-4} gram/cm^3, or

$$C_m = -(5.0\times10^{-4})\ \ln\left(\frac{I}{I_0}\right) \quad (g/cm^3)$$

This result is higher than the order of magnitude estimate, as would be expected if the effective path length was shorter than the full diameter of the jet due to the its annular geometry. The factor of 4 increase corresponds to an effective path length of 1.25 cm. This can be interpreted as meaning that the dusty jet at the laser beam location is 1,000 times its width the pintle exit (approximately 2x80 microns or 1.6×10^{-3} cm) but has not quite expanded to fill the inner and outer portions of the of the apparent conical jet. The value obtained by the integration technique is considered to be more accurate than the order of magnitude estimate, and was used to provide a conversion from relative concentration to absolute concentration in the data presentation and analysis.

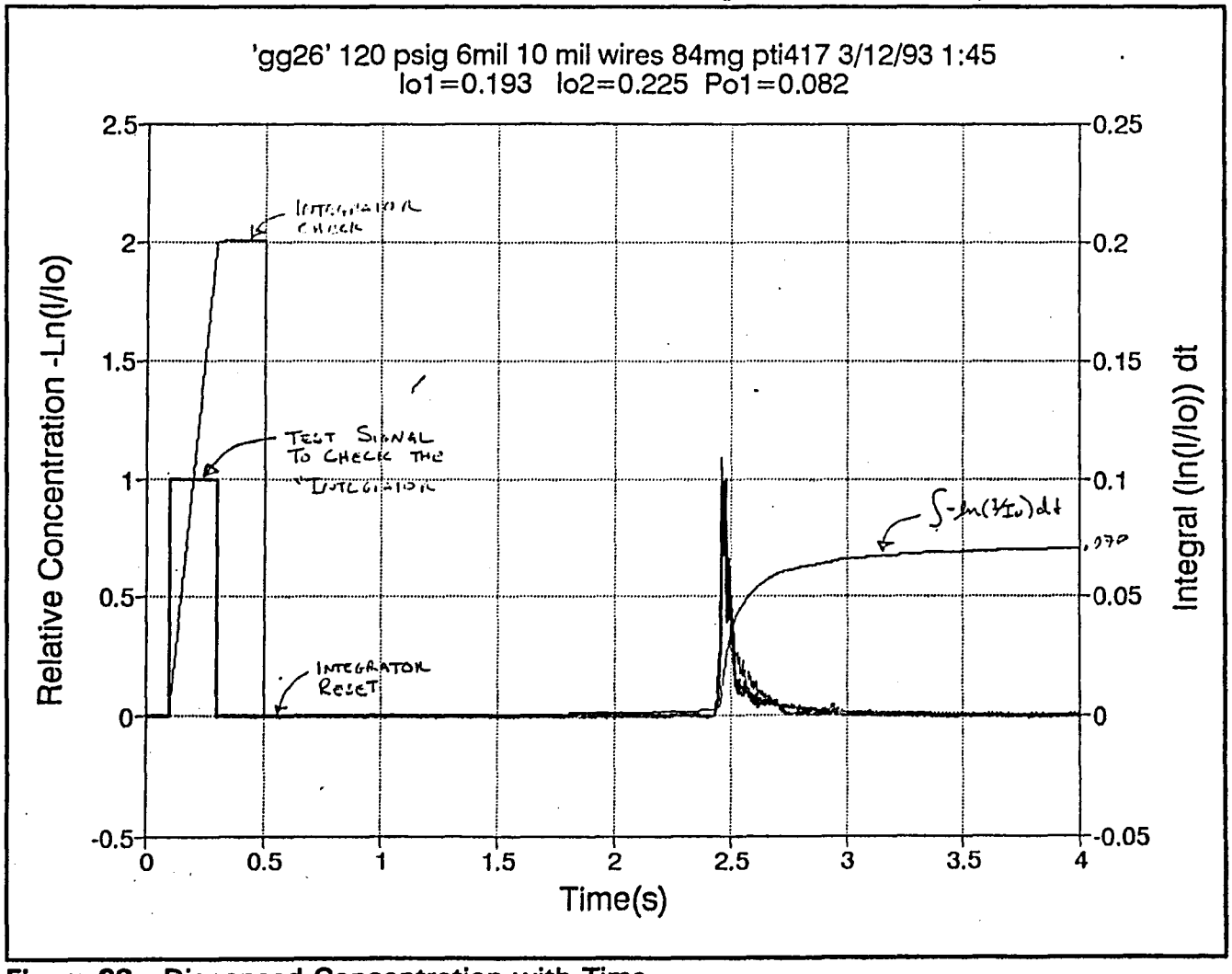

Figure 28 - Dispensed Concentration with Time.

During the development phase it was observed that, under some conditions, firing the solid particle generator after a test without reloading it with powder would exhaust some additional powder. This is an apparent indication that some of the powder was not dispensed during these test conditions. Therefore part of the test procedure was to fire the solid particle generator after each test without reloading it while recording the laser transmission signals. Using the integration procedure described above on both the test data and the post test data it is possible to estimate the fraction of dust that was not dispensed during each test.

The deagglomeration performance was determined using microscopic examination of particle sampled from the chamber. An open face Nuclepore filter holder (47 mm diameter) mounted at the bottom of the chamber sampled the partially diluted ("farfield") particle cloud produced by the solid particle generator. Previous flow field visualization had shown that, when no opposing jet is used, the dust/gas cloud impinges on the far wall of the chamber within approximately 1 second and at that time has expanded to approximately 10 times it initial diameter. Thus, the dispersed dust has had little time to agglomerate and has been diluted by entrainment. The Nuclepore filters did not have air drawn through them, since this was found to produce an undesirably high concentration of particle on the filter, leading to potential coincidence errors. The natural impingement and sedimentation that resulted from the solid particle generator jet were found to produce filter exposures with between 5 and 20 diameters between closest particles. This method of collecting particle samples follows closely the technique used by Fuchs[29] when testing a similar device.

The Nuclepore filters were covered after approximately 15-30 seconds in order to prevent reagglomerated particles from the dust cloud still circulating in the chamber from settling on the filter. The filters were then be removed and examined under an optical stereo microscope to determine the degree of deagglomeration. The microscope used for these tests was a Lietz LaborLux 12HL with 10x/18 eyepieces and 20x/0.30 DF objective. Dark-field lighting with random polarization was found to be optimum. A custom grid was made for the field stop of the ocular which divided the field of view into 6 horizontal strips, making it easier to keep track of which particles had been counted. The particles were counted and classified according to the number of individual particles (with a minimum of one) within each "aggregate". Particle counting and classification was done using the numeric keypad of a computer to enter the data into a program that recorded the data. The keypad was setup to provide auditory feedback to the operator in order to verify that the proper key was punched without having to look up from the microscope. Typically 1000 or more aggregates were counted for each test from randomly selected locations on the filter (with a step wise progression to prevent the possibility of repeating a location) in order to get a statistically significant estimate of the distribution tails.

The microscope was setup to take Polaroid still photographs, and representative photos were taken of each condition. The photos are really only good far a semi-quantitative comparison of cases, however, since the limited depth of field results in some of the particle being partly out of focus for any given setting of the focus knob. This is not a problem in real time viewing, as the focus can be adjusted for each particle, and even scanned up and down over a given particle or aggregate.

The degree of deagglomeration is defined, as in Fuchs' work, as the percentage of single particles out of total number of particles, i.e., $N_1/(N_1+2N_2+3N_3...)$ where N_n is the number of aggregates

containing n particles. It should be noted that this is a more conservative definition than the number of single particles out of the total number of aggregates, $N_1/(N_1+ N_2+ N_3...)$.

3.2 Deagglomeration performance results for PTI Dust

The test matrix was completed as planned, and a few additional exploratory points were added. Specifically, the final breadboard hardware was characterized by 36 tests using the PTI 5-10 micron dust, two tests using the Duke 10.2 micron glass beads and two tests using the Duke 2.1 micron glass microspheres. Deagglomeration data was obtained for PTI dust at 30, 60 and 120 psig pressure using 39, 79 and 118 micron slit widths and varying the concentration from approximately $1x10^{-4}$ gram/cm3 to approximately $15x10^{-4}$ grams/cm3 with at least three concentrations for each pressure and slit width. Additional data was obtained at 11 psig and 79 microns to investigate the effect of unchoked flow. Two tests were explicit repeats of one of the test conditions. The glass micro-sphere tests were done at 120 psig and a slit width of 79 microns, based on results with the PTI dust. The major findings were that it was possible to achieve better than 90% deagglomeration but not 100% deagglomeration with the PTI dust, and that these repeatability was approximately +/- 10%. The single repeated data point with Duke 10.2 micron glass microspheres lies on the curve for the PTI dust data, so it can probably be assumed that they behave similarly in general. The data with the Duke 2.1 micron glass microspheres as obtained under the optical microscope is suspect due to the difficulty is seeing the small end of size distribution (0.5 μm diameter). The limited number of particles counted using the SEM for this powder indicate that the degree of deagglomeration is significantly less for this powder than for the larger diameter powders. Unfortunately there was no chance to attempt to optimize the deagglomerator settings for the Duke 2.1 micron powder, so we do not know what the potential performance limits of the device for this powder are.

All the test conditions and data are summarized in Table 4.

The PTI dust data is presented graphically in Figure 29 through Figure 39 as deagglomeration vs. concentration for each pressure and slit width setting. There are three reason for presenting the data this way. First, the pressure and slit width settings were easy to preset and hold constant, whereas the concentration was not able to be preset. A curve fit of the data in this form, however, allows this data to be cross plotted along lines of constant concentration. A linear regression curve fit was used for this purpose, and the best fit line is shown on each plot. Second, this allows the data to be extrapolated to zero concentration. The extrapolation to zero concentration indicates the maximum performance available for a given slit width, pressure setting and dust type, as previously discussed. Third, a variant of this type of presentation has been used previously in the literature for comparing the deagglomeration performance of various devices.[30]

Table 4 - GGSF Deagglomeration Performance Data Summary.

Test #	Dust Type	Dust mass (mg)	Slit Width (um)	Peak Press (Psig)	Insitec Peak -Ln(I/Io)	Laser 1 Peak -Ln(I/Io)	Laser 2 Peak -Ln(I/Io)	avg Peak -Ln(I/Io)	Dilution Set (Psig)	Push Set (Psig)	Insert Insert (mils)	Deagglomeration N1/ Npart	N1/ Nobj	Total Object Nobj	Total Particles Npart	Number singlets N1	Number doublets N2	N3	N4	N5	N6	N7	N8
MMG-12mil setting 60 psig pb417																							
417-8	417	81	79	60	3.51			3.507			na	0.40	0.64	570	909	364	132	46	13	3	8	4	
417-3	417	??	79	60	2.12			2.120			na	0.47	0.67	261	376	175	63	18	4	1			
417-6	417	40	79	60	1.31			1.309			na	0.65	0.80	444	547	357	73	12	2				
417-9	417	20	79	60	1.20			1.204			na	0.68	0.83	334	410	277	42	12	2	1			
12mil insert 11 psig pb417																							
gg02	417	84	79	11	0.75			0.751	* 15	12	na	0.41	0.66	1017	1624	669	217	76	20	15	8	6	6
gg03	417	84	79	12	0.23			0.229	20	12	na	0.50	0.71	1003	1424	711	196	72	19	2	2	1	
12mil insert 30 psig pb417																							
gg12	417	84	79	30	0.72	0.580	0.844	0.715	60	30	na	0.68	0.83	1106	1341	916	160	20	7	2	0	1	
gg13	417	84	79	30	0.49	0.329	0.511	0.445	74	30	na	0.78	0.88	1019	1153	899	106	9	1	1			
gg14	417	84	79	30	0.15	0.163		0.157	78	30	na	0.80	0.89	1061	1205	963	112	6					
gg15	417	85	79	30	0.33	0.236	0.357	0.309	76	30	na	0.74	0.86	1049	1222	900	126	18	3				
12mil insert 60 psig pb417																							
gge8	417	85	79	53	0.92	0.755		0.836	60	60	na	0.79	0.89	1012	1138	904	93	12	3				
gge1	417	84	79	58	0.50	0.400		0.452	90	60	na	0.83	0.91	1023	1125	933	80	8	1	1			
84mgb	417	84	79	54		0.357		0.357	90	60	na	0.80	0.91	868	1009	805	55	21	5	1	1		
gge4	417	85	79	62	0.14	0.139		0.141	95	60	na	0.92	0.96	1022	1064	982	38	2					
gg11	417	84	79	60	0.84	0.892	0.968	0.901	95	60	10	0.75	0.87	1025	1186	888	116	19	1	1			
gg10	417	84	79	60		0.196	0.223	0.211	150	60	10	0.86	0.92	1026	1106	949	74	3					
gg09	417	85	79	60	0.97	3.912	2.998	2.625	140*	72	na	0.51	0.74	757	1106	560	111	49	18	11	6	2	
12mil insert 120 psig pb417																							
gge5	417	85	79	122	0.27	0.236		0.252	200	120	10	0.94	0.97	1119	1157	1082	36	1					
gge6	417	85	79	115	0.40	0.446		0.423	170	120	10	0.91	0.95	625	657	595	28	2					
gge7	417	86	79	110	0.94	1.470		1.206	120	120	10	0.78	0.88	1023	1154	904	109	8	2				
6mil insert 60 psig pb417																							
gg16	417	85	39	60	0.94	0.598	0.799	0.779	120	60	17	0.83	0.91	1254	1371	1142	107	5					
gg17	417	85	39	60	1.47	0.844	1.204	1.173	75	68	17	0.65	0.81	1150	1427	933	179	26	6	3	2	1	
gg18	417	85	39	60	0.87	0.511	0.835	0.671	100	62	17	0.73	0.86	1102	1299	946	131	18	2	2	2	1	
gg19	417	86	39	60	0.12	0.051	0.105	0.091	180	60	17	0.92	0.96	1009	1051	969	38	2					
6mil insert 30 psig pb417																							
gg20	417	86	39	30	0.73	0.844	1.204	0.927	40	32	17	0.69	0.83	1036	1247	855	161	14	3	2	1		
gg21	417	85	39	30	0.49	0.329	0.446	0.423	55	32	17	0.78	0.89	1054	1190	934	108	8	4				
gg22	417	84	39	30	0.30	0.163	0.223	0.229	68	30	17	0.81	0.90	1046	1161	937	105	3	0	1			
6mil insert 120 psig pb417																							
gg23*	417	84	39	120	0.99	0.835	0.916	0.848			17	0.83	0.81	1071	1374	868	139	41	15	2	2	2	1
gg24	417	86	39	120	0.99	0.755	1.273	1.007	240	132	17	0.78	0.89	1047	1184	826	105	12	1	0	1		
gg25	417	86	39	120	0.24	0.163	0.186	0.195	160	122	10	0.84	0.92	1044	1135	956	85	3					
gg26	417	84	39	120	1.31	1.079	0.994	1.196	140	122	10	0.77	0.88	1110	1263	978	117	10	4	1			

Test #	Dust Type	Dust mass (mg)	Slit Width (um)	Peak Press (Psig)	Insitec Peak -Ln(I/Io)	Laser 1 Peak -Ln(I/Io)	Laser 2 Peak -Ln(I/Io)	avg Peak -Ln(I/Io)	Dilution Set (Psig)	Push Set (Psig)	Insert Insert (mils)	Deagglomeration N1/ Npart	N1/ Nobj	Total Object Nobj	Total Particles Npart	Number singlets N1	Number doublets N2	N3	N4	N5	N6	N7	N8
18mil insert 60 psig pb417																							
gg27	417	84	118	60	1.08	1.309	1.139	1.176	110	75	10	0.78	0.88	1390	1578	1224	147	16	3				
gg28	417	86	118	60	0.83	0.693	0.616	0.648	150	63	10	0.79	0.89	1594	1790	1422	152	16	4				
gg29	417	86	118	60	0.58	0.562	0.580	0.574	160	60	10	0.85	0.92	1176	1271	1086	85	5					
gg30	417	86	118	60	0.37	0.261	0.357	0.330	190	60	10	0.85	0.93	1081	1173	1002	67	11	1				
18mil insert 30 psig pb417																							
gg31	417	86	118	30	0.63	0.844	0.821	0.767	* 89	30	10	0.74	0.86	1121	1311	969	121	26	3	2			
gg32	417	86	118	30	0.33	0.416	0.416	0.367	100	30	10	0.80	0.89	1016	1131	909	99	8					
gg33	417	86	118	30	1.06	1.897	1.204	1.363	55	32	10	0.65	0.81	1119	1395	905	168	36	6	2	2		
18mil insert 120 psig pb417																							
gg34	417	84	118	120	0.89	0.799	1.139	0.943	220	125	0	0.72	0.85	1456	1722	1235	183	32	5	1			
gg35	417	84	118	120	0.89	0.693	0.799	0.794	220	125	0	0.72	0.85	1120	1324	950	140	26	4				
gg36	417	86	118	120	0.31	0.315	0.329	0.319	260	120	0	0.76	0.87	1576	1807	1375	174	25	1	1			
gg37	417	86	118	120	0.25	0.211	0.223	0.227	320	120	0	0.77	0.87	1211	1380	1057	139	15					
12mil insert 120 psig pb417 "repeat" tests																							
gg38	417	86	79	120	0.42	0.511	0.478	0.468	210	120	0	0.87	0.93	1402	1510	1308	81	12	1				
gg39	417	86	79	120	0.49	0.511	0.357	0.454	210	120	0	0.89	0.94	1418	1503	1335	81	2					
12mil insert 120 psig DUKE 10.2																							
gg40	10.2	85	79	120	0.67	0.416	0.446	0.512	210	120	0	0.86	0.93	1279	1378	1187	85	7					
gg41	10.2	85	79	120	0.54	0.412	0.496	0.484	210	120	0												
gg42	10.2	85	79	120	0.51	0.417	0.499	0.476	210	120	0	0.86	0.93	1012	1090	938	71	2	1				
12mil insert 120 psig DUKE 2.1																							
gg43	2.1	85	79	120		2.996	2.303	2.648	210	120	0	0.72	0.86	637	754	645	71	17	4				
gg44	2.1	85	79	120					230	120	0												
gg45	2.1	35	79	120	1.04	0.829	0.764	0.912	230	120	0	0.82	0.91	518	574	473	38	4	2	1			

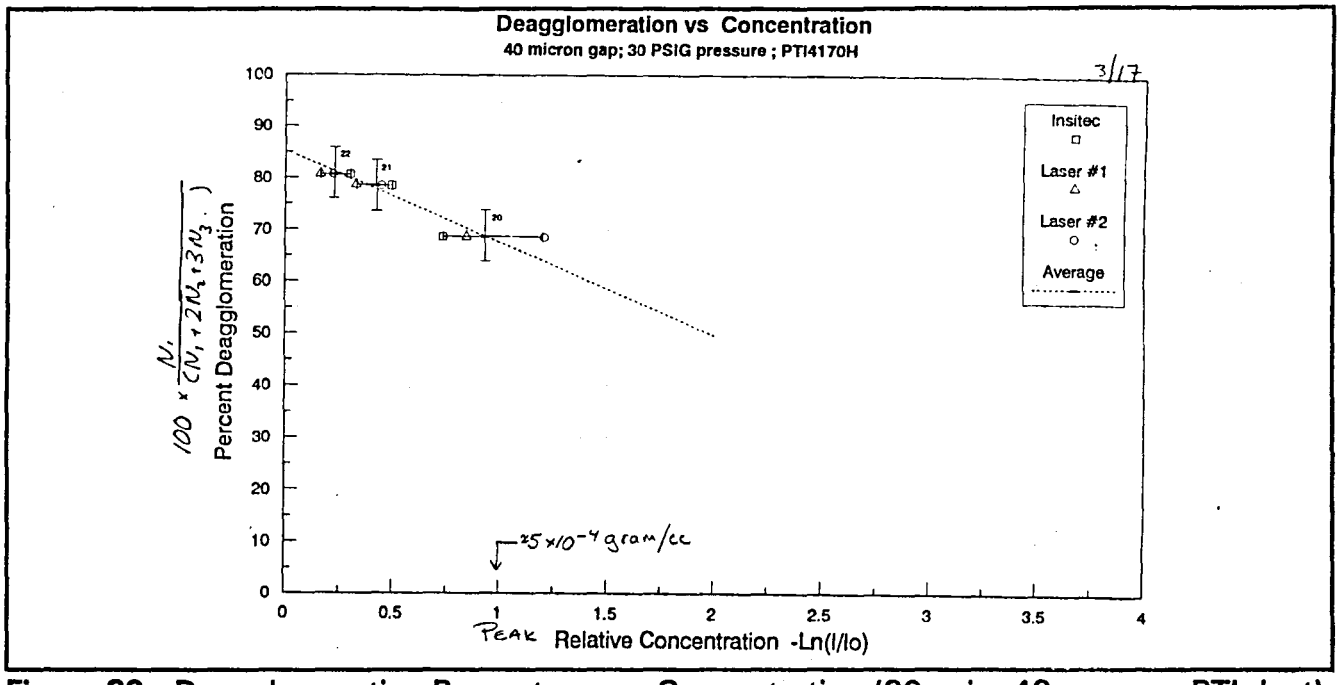

Figure 29 - Deagglomeration Percentage vs. Concentration (30 psig, 40 μm gap, PTI dust).

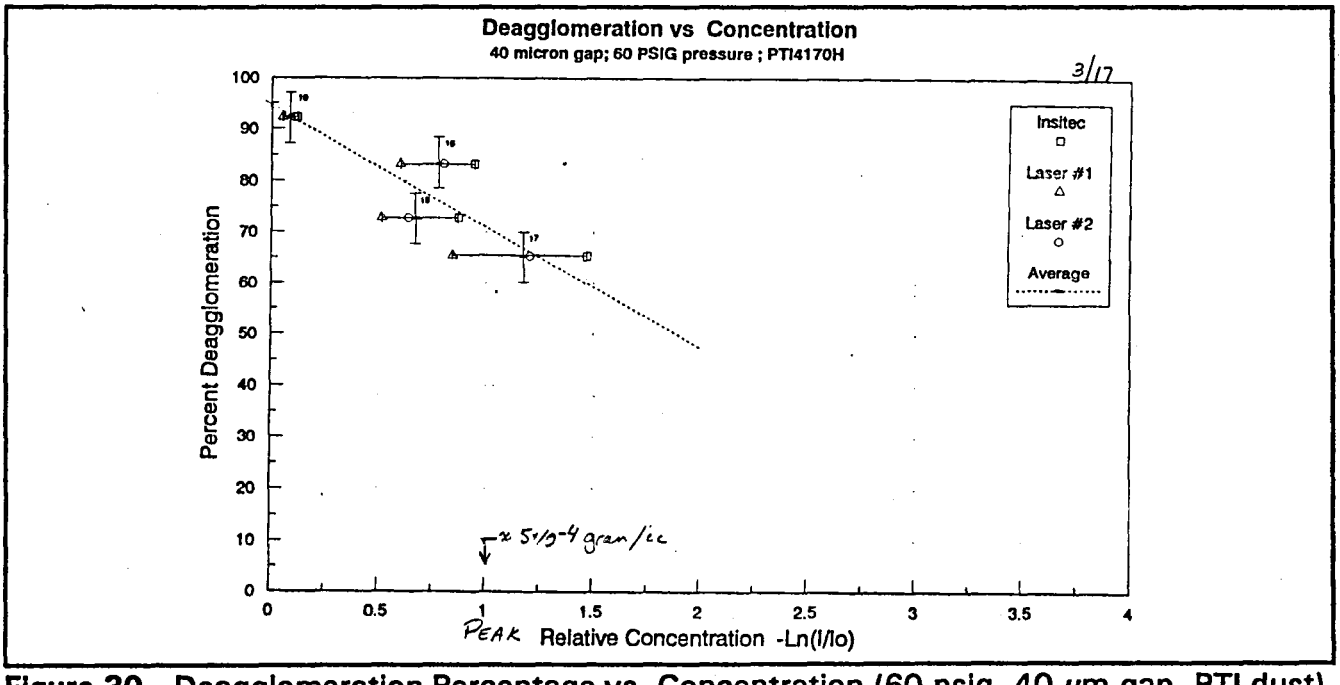

Figure 30 - Deagglomeration Percentage vs. Concentration (60 psig, 40 μm gap, PTI dust).

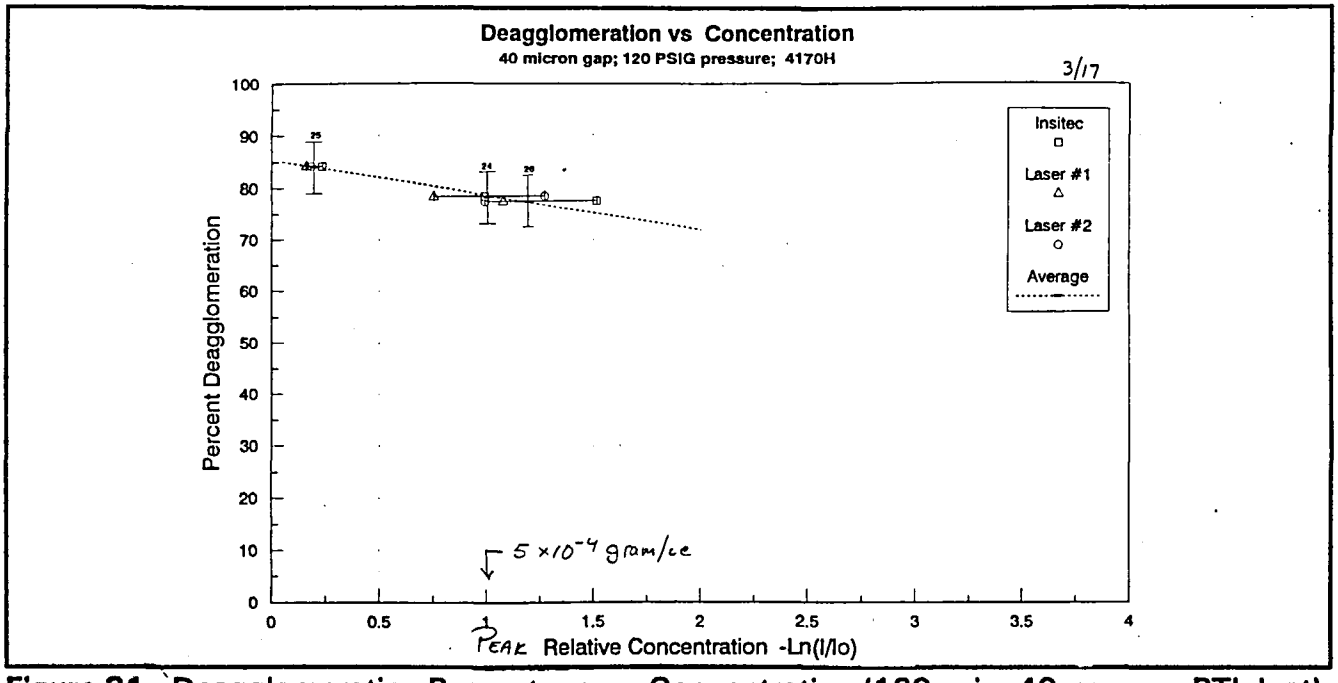

Figure 31 - Deagglomeration Percentage vs. Concentration (120 psig, 40 μm gap, PTI dust).

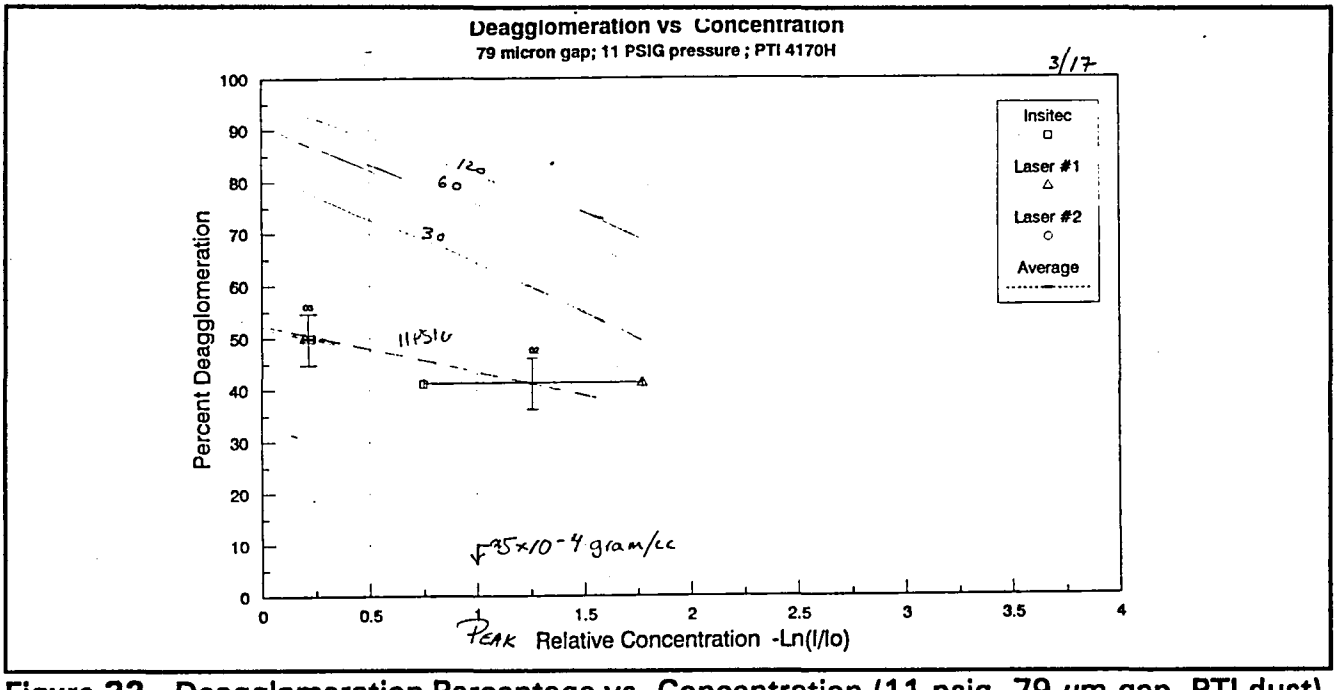

Figure 32 - Deagglomeration Percentage vs. Concentration (11 psig, 79 μm gap, PTI dust).

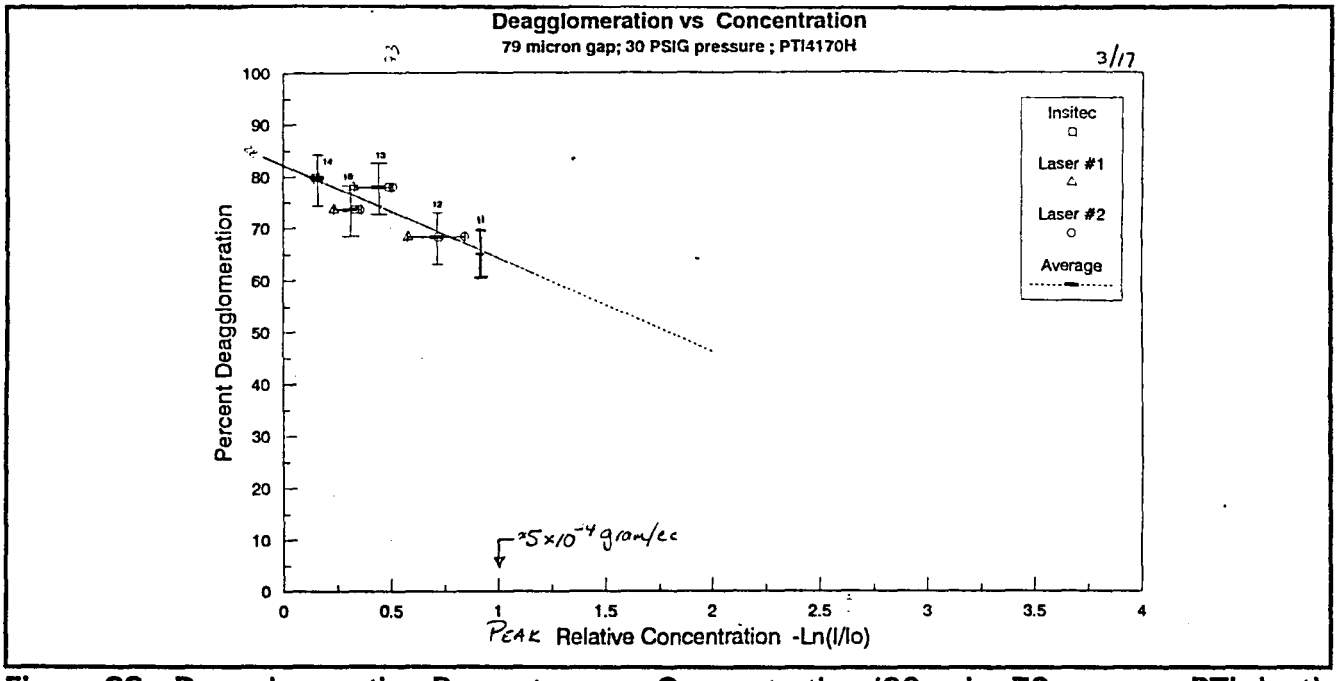

Figure 33 - Deagglomeration Percentage vs. Concentration (30 psig, 79 μm gap, PTI dust).

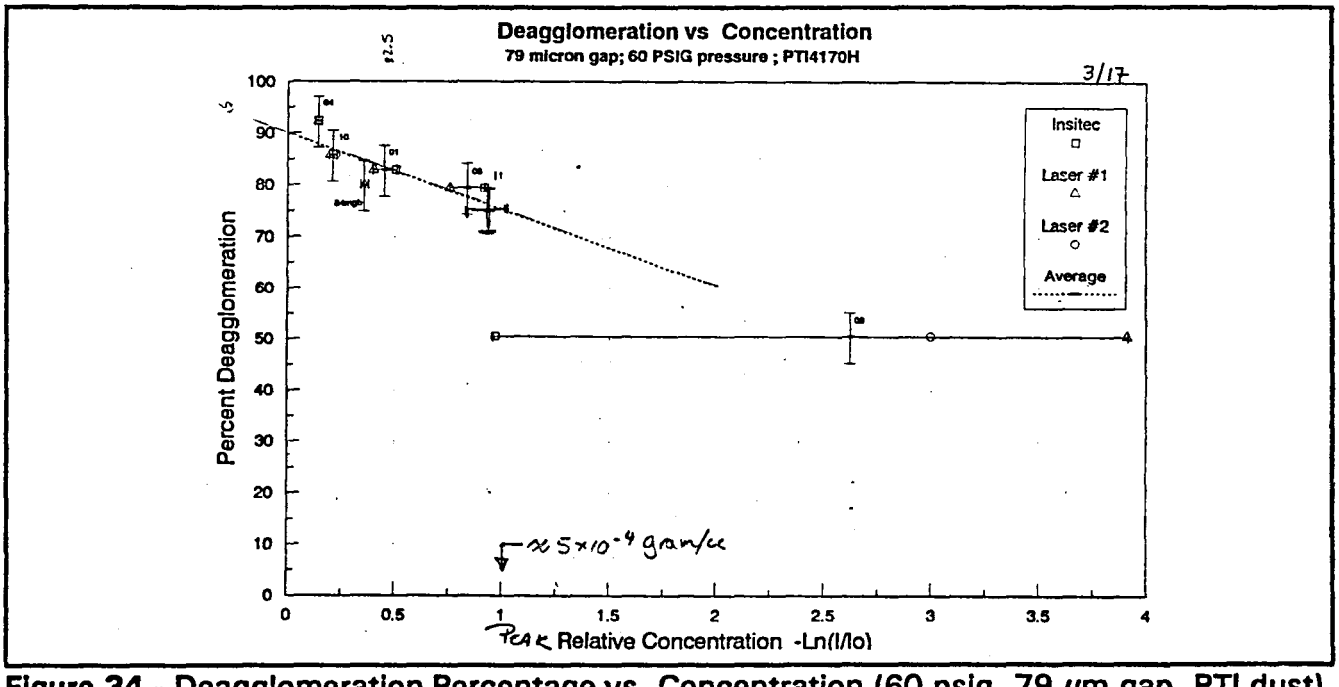

Figure 34 - Deagglomeration Percentage vs. Concentration (60 psig, 79 μm gap, PTI dust).

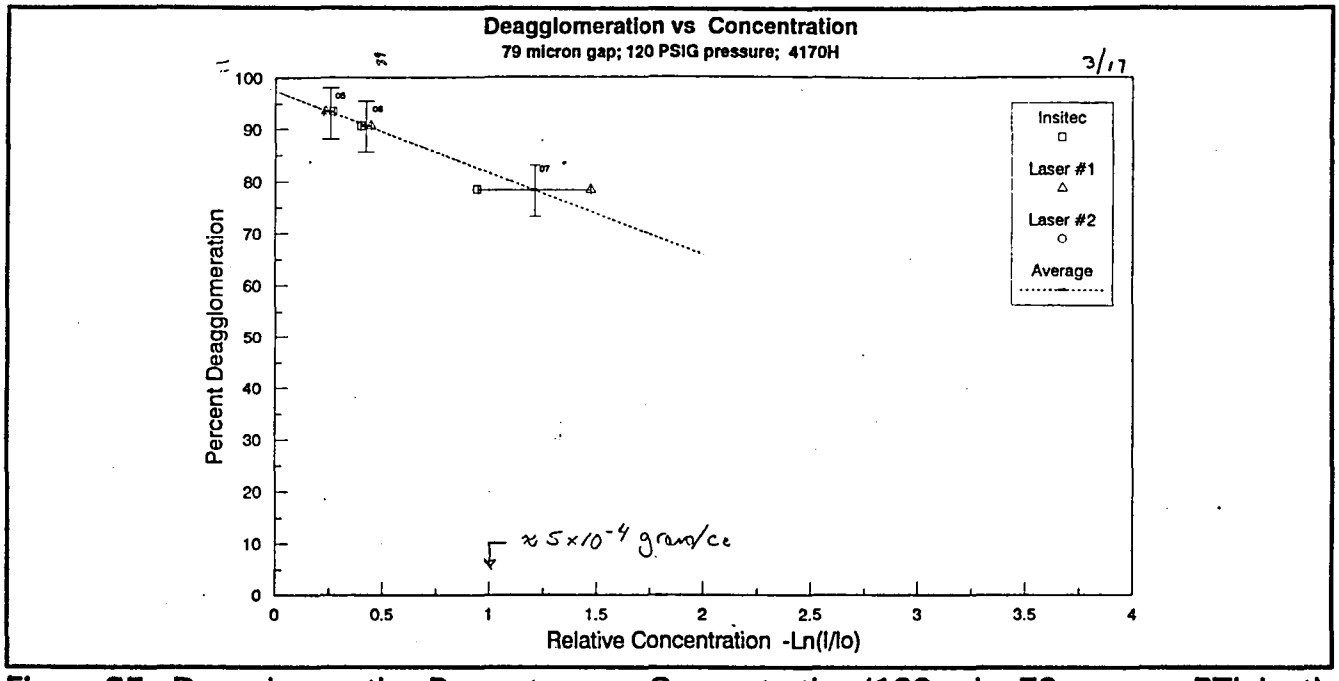

Figure 35 - Deagglomeration Percentage vs. Concentration (120 psig, 79 μm gap, PTI dust).

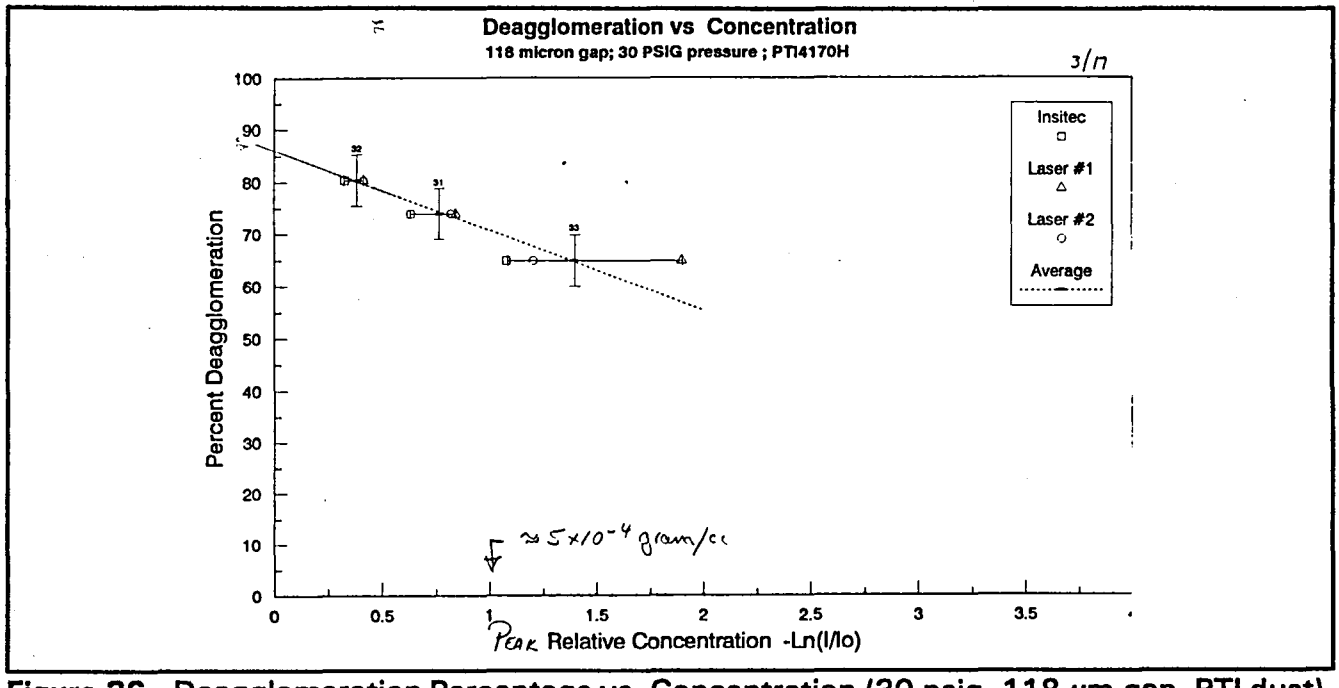

Figure 36 - Deagglomeration Percentage vs. Concentration (30 psig, 118 μm gap, PTI dust).

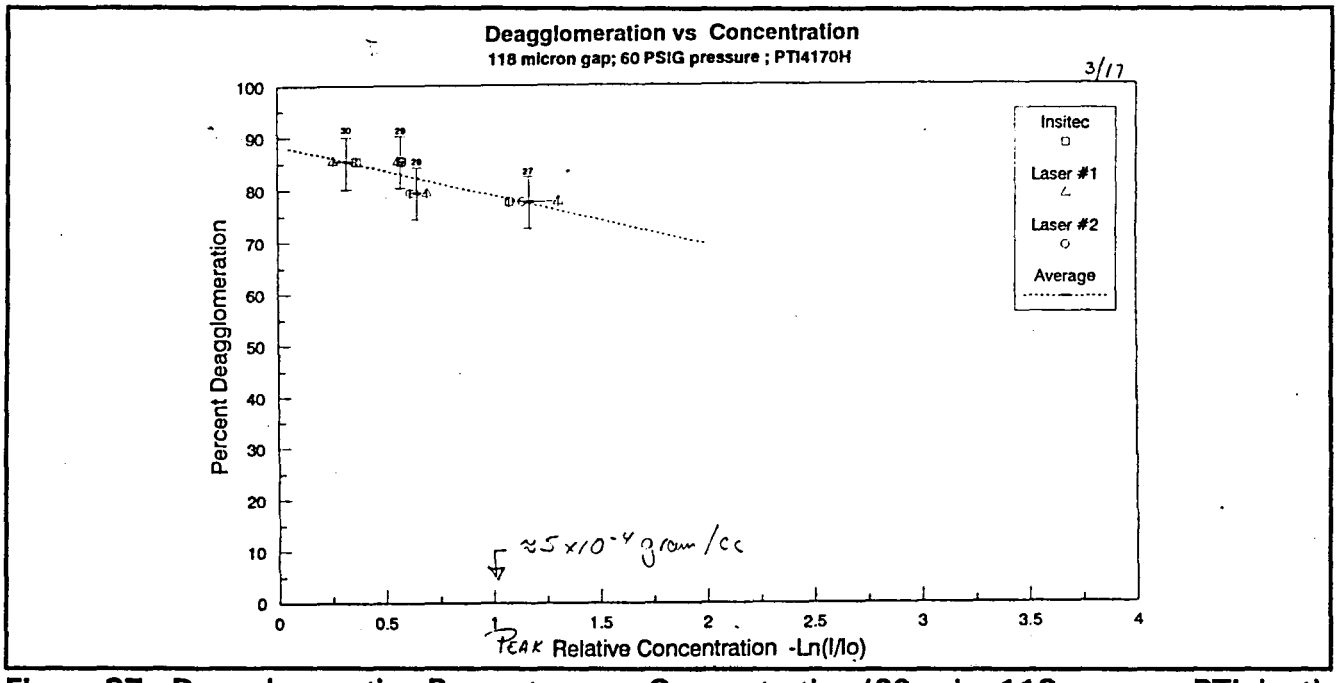

Figure 37 - Deagglomeration Percentage vs. Concentration (60 psig, 118 μm gap, PTI dust).

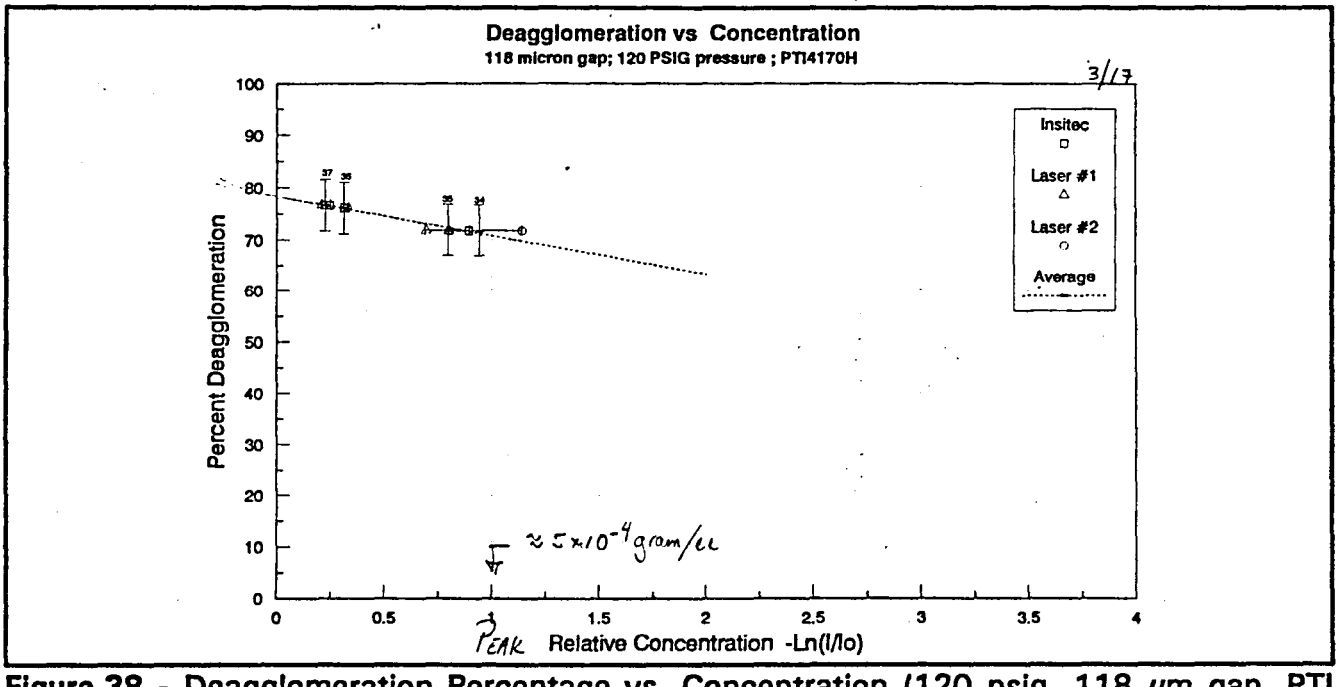

Figure 38 - Deagglomeration Percentage vs. Concentration (120 psig, 118 μm gap, PTI dust).

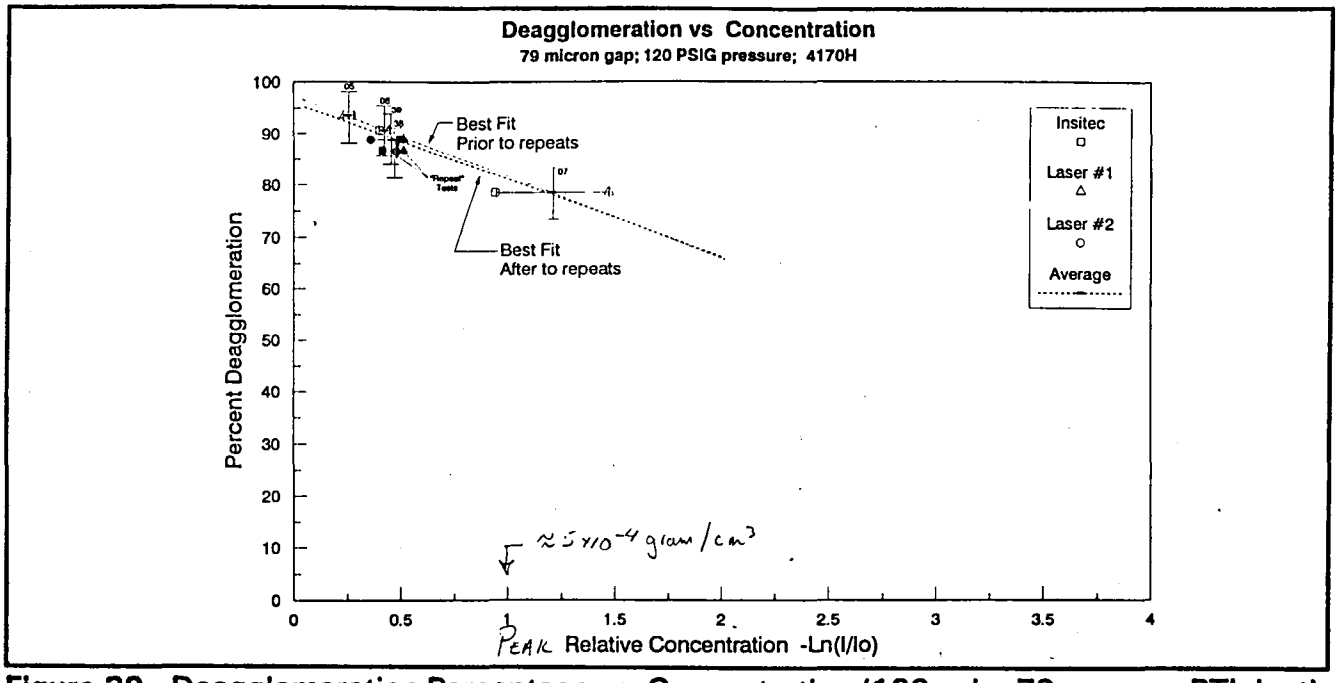

Figure 39 - Deagglomeration Percentage vs. Concentration (120 psig, 79 μm gap, PTI dust).

The vertical axis shows percent deagglomeration (percentage of single particles out of total number of particles, i.e., $N_1/(N_1+2N_2+3N_3...)$ where N_n is the number of aggregates containing n particles) as determined using the optical microscope. An accuracy of +/- 5% has been assigned to these measurements, based on the spread in the data obtained with similar conditions. The horizontal axis shows the relative dust concentration at the exit plane as measured by the three laser beams. The data obtained from each of the laser beams is shown, and the deagglomeration performance is plotted at the location of the average of the three beam's data. The approximate absolute particle mass concentration for a relative concentration value of $-\ln(I/I_o) = 1$ is also indicated on the horizontal axes so that approximate absolute concentrations can be obtained for all the data.

Cross plots of the data as deagglomeration vs pressure at constant slit width and constant concentration are shown as Figure 40 and Figure 41. The exit plane concentrations that were chosen were the extrapolation to zero grams/cm^3 and the interpolation to 2.5×10^{-4} grams/cm^3 ($-\ln(I/I_o) = 0.5$). The choice for the interpolated concentration value to use for the cross plots was simply to illustrate the pressure and slit width trends at a convenient low-concentration operating point. Similar cross plots could be constructed at any other concentration in the range tested.

On these cross plots, a comparison of the data obtained at the different pressures with the 79 micron gap shows that there is a significant difference between the choked conditions (30, 60, 120 psig) and the unchoked condition (11 psig). This would be expected since in the choked case the flow goes supersonic in the converging section. There is a much less pronounced difference among the choked condition cases that were tested. For a given relative concentration and slit width, the deagglomeration performance increases with increasing pressure, as would be consistent with the

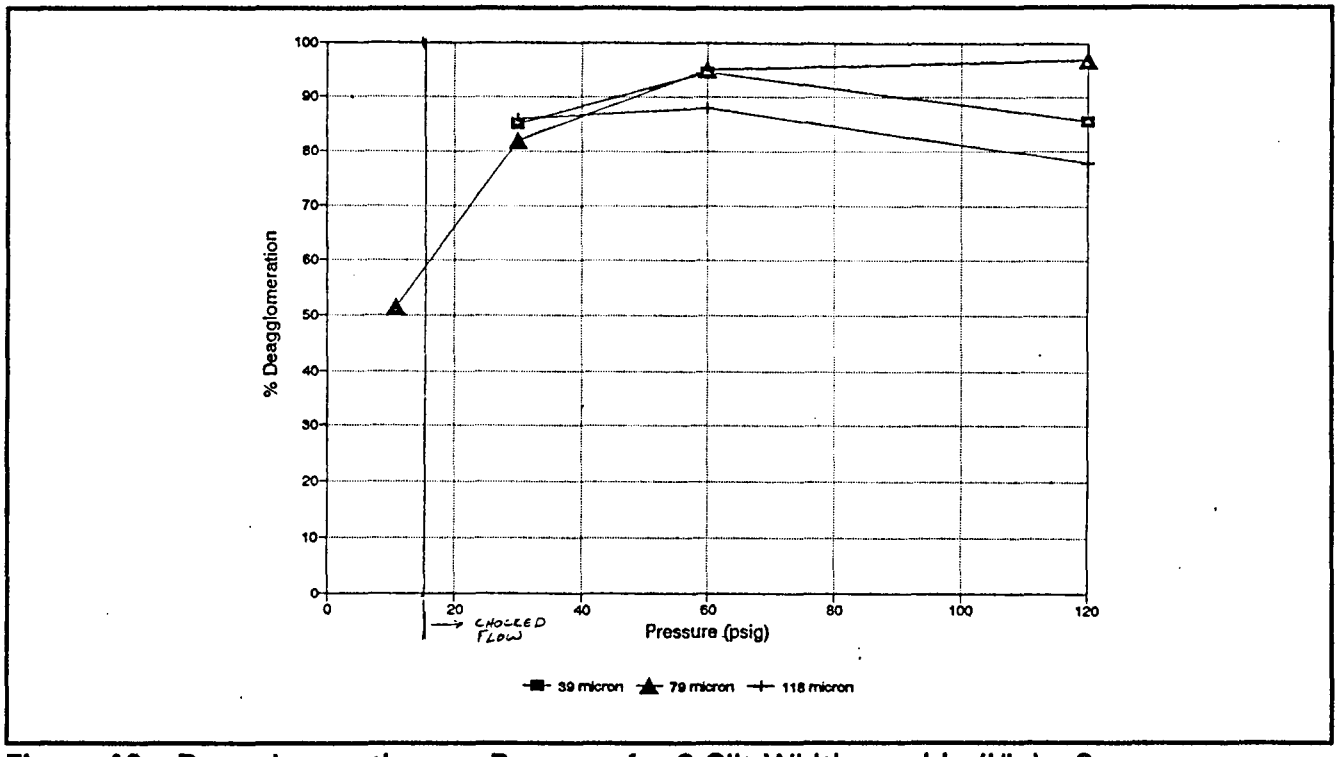

Figure 40 - Deagglomeration vs. Pressure for 3 Slit Widths and Ln(I/Io) = 0.

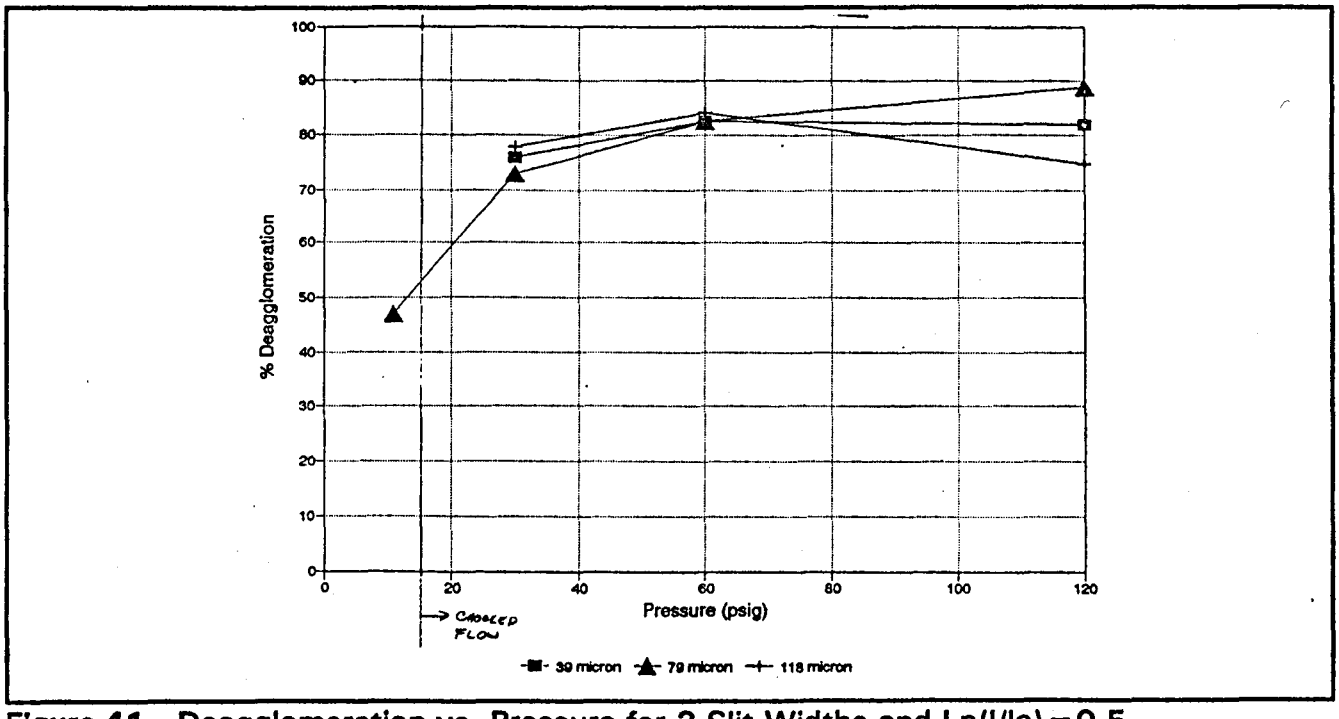

Figure 41 - Deagglomeration vs. Pressure for 3 Slit Widths and Ln(I/Io) = 0.5.

increase in shear.

The data obtained at the different pressures with the 39 and 118 micron gaps indicates that the deagglomeration performance increases as the pressure is raised from 30 to 60 psig, but then levels off or even decreases slightly as the pressure is raised from 60 to 100 psig. This result is counter intuitive, but at the present time we do not have an explanation for it.

There was very little deagglomeration performance difference between the three slit widths that were chosen. In fact, the difference between the slit widths typically falls within the data scatter of the individual data points used to make the cross plots. This is an unexpected result, and should be investigated further.

SEM photographs of the PTI dust samples are shown in Figure 42.

3.3 Repeatability of deagglomeration performance, PTI dust

Two tests (test #gg38 and #gg39) were performed as explicit repeats of an existing data point (test # gg06) to characterize the device's repeatability. Both the concentration achieved and the degree of deagglomeration achieved fall within the uncertainty of the existing data point. The three data points lie within a 5% spread in deagglomeration and within a 15% spread in exit plane concentration. The particles from one of the repeat tests were sampled on an SEM stub instead of the Nuclepore filter holder. The SEM photos of this case (test # gg38) are shown in Figure 42, labeled as "Sample 1".

3.4 Comparison of similarly sized glass micro-sphere results with geological dust results

Two tests (test #gg40 and #gg42) were performed using the Duke Scientific Corp P/N 364 10.2 μm diameter glass beads at the settings used for the repeated tests with the PTI dust described above. Both the concentration achieved and the degree of deagglomeration achieved with the glass microspheres fall within the scatter and uncertainty of the three PTI data points (Figure 43). This is somewhat surprising considering the very different morphologies of these powders. The particles from these tests were sampled on an SEM stub instead of the Nuclepore filter holder. The SEM photos for this case (#gg40 and #gg42) are shown in Figure 44 as "Sample 3" and as "Sample 4" in Figure 45.

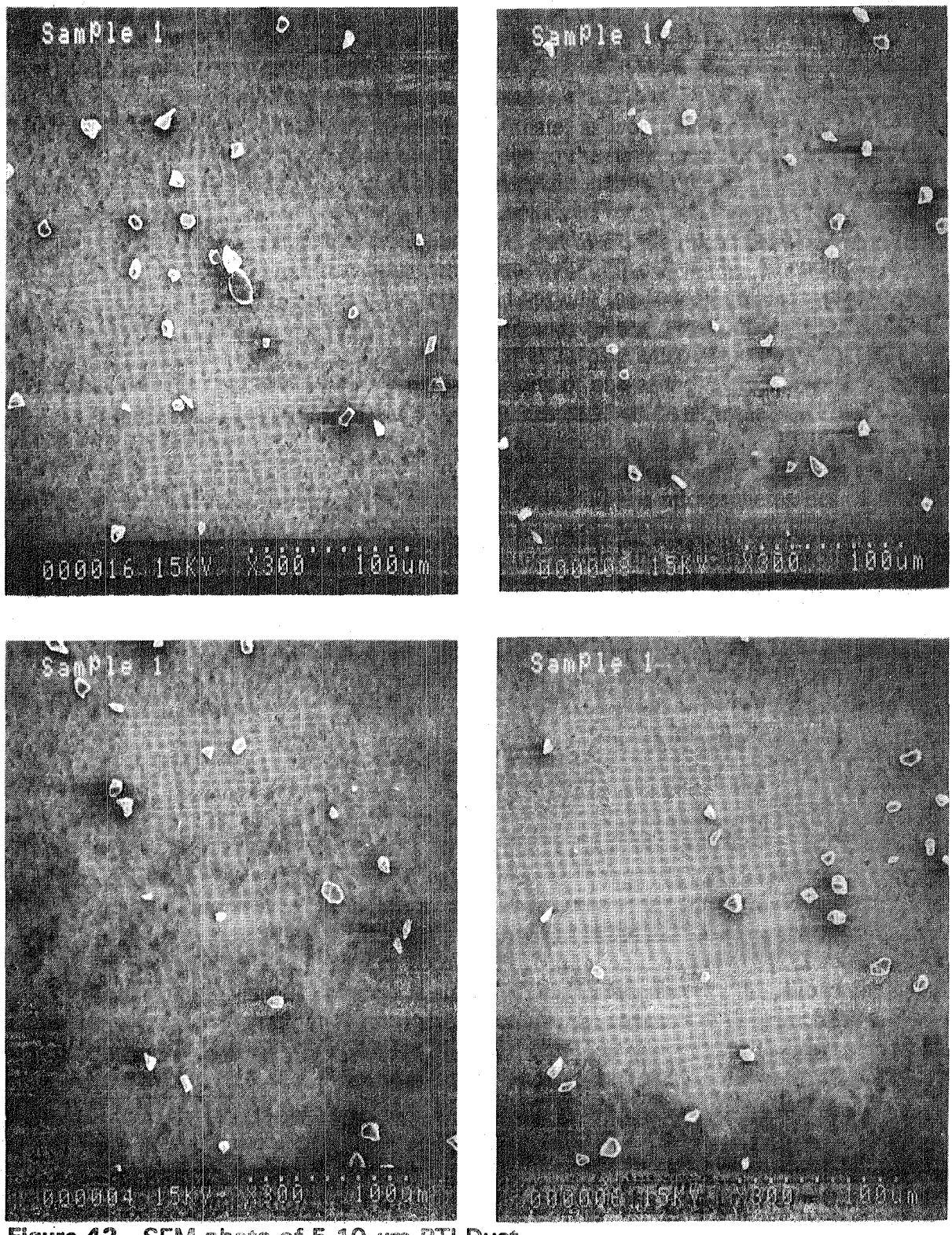

Figure 42 - SEM photo of 5-10 μm PTI Dust.

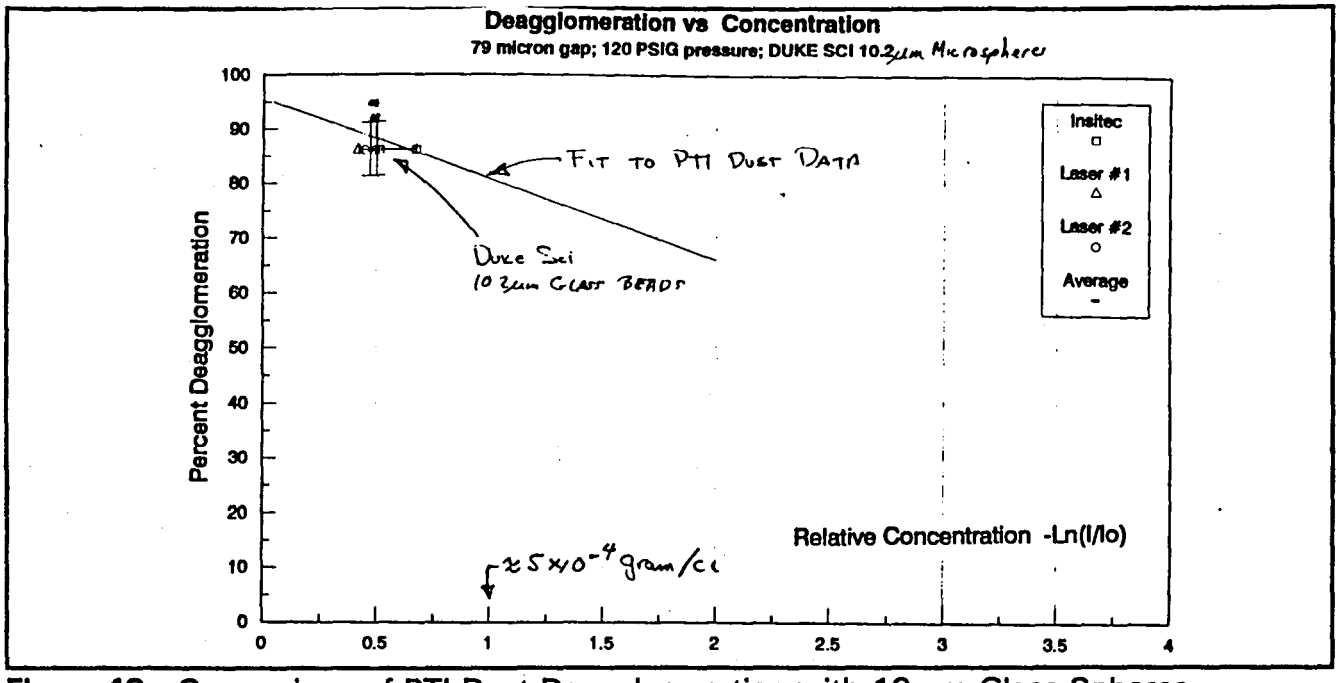

Figure 43 - Comparison of PTI Dust Deagglomeration with 10 μm Glass Spheres.

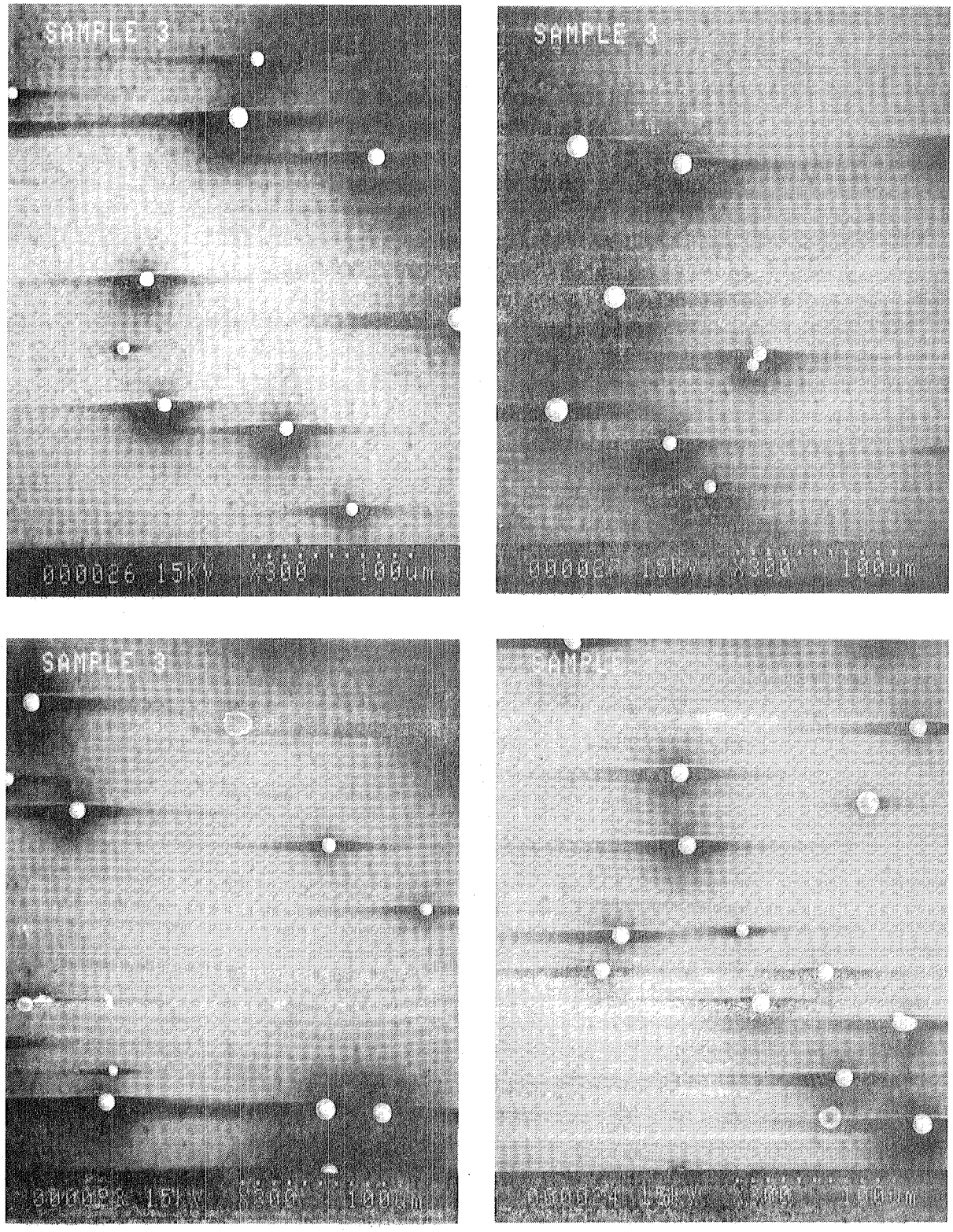

Figure 44 - SEM photo of 10 μm spheres.

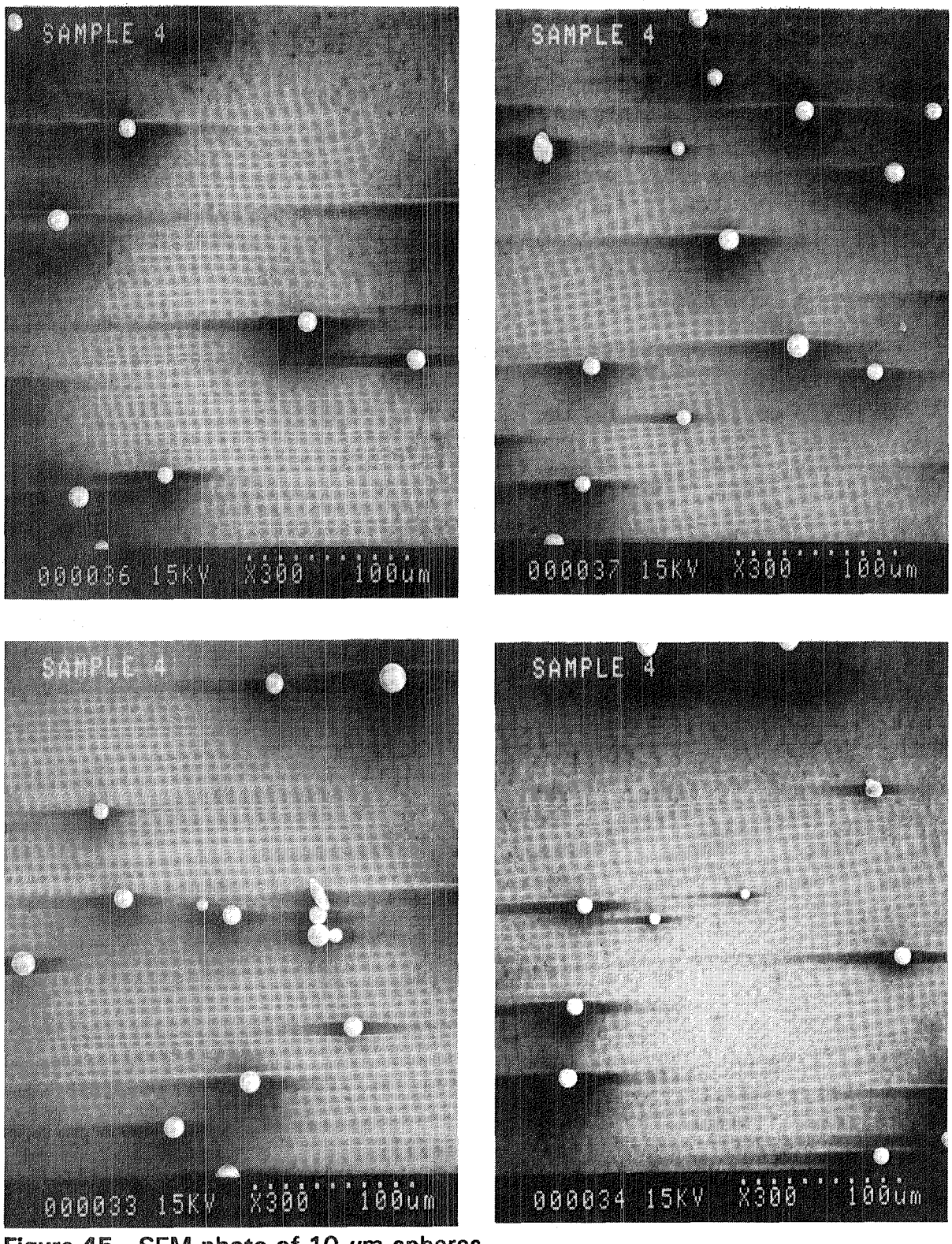

Figure 45 - SEM photo of 10 μm spheres.

3.5 Result for tests with 2.1 μm glass microspheres

Two tests (test #gg43 and #gg45) were performed using the Duke Scientific Corp P/N 547 2.1 μm diameter glass beads. The first test was done at the settings used for both the PTI dust repeated tests and the 10.2 micron glass bead tests described above. This resulted a very high particle loading on the sampling filter, so the second test was done with the same pressure settings and slit width but with less powder. This resulted in a nominally acceptable particle loading on the filter. An attempt was made to characterize this collected sample under the optical microscope, but it was very difficult to see particles smaller than 1 μm diameter so the deagglomeration estimated this way is probably under-estimated. The SEM photos for the second test (Test # gg45) are shown in Figure 46 as "Sample 6". The very limited number of particles counted using the SEM for this powder indicate that the degree of deagglomeration is significantly less (approximately 66% vs approximately 85%) for this powder than for the larger diameter powders.

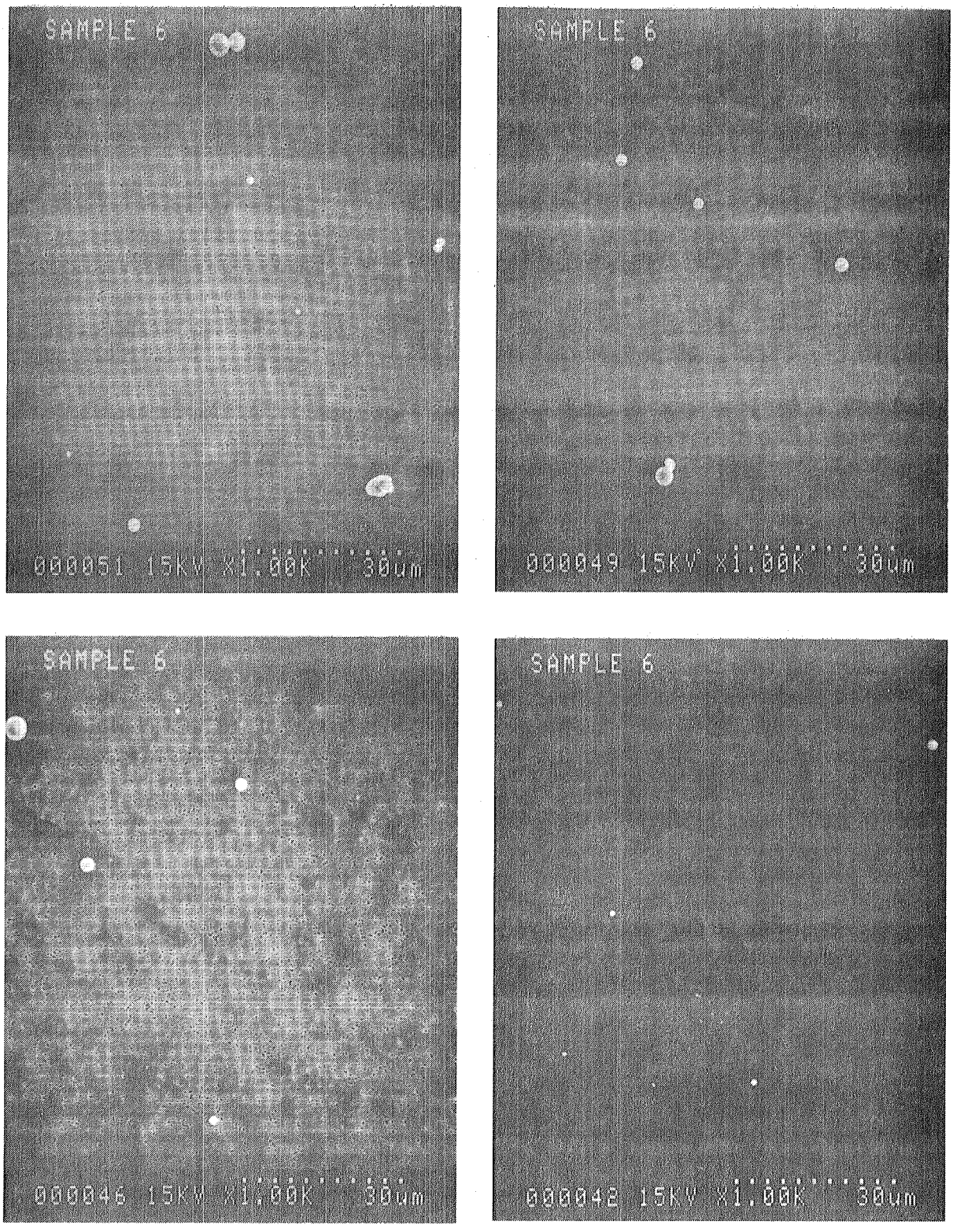

Figure 46 - SEM photo of 2.1 μm spheres.

4 SUMMARY AND SIGNIFICANT FINDINGS

4.1 Deagglomeration Performance characterization Test Results

The test matrix for the deagglomeration performance tests was completed as planned, and a few additional exploratory points were added. Specifically, the final breadboard hardware was characterized by 36 tests using the PTI 5-10 micron dust, two tests using the Duke 10.2 micron glass beads and two tests using the Duke 2.1 micron glass microspheres. Deagglomeration data were obtained for PTI dust at 30, 60 and 120 psig pressure using 39, 79 and 118 micron slit widths and varying the concentration from approximately $1x10^{-4}$ gram/cm^3 to approximately $15x10^{-4}$ grams/cm^3 with at least three concentrations for each pressure and slit width. Additional data was obtained at 11 psig and 79 microns to investigate the effect of unchoked flow. Two tests were explicit repeats of one of the test conditions. The glass microsphere tests were done at 120 psig and a slit width of 79 microns, based on results with the PTI dust.

The most significant finding is that the breadboard solid particle generator can achieve better than 90% deagglomeration but not 100% deagglomeration with the PTI dust, and that the repeatability was approximately +/- 10%.

Additional important results were also obtained for other powder types also. First, the single repeated data point with Duke 10.2 micron glass microspheres lies on the curve for the PTI dust data, so it can probably be assumed that they behave similarly in general. Second, the deagglomeration data for Duke 2.1 micron glass microspheres as obtained under the optical microscope is suspect due to the difficulty is seeing the small end of size distribution (0.5 μm diameter). The limited number of particles counted using the SEM for this powder, however, indicate that the degree of deagglomeration is significantly less for this powder than for the larger diameter powders. Optimizing the deagglomerator settings for the Duke 2.1 micron powder was beyond the scope of this study.

The repeatability of the breadboard solid particle generator was characterized by performing three tests with the same settings. The resulting data points lie within a 5% spread in deagglomeration and within a 15% spread in exit plane concentration.

4.2 Carrier gas effect on minimum chamber pressure achievable

The amount of carrier gas injected into the chamber is important because of the chamber pressure requirements. It is virtually impossible to draw gas out of the chamber without also removing particles. Therefore any gas used to deagglomerate the particles will cause a rise in the chamber pressure (either from some initial chamber pressure or from initial vacuum conditions). It is important, therefore, to be able to estimate the amount of gas used per mass of powder. This information is available in the presentation of the deagglomeration vs exit-plane mass concentration

data plots. Since the deagglomeration performance improves as the amount of gas used per mass of powder increases, a trade-off between the deagglomeration requirements and the minimum chamber pressure requirements is needed. The relative importance of these parameters will need to be decided by the experimenters if this device is used. In order to illustrate the order of magnitudes in this trade-off, first assume that all of the deagglomeration is done at the peak concentration. Then assume that 80% deagglomeration is acceptable and that a 67,000 cc liter chamber initially at vacuum is used. From the deagglomeration tests, a particle sample concentration of approximately $5x10^{-4}$ grams per cm^3 of carrier gas at STP are required for 80% deagglomeration of PTI dust. If approximately 0.1 grams of PTI dust are used to produce a particle number concentration of 10^3 particles/cm^3 in the chamber then 2000 cm^3 scc of gas are used, which will raise the chamber pressure to approximately $3x10^{-2}$ atm. If a particle number concentration of 10^5 particles/cm^3 is desired in the chamber, the minimum chamber pressure would be 3 atm.

4.3 Gravity independent design concept developed and tested

Several gravity independent sample holder design concepts were fabricated and tested. Based on these tests, a design concept was developed for a gravity-independent sample holder, and a prototype sample holder was fabricated for the final version of the breadboard. The mass of powder stored in this sample holder "cartridge" (on the order of 100 milligrams) covers portions of the required number density space (assuming the 67 liter GGSF chamber) required by most of the experiments in the 1-10 particle diameter range (experiments no. 5, 13, and 18) as shown in **Fig. 1.** The design can be extended to dispense larger masses of powder by adding a mechanical device (e.g., stepper motor) to sequentially bring powder "cartridges" into position, although such a design was not built as part of this effort. The deagglomeration performance testing in this effort was done with a single powder "cartridge". The present design and hardware can be easily modified to reduce the total mass of powder dispensed simply by reducing the length and/or diameter of the dust plug in the "cartridge". In its present form, the sample holder cannot be used for KC-135 flights because it depends on the powder cohesion to hold the powder in place and the vibration associated with a KC-135 flight would cause the powder to move undesirably. A design modification for a KC-135-ready version of the sample holder cartridge is proposed in section 9.2 "Design and Engineering Improvements".

4.4 Preliminary design concept for controlling flowfield and penetration into chamber

Flow visualization tests indicated that at nominal deagglomerator operating conditions and with the chamber at ambient pressure the dusty gas jet impinged on the far wall of the chamber. We were able to "stop" the transient dust/gas jet in the center of the chamber by using an opposed transient jet of pure gas produced by a second simulated deagglomerator.

At NASA's direction, no further work was done concerning the control of the powder penetration into the chamber and its subsequent impugnment on the far wall of the chamber. The opposed jet hardware was not included in the deliverable hardware.

5 RECOMMENDATIONS FOR FURTHER STUDIES

All of the following recommendations are based on the assumption that the results of the preliminary characterization of the deagglomeration performance, and the carrier gas issues raised do not preclude the use of the generic design that resulted form this effort.

A carefully focused but limited set of data was obtained during this effort. A more complete data set should be obtained to better quantify the performance of the blast deagglomerator under the operating conditions required for the GGSF S&T requirements. These data should be acquired on the breadboard device so deficiencies can be identified prior to the flight hardware design, and flexibility in the science requirements, if any, can be accommodated.

- The mass of particles during this test series was limited to 85 mg. The sample holder can contain up to 200 mg. The test matrix should be expanded to increase the sample quantities as well as other sample material types.

- The accomplished test matrix focused on 10 μm particles, with limited data and no optimization for 2 μm particles, and no data for smaller than 2 μm or larger than 10 μm particles. The breadboard particle generator should be tested with other particle sizes to verify the ability to optimize for, and deagglomerate various particle sizes outside of 10 μm.

- The deagglomeration percentage is very dependent on the dilution of the particles in the carrier gas. The carrier gas can affect the chamber environment detrimentally for some GGSF experiments. A thorough characterization matrix will result in a gas requirement vs. deagglomeration percentage that can be used to better define the GGSF experiments or changes to science requirements that can allow this type of particle generator to be used.

5.1 Further analytical studies and data analysis

The existing quantitative theory of particle deagglomeration in shear flows appears to be virtually nonexistent, based on a search of the literature. If a more thorough search fails to find a relevant and sufficient theoretical development, then it may be desirable to pursue a theoretical development. This is a more difficult and extensive task than it might appear at first glance. The theory, even if completely developed, would require knowledge of the initial powder condition, such as aggregate binding forces. Thus some level of experimentation and empiricism is likely to creep into the analysis. Therefore, it would appear that only a first order analysis would be warranted.

The coincidence error in the particle sampling procedure that occurs when particles fall on top of each other (and falsely appear as aggregates) has not been estimated. This could be estimated theoretically based on the particle loadings achieved. A more straightforward approach would be to obtain "nearest neighbor distance" data for each particle from the photos, then plot the data as

number of occurrences less than a given distance vs. the distance. This plot could then be extrapolated to a distance of one particle diameter to find the number of occurrences that would produce apparent doublets.

5.2 Design and engineering improvements

An important design improvement is the implementation of a low-gravity laboratory, such as the KC-135, breadboard of the sample holder described previously. The most basic form of this consists of a modification of a standard ball valve, which holds the sample in the rotating section.

Another important improvement would be to optimize the dilution jet system based both on deagglomeration/concentration and weight/space considerations. The number of jets was chosen in a relatively ad-hoc fashion, and it is possible that the number of jets could be reduced. The mixing distance between the jets was not optimized, and further testing might indicate that this distance needs to be changed. Once the design has been fully optimized for deagglomeration performance its size and weight could easily be reduced.

The wear characteristics of the male and female cones could be improved by plating or other surface processes to provided a harder surface, as was done in the original Micromerograph which used a chrome plate.

5.3 Suggested Further 1-g lab characterization tests

There are several near-term tests that can be done in a 1-g lab. A study of the systems performance with particles in the 0.5 to 1 micron range is suggested, and, if successful, could then be extended down to 0.1 microns. There is no indication from the literature that an aerodynamic device such as this will work below 0.1 μm.

The G-independence of the sample holder could be further investigated by conducting tests with the sample holder in a vertical position as well as a horizontal position, however this is not as usefull as demonstrating this device in a low-gravity laboratory.

The amount of powder left in the device when it is operated in different conditions should be investigated more fully. In its present design state the amount of mass dispensed is probably known to a satisfactory degree. However, there is some level of particulate coating in the device. No cleanliness requirements were provided, but it seems apparent that it is undesirable for the various experiment's powders to intermix.

The charge imparted on the particles through contact charging and/or the triboelectric effect should be investigated. It is possible that the charge buildup could be minimized with different choices of deagglomerator material. The integration of a charge neutralization section containing a radioactive source following the deagglomerator should be investigated if charge buildup is found to be a

problem. The radioactive source could be incorporated into either the female cone or male cone in their final design.

In addition, any or all of the engineering and design improvements suggested in the previous section could be characterized (at least in a preliminary sense) in a 1-g laboratory setting.

6 REPRESENTATIVE PHOTOGRAPHS OF PARTICLE SAMPLES

This section provides more representative photographs (others were in Section 3.2 through 3.5 of the data acquired during the characterization of the breadboard deagglomerator. These photos were obtained using a Scanning Electron Microscope.

SEM Photos of 5–10 μm Arizona Dust.

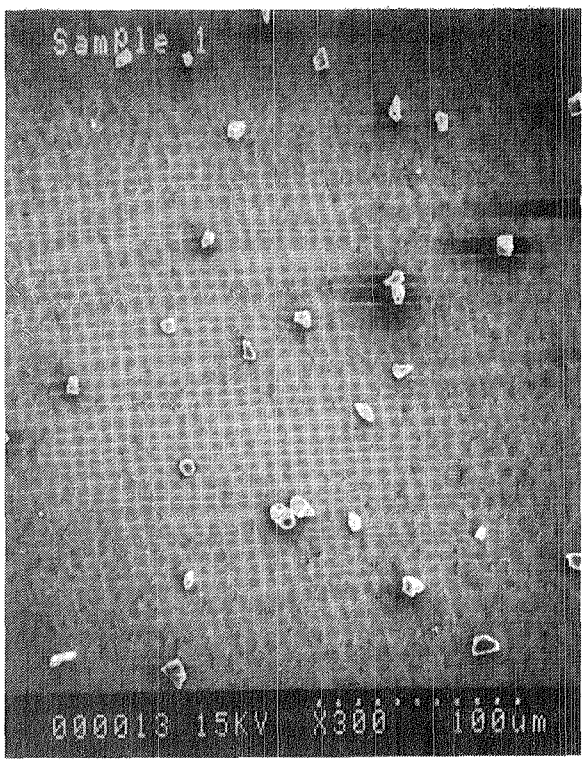

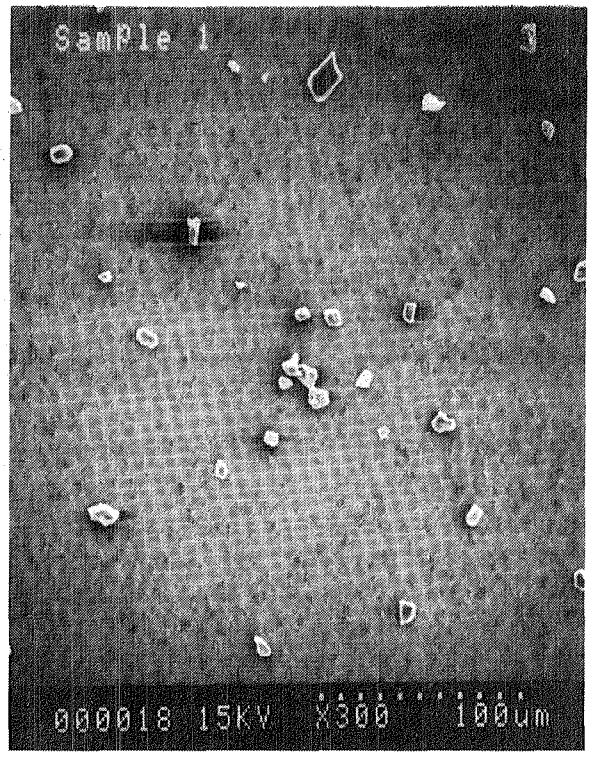

SEM Photos of 5–10 μm Arizona Dust (continued).

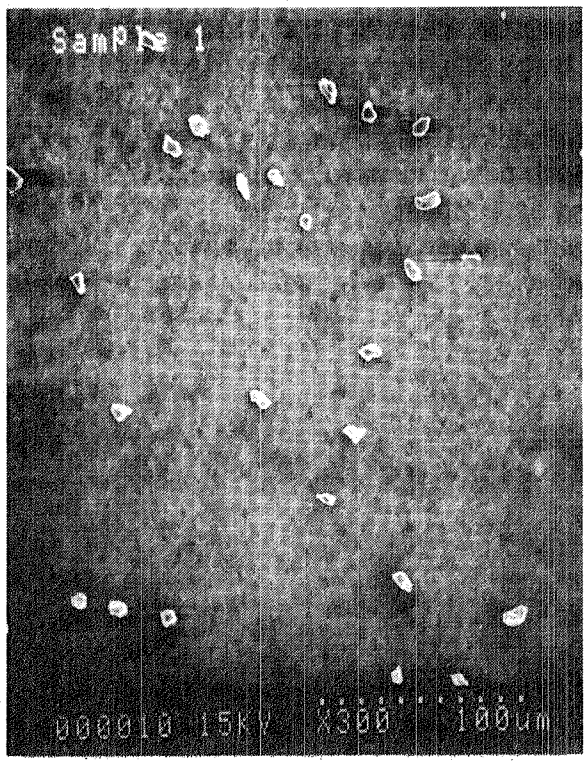

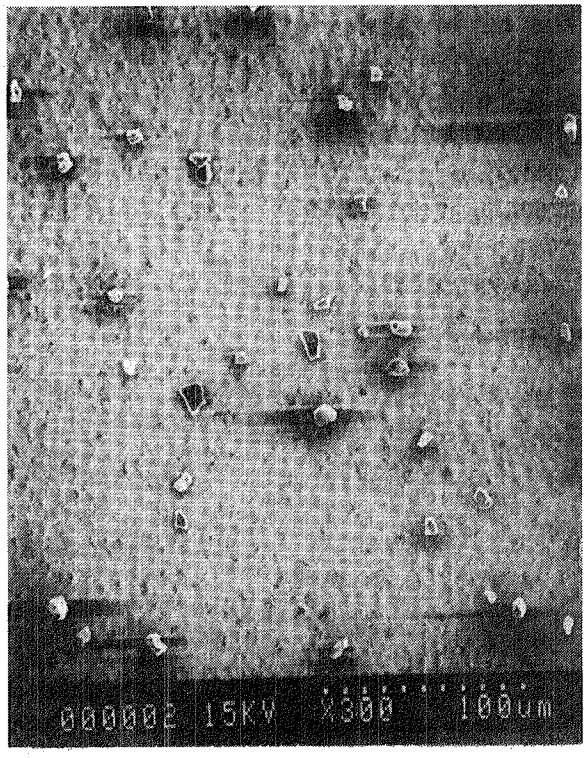

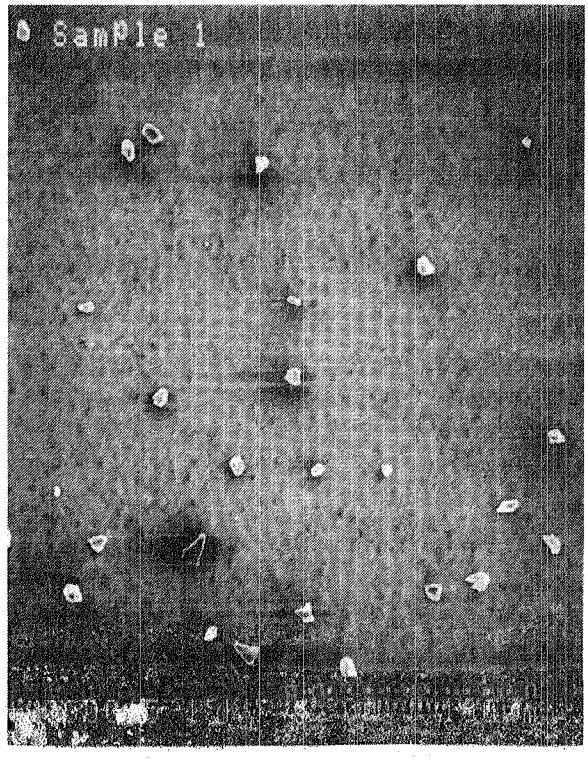

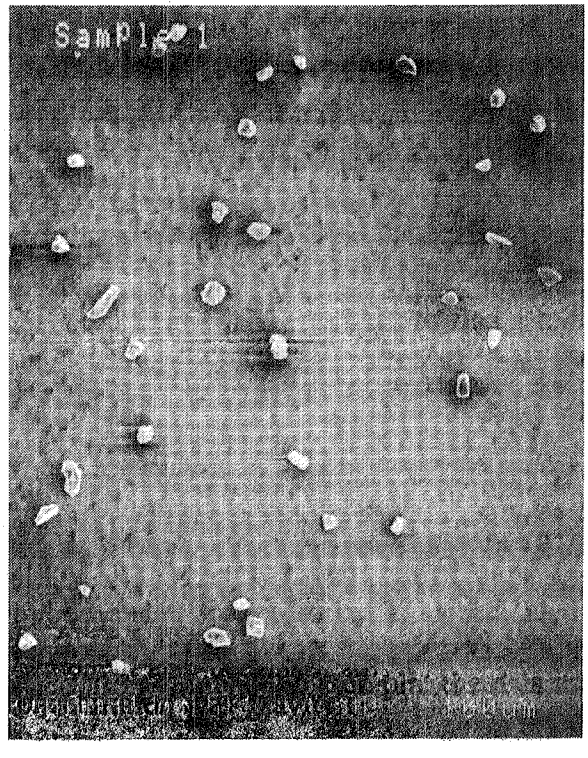

SEM Photos of 10 μm Glass Microspheres.

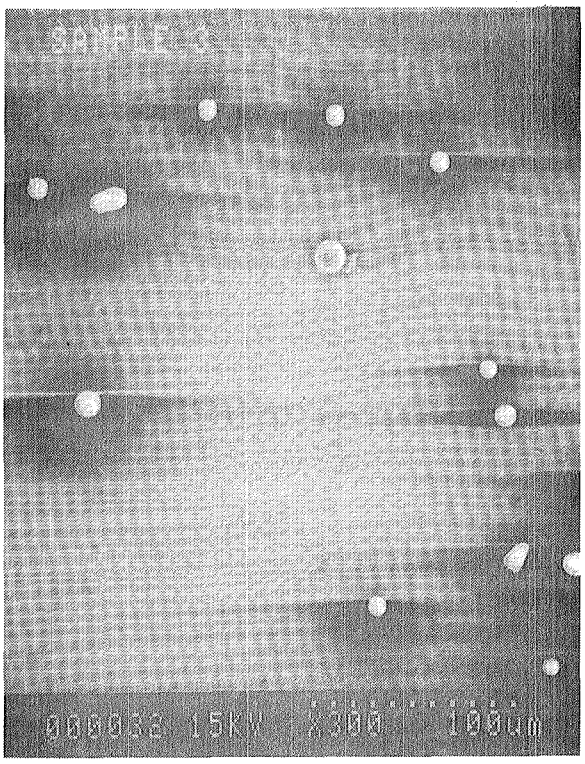

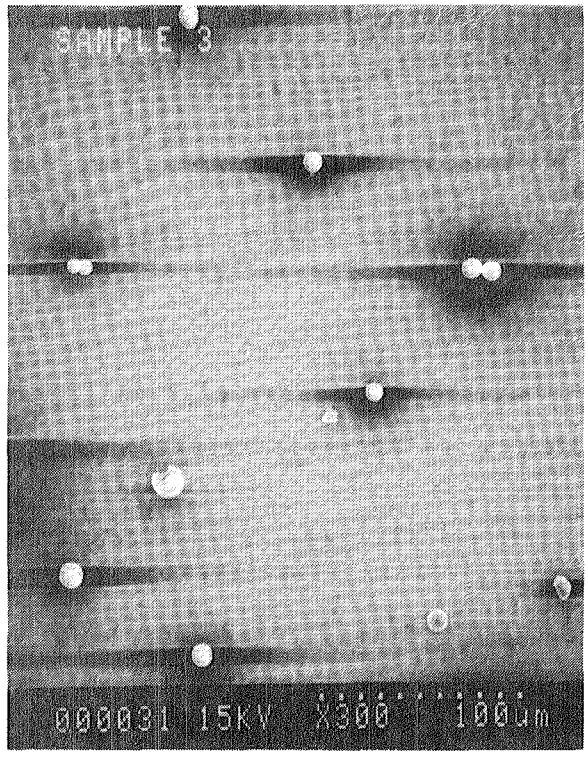

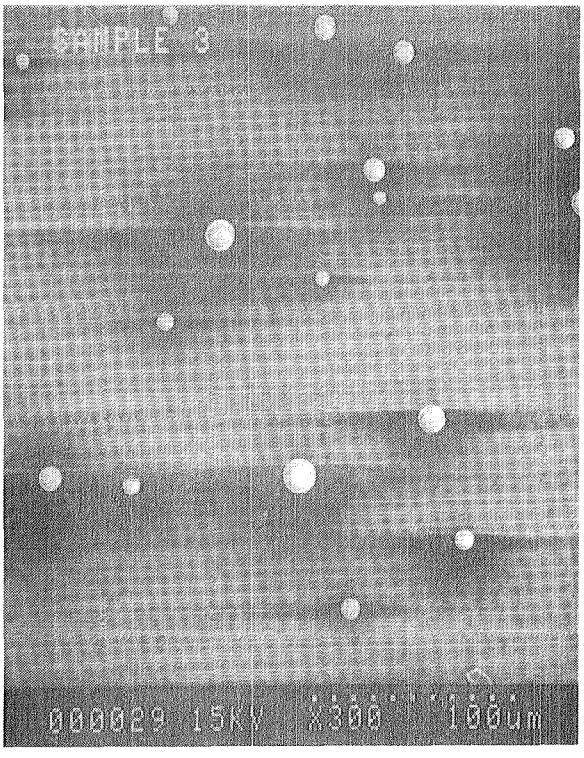

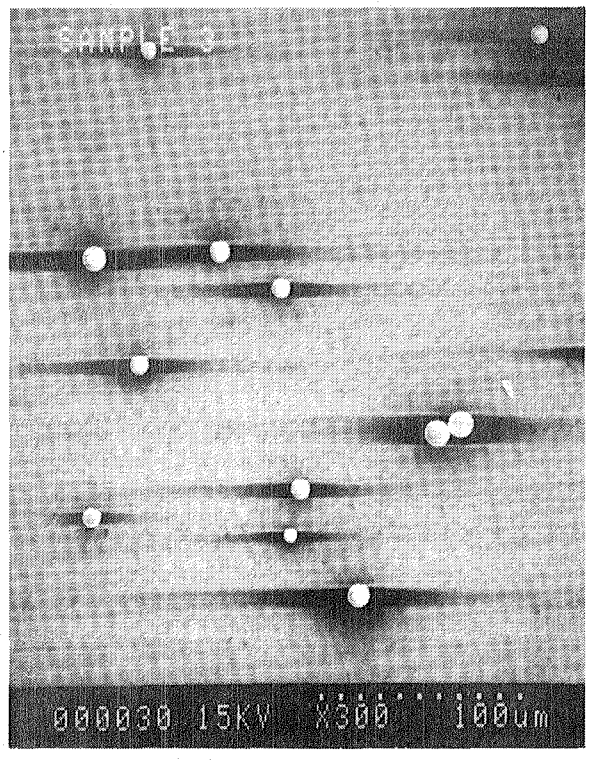

SEM Photos of 2.1 μm Glass Microspheres.

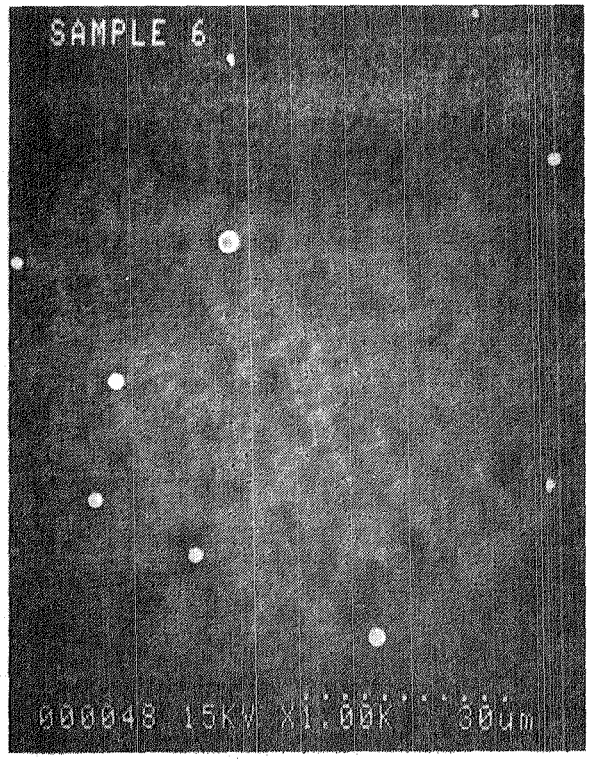

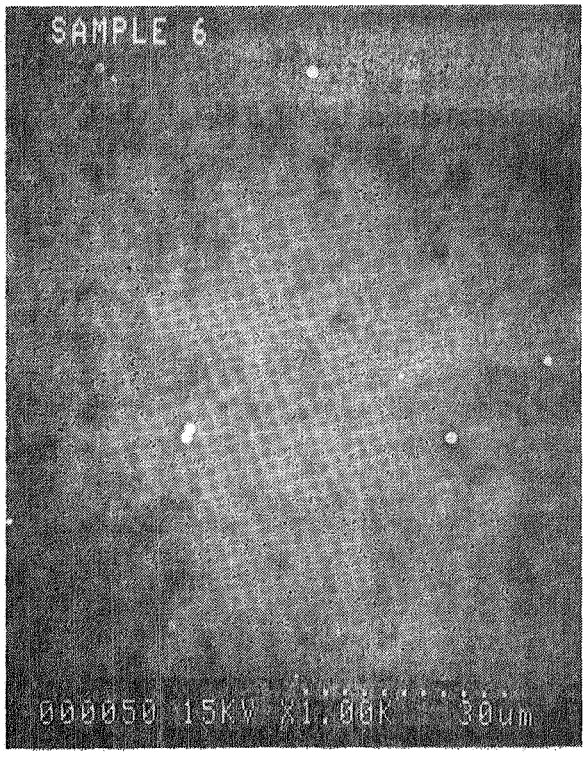

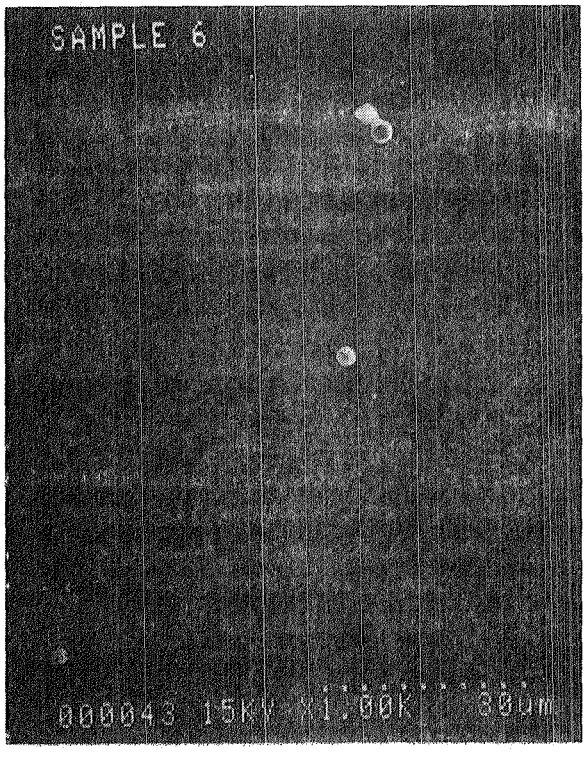

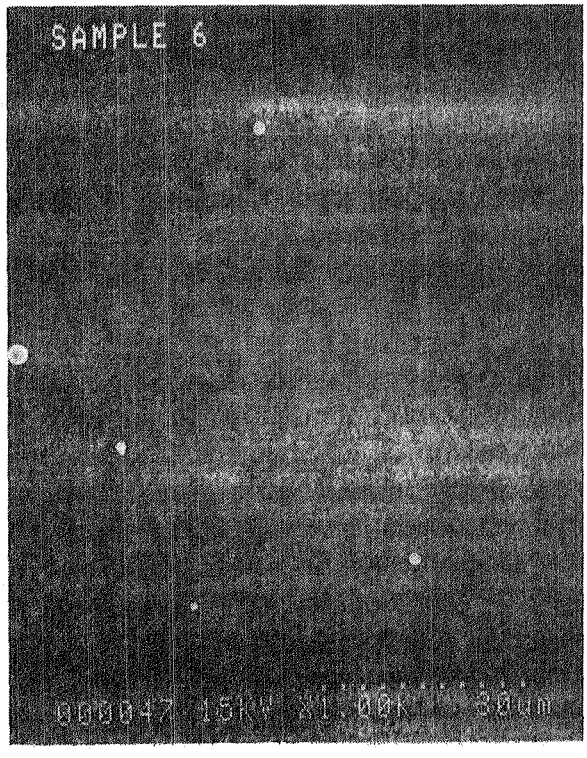

SEM Photos of 2.1 μm Glass Microspheres (continued).

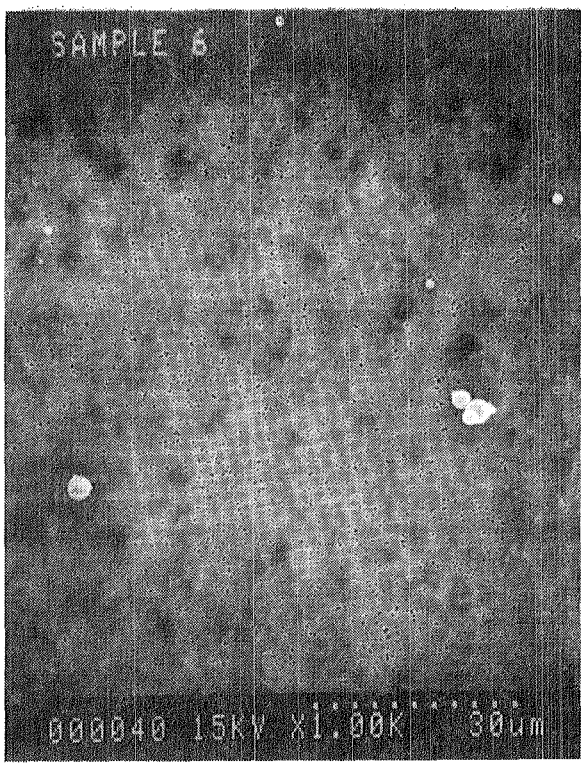

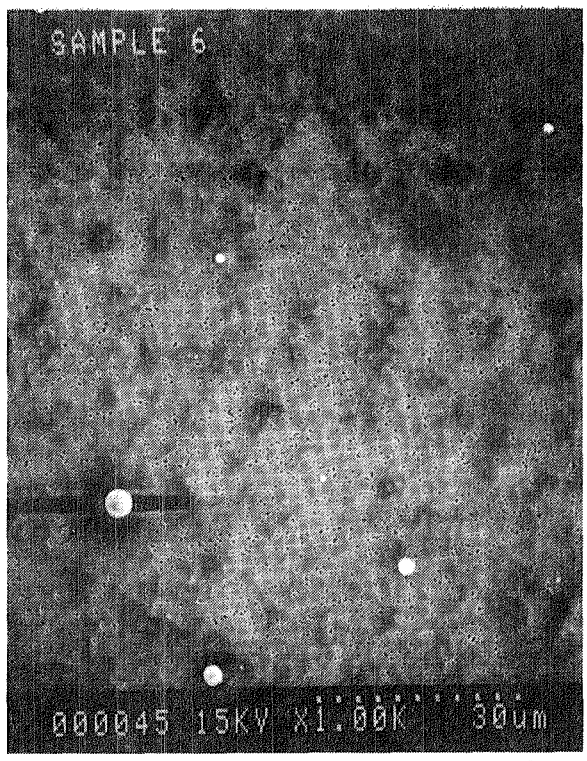

7 PARTS LIST OF DELIVERED BREADBOARD

This list represents the breadboard hardware that was delivered under this contract:

Plexiglass Chamber
- Plexiglass 2 ft diameter X 2 ft long Cylinder
- Plexiglass Chamber-2 ft diameter Top
- Plexiglass Chamber-2 ft diameter Bottom
- Tie rods
- Spare Top with large opening

Deagglomerator Assembly
- Mounting plate and frame
- Deagglomerator head
- Dilution flow section
- Dilution flow solenoid valve
- Dilution flow pressure transducer (mounted in valve body)
- Powder storage camber
- Dispersion flow solenoid valve
- Dispersion flow pressure transducer (mounted in solenoid valve body)
- laser diodes (3)
- laser diode mounts (3)
- laser diode powder supplies
- PIN photodiodes (3)
- PIN photodiodes mounts (3)
- Laser Line filters (3)
- PIN photodiode load resistors and cables (3 sets)

Control circuit
- Control circuit box
- Schematic diagram

Accessories
- Additional spacer rings (4)
- Spare Pintle (1)
- Powder Technology in 4161D Arizina road dust (approximately 1/2 lb)
- Powder Technology in 4170H Arizina Road Dust (approximately 1/2 lb)
- Customized spatula for loading powder (1)
- Adjustment key for laser diodes (3)
- Laser diode manuals
- PIN photodiode data sheets
- laser line filter data sheets
- solenoid valve data sheets
- PTI dust data sheets
- PTI dust MSDS sheet
- Nuclepore filter (4) - Brown Box
- Packing list

8 REFERENCES

1. N. Gat, "Gas-Grain Simulation Facility (GGSF) Phase A Study -- Final report Volume 1. Stage 1. Facilities Definition Studies" (NASA CR177606), Nov. 1992.

2. *Ibid.*

3. *Ibid.*

4. W. C. Hinds, *Aerosol Technology, Properties, Behavior and Measurement of Airborne Particles* (John Wiley and Sons), 1982, pp. 383-395.

5. K. Willeke, *Generation of Aerosols and Facilities for Exposure Experiments* (Ann Arbor Science Pub.), 1980.

6. *Fine Particles, Aerosol Generation, Measurement, Sampling and Analysis* (B.Y.H. Liu, Ed., Academic Press Inc.), 1976, pp. 57-275.

7. M. Corn and M. Esmen, "Aerosol Generation", Handbook on Aerosols, (USERDA), 1976.

8. W. C. Hinds, *Aerosol Technology. Properties, Behavior and Measurement of Airborne Particles*, (John Wiley and Sons), 1982, pg. 387.

9. *Ibid.*, pg. 392.

10. U. Katz, "Study to Perform Preliminary Experiments To Evaluate Particle Generation and Characterization Techniques For Zero-Gravity Cloud Physics Experiments", (NASA Contractor report 3486, 1981), pg. 185.

11. K. Iinoya and H. Masuda, "Experimental Study on the Dispersion of Fine Particles into Air", *Generation of Aerosols and Facilities for Exposure Experiments*, (Ann Arbor Science, 1980).

12. F. S. Eadie and R. E. Payne, "Particle Size Distribution Analyzed Quickly, Accurately", *Iron Age*, (No. 10, 1954), pg. 99.

13. F. S. Eadie and R. E. Payne, "The Micromerograph - A New Instrument For Particle Size Distribution Analysis", (British Chemical Engineering, 1956), pp. 306-311.

14. L. M. Cohen, M. R. Denison, N. Gat, and A. B. Witte, "Comparison of Sieve Diameter to Stoke's Diameter Distribution for Pulverized Coal Particles", *Combustion Science & Technology*, (Vol. 27, 1981), pp. 79-82.

15. N. A. Fuchs, *The Mechanics of Aerosols*, (Translated from Russian, Dover Pub.), 1964, pg. 375.

16. R. R. Irani, and C. F. Clayton, *Particle Size: Measurement, Interpretation, and Application*, (Wiley, New York), 1963, pp. 77 and 145.

17. T. Allen., *Particle Size Measurement*, (Chapman and Hall), 1974, pp. 230-232.

18. C. Orr, and J. M. Dallavalle, *Fine Particle Measurement*, (Macmillan), 1959, pg. 71.

Y. V. Mirskii and T. S. Nesmeyanova, et al., "Rapid Determination of Particle Size Distribution of Microbead Catalysts", *Chemistry and Technology of Fuels and Oils*, (1985), pp. 489-492.

20. A. C. Bryant, D. S. Freeman, and F. L. Tye, "An Appraisal of the Micromerograph for Particle Size Analysis of Manganese Dioxide", Particle Size Analysis Conference, Society for Analytical Chemistry, (1966), pp. 154-165.

21. A. I. Michaels, T. L. Weaver, and R.C. Nelson, "Effect of Dispersion Techniques Upon the Measured Particle Size and Distribution of Tungsten Powder", ASTM Bulletin No. 247, (1960), pp. 74-77.

22. S. M. Kaye, D. E. Middlebrooks, and G. Weingarten, "Evaluation of the Sharples Micromerograph for Particle Size Distribution Analysis", Feltman Research Laboratories, Picatinny Arsenal, Dover, N.J., Technical Report FRL-TR-54, (1962).

23. Fuchs, N. A., and Selin A. N., "Pneumatische Zerstabung von Pulvern (Pneumatic Dispersion of Powders)", (Inzhenierno - Fizicheskii Zh. Vol. 7, No. 1, 1964), pp. 124-126 (in Russian): Staub Vol. 24, No 5. (1964), pg. 817.

24. N. A. Fuchs and F. I. Murashkevich, "Laboratory Powder Dispenser", (Staub-Reinhalt Luft (English) Vol. 30, No. 11, November 1970).

25. Fuchs, *The Mechanics of Aerosols*, op. cit, pg. 375.

26. I. Koichi and H. Masuda, "Dispersion of Fine Powders", *Generation of Aerosols and Facilities for Exposure Experiments*, (Ann Arbor Science, 1980).

27. Fuchs and Murashkevich, "Laboratory Powder Dispenser", loc. cit.

28. A. Zahrdnicek and F. Loffler, "Deagglomeration of Fine Powders in Gas Streams", International Chemical Engineering, (Vol. 19, No. 1, Jan. 1979), pp. 40-45.

29. Fuchs and Selin, *loc. cit.*, pg. 817.

30. I. Koichi and H. Masuda, "Experimental Study on the Dispersion of Fine Particles into Air", *Generation of Aerosols and Facilities for Exposure Experiments*, (Ann Arbor Science, 1980).

APPENDIX B: Particle Generator Theory, Analysis, and Modeling

This section will provide background information to the task of a comprehensive investigation for the development of an analytical model and theoretical understanding of the performance and operations of the deagglomerator. After an initial estimation of the requirements for the analytical model development, it became apparent that there is a significant effort required to properly identify the relevant parameter interactions and to plan the development of a model.

The performance of the particle generator is in a dual capacity as a deagglomerator and a disperser of particles. These operations are interdependent and cannot be totally separated. The performance also depends on various experiment chamber parameters. This discussion is broken into **Powder Sample Lofting, Fluid Mechanics of a Dense Two-Phase Flow, Forces Acting on the Particles,** and **Free Jet Dispersion.** It is not implied that these topics can be treated independently, though. This write-up is not a comprehensive discussion but points out to the scope of the physical/mechanical effects, their interactions and the state of the present knowledge. Some of the parameters affecting the system performance are listed in the table below.

Deagglomeration	Dispersion
Powder Material	Blast Pressure
Particle Size Distribution	Pulse Duration
Gap Size	Chamber Pressure
Cone Geometry and	Opposing Jet(s)
Blast Pressure	Exit Cone Angle
Blast Duration	Chamber Size
Powder Mass	Chamber
Carrier Gas Flow Rate	
Moisture	
Inter-, and Intra-Particle	
Particle Shape	

The model is divided into four modules, or subroutines. The output of each serves as input into the subsequent module. This is not to imply that the effects are independent but such an approach provides a logical approach to the solution of a complex physical phenomena.

a) Powder Sample Lofting and Entrainment: This module relates to the initial lofting of the particles from the sample cup.

Physics: This effect depends on the geometry of the sample cup, the flow parameters (e.g., pressure, pulse duration, particle size, morphology, inter-particle forces [cohesion, adhesion, electrostatic, moisture, etc.]).

Relevant Background information: Some relevant literature and investigations of similar effects (under entirely different geometries and flow regimes, however) may be found in the literature generated by various Defense Nuclear Agency (DNA) studies. As a participant in the DNA program, TRW has extensive experience in developing instrumentation for dusty field flow, quantification of the particle number density, high speed micro-photography, other flow field measurements and modeling.

Approach: As a first step, an experimental approach should be considered using high speed micro-photography. By observing the surface of the powder during the carrier gas blast, one may clarify, for instance, whether surface-shear forces, jet impingement effects, or other mechanisms play a role in the lofting of the particles. These experiments should be repeated in a microgravity environment since the initial state of the particles (e.g., location in the cup) is not as well defined as in one-g. A model of the flow over the particle bed may then be used to calculate the boundary layer shear force, from which the force on the particles is determine. The mechanism of lofting, however, is unclear (at least intuitively), and the shear force, or momentum transfer, must somehow be translated to momentum imparted to the particles, as well as aerodynamic lift that causes the particle entrainment into the flow field. The output of this module, a time-dependent flow field with particle concentration, serves as input to the next module.

Parameters to be considered: gas blast flow rate and pressure; powder cup geometry; amount of particles; particle size, size distribution, and geometry; density; g-level.

b) Dense, two-phase flow.
This module relates to the flow of the gas/particle mixture in the passage leading to the deagglomerator and within the deagglomerator all the way to the exit plane.

Physics: The flow field exerts forces on the particles, while the present of the particles modifies the flow field.*,**,***,****

Approach: The flow field exerts forces on the particles. Because of the dense phase, the particles' flow can not be superimposed over the single-phase flow field. The volume fraction occupied by the particles is probably significant to alter the (unloaded) fluid flow field. Therefore, both the

---

*"Dynamics of Dusty Gases." Frank Marble, Annual Review of Fluid Mechanics, Vol. 2, 1970, pp. 397-446.

**"Fundamental of Gas-Particle Flow." G. Rudinger, Handbook of Powder Technology, Vol. 2, Elsevier, 1980.

***"Flow of Solid Particles in Gases." G. Rudinger, NATO Report AGARDograph No. 222, 1976

****"Fluid Mechanics of Multiphase Systems." S.L. Soo, Blaisdell Publishing, Co., 1967.

continuity and momentum equations for each of the phases are coupled and must be solved simultaneously. As the flow enters the narrow passage of the deagglomerator, both viscous and compressibility effects become important. The equations should, therefore, account for the (dusty) boundary layer, and eventually for the possibility of flow through a shock wave in the diverging section. In this region, the energy equation is also required and coupled to the momentum and continuity equations. Depending on the particle size and their thermal properties, the energy equation for the solid phase may or may not be required. This can be determined by an order of magnitude analysis. The flow is axisymmetric and a 3-D solution is probably not be required. A channel flow geometry may be relevant to this situation. Because of the narrow passage geometry, the degree of turbulence may be affected. This is to be determined, though, by parametric analysis. The adhesive properties of the particles should be known here in order to determine if any of the aerodynamic forces are sufficient to breakup the agglomerates. Similarly, the flow in a velocity gradient field may cause some agglomeration.

Background and relevant information: Two-phase flows have been extensively investigated over the years, and classical books were published in the field. TRW has extensive experience in this area. A model for a two-phase counter-flow heat exchanger that couples the solid and fluid phases continuity, momentum and energy equations was published.*

Parameters to be considered: Particle size; Size distribution; shape (ballistic coefficient); total particle mass; blast pressure; blast duration; deagglomerator internal cone angle and gap size; inter- and intra-particle forces.

c) Deagglomeration & Forces acting on the particles

This module relates to the break-up of the powder sample during the entrainment process and of the particle aggregates within the flow field within the deagglomerator. The results may be strongly coupled to the previous module and a stepwise solution may be required.

Physics: One single topic that bears relevance to, and may dominate all the areas discussed herein, is the physics of the sample powder. The forces holding the particles together and their nature, should be well understood if a valid model is to be developed to describe both deagglomeration and dispersion. These forces are particle- and environment-dependent. Examples of such forces include electrostatic (the magnitude of which depends on the electrical properties of the particles), surface tension due to moisture, etc. Forces that breakup the particles: while in the deagglomerator, the particles are exposed to a velocity gradient, and at some point they may pass through a shock wave. Both these effects may cause the breakup of agglomerates. The friability of the particles may also be considered for some types of particles.

---

*"The Circulating Balls Heat Exchanger (CIBEX)." Nahum Gat, J. Thermophysics and Heat Transfer, Vol. 1, No. 2, April 1987, pp. 105-111.

In addition to the inter-particle forces, there are intra-particle forces that may be relevant to the breakup of particles in the flow field due to aerodynamic shear, as well as mechanical forces due to collisions and impacts.

Background and relevant data: The objective of the GGSF experiments is to allow the investigation of many of these forces, and the GGSF experiments and investigators may be a good source of information. There have been some papers published on the subject of the deagglomeration of dry powders using aerodynamic techniques.

Approach: It is recommended that before, or in parallel to, any modeling effort, these effects should be properly identified and quantified (at least to a first order approximation). The usefulness of the model depends on the reliability of this portion of the model. The approach may combine theoretical/experimental investigations.

Parameters to consider: All types of aerodynamic forces; electrical and electrostatic forces; mechanical forces; etc. mechanical properties; electrical properties; particles size and distribution.

d) Dispersion.
This module relates to the free jet flow of the particle-laden gas from the exit plane of the deagglomerator into the experiment chamber.

Physics: A particle laden, axisymmetric jet is introduced into a quiescent fluid. The jet has temporal/transient properties.

Background and relevant data: probably very little was published or researched in the areas of direct relevance to the parameter space of interest to GGSF. One-phase free jets have been investigated extensively, however, and this could serve as a starting point for the two-phase modeling effort.

Approach: Use one-phase, transient, free jet model, assume to a first approximation that the solid-phase concentration (or volume fraction) is small and, therefore, has no effect on the gas-phase flow field. Develop an axisymmetric flow model with an initial radial distribution function of the particles. To the first approximation ignore gravity, otherwise, a full 3-D model is required. Since the solution to the gas jet flow field is possible, particle trajectories can be calculated using conventional drag, accounting for Knudsen and Reynolds number effects as necessary.

Parameters to consider: Output of the deagglomerator channel flow field; experiment chamber pressure; [g-level and orientation;] Knudsen number and Reynolds Number; particle ballistic coefficient and distribution.

Experimental Validation of Theory and Modeling

The value of an analytical/numerical model is only as good as the quality of the validation and verification data associated with the model. It is imperative to carry out a parallel experimental effort to validate the model performance. Moreover, several areas were described above in which

the theoretical state of knowledge may be relatively lacking or poor. This may not allow the development of a model solely on a theoretical basis. Experimental data, and empirical correlations may be required in order to take the place of theoretical considerations. An example of these effects is the noticeable difference between various powders. For instance, P-K and talcum powders clearly behave in a different manner when handled or used in the deagglomerator. It is not clear what properties of the two powders produce this difference in behavior and how to quantify these properties. Several other areas come to mind in which the above may be true:

- The adhesive properties of particles and the type of forces that dominate agglomeration and coagulation.

- Particle morphology (or shape); for angular particles the ballistic coefficient can be assigned only on a statistical basis because it changes depending on the orientation of each particle in the flow field. This effect may dominate the lofting of the particles, their entrainment into the gas steam, and their sedimentation. Further, this effect may be dependent on the Reynolds number and change as the flow regimes vary.

- Inter-particle forces and the breakup of particles due to aerodynamic and mechanical forces may have a significant effect on the nature of the deagglomeration and dispersion processes.

For the reasons listed above, an experimental validation of the various elements of the analytical model should be carried out carefully. The modeling activity should be utilized to identify areas that require experimental or empirical data.

Test Matrix: The experimental conditions under which the system should be characterized are to be determined in conjunction with the model development.

Diagnostics for Theory and Modeling Validation.

Several types of diagnostics are required to support the model development since there are many different parameters that must be characterized. An abbreviated list of such parameters would include; inter-particle forces, powder moisture content, carrier gas humidity, particle charge as a function of time, gas velocity and turbulent intensity at various locations in the system (including boundary layer profiles), particle concentration at various locations in the system (also including boundary layer profiles), and ,of course, the degree of deagglomeration at various locations in the system.

a) Powder sample lofting and entrainment

The use of high speed microphotography for qualitative visualization of the entrainment process has been discussed previously. Additional instrumentation would be required in order to make quantitative measurements. For example, X-ray transmission measurements could be used to obtain spatially and temporally resolved mass densities, as is presently done in our DNA dust lofting

experiments. Other measurements that are necessary to characterize the entrainment process are dense two phase flow velocity and turbulence measurements and inter-particle forces.

b) Dense two phase flow measurements

The two phase flow measurements of velocity, turbulence and particle size distribution in the very small physical dimensions of the deagglomerator would require a two-component particle sizing LDV (laser Doppler velocimeter) system, preferably a fiber optic system for convenience. Such systems are commercially available from TSI, DANTEC or Aerometrics but are very costly.

c) Forces acting on the particles

The aerodymanic forces acting on the particles could be determined using an LDV system. The forces between particles such as electrostatic attraction, surface tension due to moisture, mechanical packing etc. are much harder to measure, especially for the powder in its initial state prior to entrainment. The instrumentation required for these measurements is still to be determined.

d) Dispersion

A combination of LDV and flow visualization should be sufficient for characterizing the dispersion of the dusty gas cloud. Theses techniques could be augmented by light or X-ray extinction measurements.

e) Extended range particle sizing instrumentation

The deagglomeration diagnostics may be divided into on-line and off-line methods. The on-line include optical methods such as absorption, scattering, etc. as appropriate for the range of particle size and concentrations. Off-line technique include sample removal for morphological analysis using light microscopy or SEM as appropriate for the size range, and other techniques for particle characterization. Sample removal methods should be specific and non controversial in that the sample may not be altered while being manipulated.

Off-line sampling instruments can be developed for sampling in two regimes of the GGSF. Dilute phase particle (e.g., in the experiment chamber, far from the exit plane of the deagglomerator) sampling may be done with a simple suction probe equipped with a Nuclepore filter. Such a system, one should realize, does not operate in an iso-kinetic mode and therefore may remove a biased sample (e.g., a higher fraction of small particles), may have low temporal and spatial resolution, since sampling is not instantaneous, and may be affected by gravity. Overall, however, this is a simple probe and the morphology of the samples in the dilute phase may reveal some information on the performance of the deagglomerator.

Sample collection near the deagglomerator exit plane is more involved. In that area, the number density of particles is much higher than at any other location in the chamber. If sufficient attention is not given, sample alterations may occur within the particle sampling and handling system. As indicated by Dr. Fred Rogers, there is a need for a strong and rapid quenching of any of the coagulation and agglomeration processes. Thus the sampling probe requires custom development of a system that can provide the required suction and dilution. The probe will have to undergo extensive testing and performance characterizations.

REPORT DOCUMENTATION PAGE

Form Approved
OMB No. 0704-0188

1. AGENCY USE ONLY *(Leave blank)*	2. REPORT DATE	3. REPORT TYPE AND DATES COVERED
	December 1993	Contractor Report

4. TITLE AND SUBTITLE
Gas-Grain Simulation Experiment Module Conceptual Design and Gas-Grain Simulation Facility Breadboard Development

5. FUNDING NUMBERS
NAS2-13408

6. AUTHOR(S)
J. M. Zamel and M. Petach

7. PERFORMING ORGANIZATION NAME(S) AND ADDRESS(ES)
TRW Space & Electronics Group
Applied Technology Division
Redondo Beach, CA 90278

8. PERFORMING ORGANIZATION REPORT NUMBER
A-94034

9. SPONSORING/MONITORING AGENCY NAME(S) AND ADDRESS(ES)
National Aeronautics and Space Administration
Washington, DC 20546-0001

10. SPONSORING/MONITORING AGENCY REPORT NUMBER
NASA CR-177632

11. SUPPLEMENTARY NOTES
Point of Contact: M. L. Fonda, Ames Research Center, MS 239-12, Moffett Field, CA 94035-1000
(415) 604-5744

12a. DISTRIBUTION/AVAILABILITY STATEMENT
Unclassified-Unlimited
Subject Category – 88

12b. DISTRIBUTION CODE

13. ABSTRACT *(Maximum 200 words)*

This report delineates the Option portion of the Phase A Gas-Grain Simulation Facility study. The conceptual design of a Gas-Grain Simulation Experiment Module (GGSEM) for Space Shuttle Middeck is discussed. In addition, a laboratory breadboard was developed during this study to develop a key function for the GGSEM and the GGSF, specifically, a solid particle cloud generating device. The breadboard design and test results are discussed and recommendations for further studies are included.

The GGSEM is intended to fly on board a low earth orbit (LEO), manned platform. It will be used to perform a subset of the experiments planned for the GGSF for Space Station Freedom, as it can partially accommodate a number of the science experiments. The outcome of the experiments performed will provide an increased understanding of the operational requirements for the GGSF.

The GGSEM will also act as a platform to accomplish technology development and proof-of-principle experiments for GGSF hardware, and to verify concepts and designs of hardware for GGSF. The GGSEM will allow assembled subsystems to be tested to verify facility level operation. The technology development that can be accommodated by the GGSEM includes:

- GGSF sample generation techniques
- GGSF on-line diagnostics techniques
- sample collection techniques
- performance of various types of sensors for environmental monitoring
- some off-line diagnostics

Advantages and disadvantages of several LEO platforms available for GGSEM applications are identified and discussed.

Several of the anticipated GGSF experiments require the deagglomeration and dispensing of dry solid particles into an experiment chamber. During the GGSF Phase A study, various techniques and devices available for the solid particle aerosol generator were reviewed. As a result of this review, solid particle deagglomeration and dispensing were identified as key undeveloped technologies in the GGSF design. A laboratory breadboard version of a solid particle generation system was developed and characterization tests performed. The breadboard hardware emulates the functions of the GGSF solid particle cloud generator in a ground laboratory environment, but with some modifications, can be used on other platforms.

14. SUBJECT TERMS
Particle dispersion, Deagglomeration percentage, Particle generation

15. NUMBER OF PAGES
143

16. PRICE CODE
A07

17. SECURITY CLASSIFICATION OF REPORT	18. SECURITY CLASSIFICATION OF THIS PAGE	19. SECURITY CLASSIFICATION OF ABSTRACT	20. LIMITATION OF ABSTRACT
Unclassified	Unclassified		

End of Document